MOLECULAR DETERMINANTS OF HUMAN ANTIBODY MEDIATED INHIBITION OF HUMAN NOROVIRUS

By

Gabriela S. Alvarado

Dissertation

Submitted to the Faculty of the

Graduate School of Vanderbilt University

in partial fulfillment of the requirements

for the degree of

DOCTOR OF PHILOSOPHY

in

Microbiology and Immunology

March 31, 2019

Nashville, Tennessee

Approved:

Christopher R. Aiken, Ph.D.

Amy S. Major, Ph.D.

Peggy L. Kendall, M.D.

James R. Goldenring, M.D., Ph.D.

James E. Crowe, Jr., M.D.

To my parents, Yamileth and Luis Alvarado, I am eternally grateful for your love, support and the sacrifices you made

ACKNOWLEDGMENTS

I would first like to express my sincere gratitude to my mentor, Dr. James E. Crowe. His work ethic and passion for science has inspired to become a better scientific researcher. He gave me the opportunity to work in an environment full of cutting edge resources and always encouraged my independence and freedom.

I would also like to thank Vanderbilt University and the Department of Pathology, Microbiology and Immunology for letting me join their graduate program. I am greatly indebted to the Initiative for Maximizing Student Diversity (IMSD), specifically Dr. Linda Sealy and Dr. Roger Chalkey for providing a nurturing environment for graduate students. I am also thankful for my dissertation committee, Dr. Christopher Aiken (Chair), Dr. Peggy Kendall, Dr. Amy Major and Dr. Jim Goldenring. I always appreciated your valuable insight and guidance.

I am very thankful for having such amazing colleagues. I am extremely grateful to have been trained by Nurgun Kose. Your patience, technical expertise and kindness are irreplaceable. To all my fellow laboratory mates and friends, I thank you for your constant support and words of encouragement.

This work would not have been possible without my collaborators in the laboratories of Dr. Mary Estes and Dr. B.V. Venkatar Prasad at the Baylor College of Medicine who provided critical reagents and experimental results to complete my graduate studies. My research was financially supported by the National Institute of Health (NIH), the National Institute of Allergy and Infectious Diseases (NIAD), the Vanderbilt Digestive Disease Research Center and the Vanderbilt University Trans-Institutional Program.

Most of all, I am fully indebted to my family. To my sister and mother, thank you for always being so understanding, reassuring and giving me your unconditional love. To my grandmother and father, I will always treasure our memories together. You have all helped me become who I am today.

TABLE OF CONTENTS

Page

LIST OF FIGURES

LIST OF ABBREVIATIONS

BLI	Bio-layer interferometry
CDC	U.S. Center for Disease Control
dIgA	Dimeric IgA
EC50	Half-maximal effective concentration
EBV	Epstein-Barr virus
ELISA	Enzyme-linked immunosorbent assay
FBS	Fetal bovine serum
GI	Genogroup I
GII	Genogroup II
GST	Glutathione S-transferase
HBGA	Histo blood group antigen
HIE	Human intestinal enteroid
HPI	Hours post-infection
HuNoV	Human norovirus
IC50	Half-maximal inhibitory concentration
Ig	Immunoglobulin
kDa	Kilodaltons
LCL	Lymphoblastoid cell line
mAb	Monoclonal antibody
MBP	Maltose binding protein
mIgA	Monomeric IgA
P	Protruding
ORF	Open reading frame
PGM	Porcine gastric mucin

PBMC	Peripheral blood mononuclear cell
RBC	Red blood cell
S	Shell
TEV	Tobacco etch virus
US	United States
VLP	Virus-like particle

CHAPTER I

INTRODUCTION

Thesis overview

Documented in my thesis is a summary of the work I have done to characterize the molecular basis of human antibody-mediated inhibition of human norovirus (HuNoV). I divided my work into five chapters; the first chapter contains a thorough review of background information pertaining to the discovery, classification and epidemiology of noroviruses, as well as available vaccines, therapeutics and the human immune response to infection.

In the second chapter I begin to discuss my dissertation research. This chapter focuses on my work towards elucidating the human antibody response to norovirus GI.1, or Norwalk virus, infection. I describe the isolation and characterization of a panel of fourteen human monoclonal antibodies (mAbs), seven IgGs and seven IgAs, specific to NoV GI.1 virus-like particles (VLPs). We also used one of the isolated IgAs to identify and describe the structural basis for neutralization, or inhibition of receptor binding, of GI.1 VLPs.

The third chapter focuses on the discovery and study of human monoclonal antibodies that bind and neutralize a pandemic strain of HuNoV, GII.4 Sydney 2012. I isolated a panel of twenty-five human mAbs, twenty-one IgGs and four IgAs, and describe their ability to inhibit GII.4 Sydney 2012 VLPs from binding to histoblood group antigens (HBGAs). Using stem cell derived enteroids, five of the isolated mAbs were also tested for *in vitro* neutralization of live GII.4 Sydney 2012 virus. Binding studies using real-time bio-layer interferometry (BLI) also revealed at least three potential binding groups on the GII.4 Sydney 2012 major capsid protein.

In the fourth chapter, I describe the work I have done to isolate anti-NoV human mAbs with breadth. Specifically, human mAbs that bind, or bind and neutralize, more than one genotype within a NoV genogroup or strains across both genogroup I and II (GI and GII). I

focused on isolating IgGs, IgAs and IgMs, that bound to VLPs representing current circulating strains of NoV. In this chapter I describe fourteen, five IgMs, seven IgGs and two IgAs, with genogroup specific cross-reactivity or reactivity across both genogroups. Eleven of the fourteen mAbs inhibited VLP HBGA binding with at least one of the NoV strains tested. I also include crystallographic studies which identify a potential neutralizing mechanism for a cross-reactive neutralizing mAb.

The fifth and final chapter, describes a summary of my findings and suggests future directions for my studies. I believe the work I have done to identify the determinants of antibody-antigen recognition and mapping blockade, or neutralizing, epitopes will provide insight into HuNoV antigenic sites that in the future can be used to design prophylactics and therapeutics, broadly protective vaccine candidates and sensitive diagnostics.

Introduction to norovirus

Initially discovered by Albert Kapikian over 40 years ago, HuNoVs have now become the leading cause of epidemic and sporadic non-bacterial gastroenteritis worldwide and the principle cause of foodborne disease outbreaks in the United States (Glass et al. 2009; Lopman et al. 2016). NoVs persistence is attributed to many factors, such as a low infectious dose, extreme environmental viral stability, high levels of viral shedding, and prolonged shedding even after symptoms have resolved (Teunis et al. 2008). Each year on average worldwide, HuNoVs cause approximately 267 million cases of infection and over 200,000 deaths in children under the age of five (Debbink, Lindesmith, et al. 2012). The global economic burden is estimated to be about $4.3 billion in direct health system costs and $60.3 billion in societal costs each year (Bartsch et al. 2016). HuNoVs infect people of all ages and, even though infection is characteristically acute and self-limiting, it can become life threatening in children, the elderly, and the immunocompromised (Bok & Green 2012).

Discovery and classification of noroviruses

The first reports of “winter vomiting disease” date back as far as 1929. Dr. J Zahorsky noted sporadic cases of sudden-onset of vomiting and diarrhea among his patients with prevalence peaking in the winter months, but we now know NoV outbreaks can occur year-round (White 2014). The etiologic agent responsible for “winter vomiting disease” was not discovered until 1972 and was named Norwalk virus following a 1968 outbreak in an elementary school in Norwalk, Ohio (Kapikian et al. 1972). Initial attempts to identify the agent responsible for the 1968 outbreak using a traditional tissue culture approach were not successful. Fortunately, immune electron microscopy, using convalescent serum and stool filtrates derived from patients infected during the outbreak, facilitated the visualization of the highly infectious virus (Figure 1-1) (Kapikian et al. 1972; Kapikian 2000). The antibody-antigen interaction formed complexes which allowed easier detection by electron microscopy and were critical to the determination that these particles were responsible for the acute gastroenteritis outbreak. This strain would eventually become the prototype virus for all noroviruses.

We now know that NoVs, or Norwalk-like viruses, are icosahedral, nonenveloped, positive sense single-stranded RNA viruses and are classified as a genus within the *Caliciviridae* family of viruses. The RNA genome typically ranges from 7.3 to 8.5 kilobases in length and is polyadenylated on the 3’-end. The genome is also separated into three open reading frames (ORF) and is surrounded by a capsid anywhere between 27 to 40 nm in diameter (Fields et al. 2013; Xi et al. 1990). ORF1 encodes a large polyprotein which is proteolytically cleaved into six non-structural proteins, most of which are believed to be essential for viral replication. The major and minor capsid proteins, viral protein 1 and 2 (VP1 and VP2), are encoded by ORF2 and ORF3, respectively.

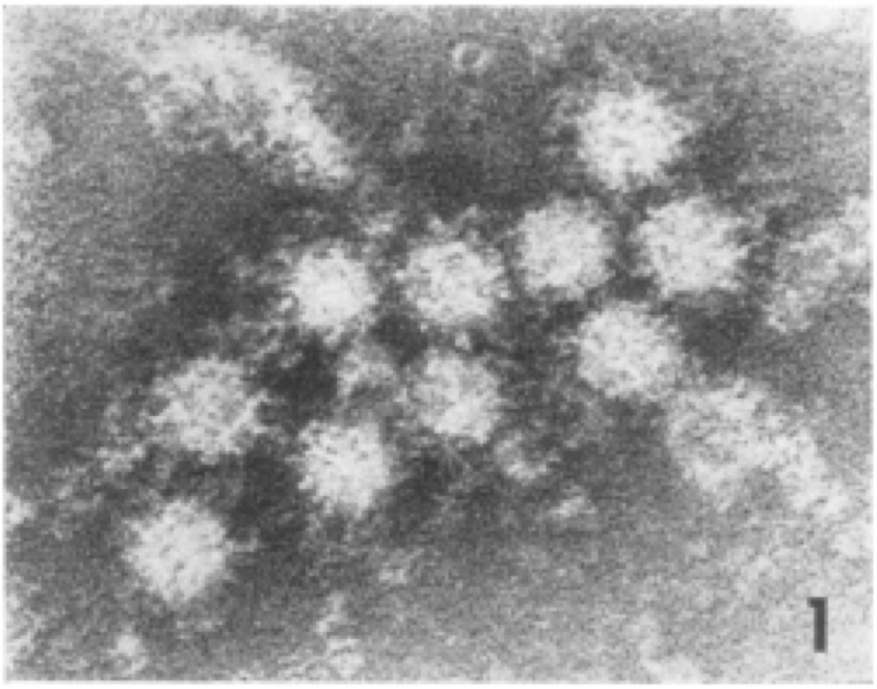

Figure 1-1. Immune electron micrograph of Norwalk virus. Stool filtrate from a challenged patient was incubated with post challenge antiserum and visualized using immune electron microscopy. From (Kapikian et al. 1972)

The NoV capsid exhibits T=3 icosahedral symmetry and is formed by 180 molecules of VP1, which organize themselves into 90 dimers of capsid protein. The VP1 amino acid sequence is also used to phylogenetically classify noroviruses into seven distinct genogroups (Figure 1-2) (Vinjé 2015). Genogroups I, II and IV (GI, GII and GIV) infect humans, but GI and GII are responsible for the majority of human cases of infection (Zheng et al. 2006). Based on sequence conservation, each genogroup is further subdivided into genotypes. GI and GII are divided into at least thirty-one different genotypes (Vinjé 2015). Each genotype is also separated into different strains from specific outbreaks. For over two decades, Genogroup II genotype 4 (GII.4) NoVs have been responsible for the majority of NoV outbreaks (Figure 1-2). Rapidly evolving GII.4 viruses result in the emergence of new variant strains every 2-3 years (Lindesmith et al. 2013).

Structure of noroviruses

The major capsid protein, VP1, consists of an internal shell (S) domain and a protruding (P) domain, as seen on the three-dimensional ribbon representation of Norwalk virus in Figure 1-3. The S domain forms the interior core of the capsid and surround the viral genome. The P domain contains determinants for antibody and receptor binding and is further subdivided into the P1 subdomain, which is exposed and projects out to form an arch-like structure, and a hypervariable surface-exposed P2 subdomain (Koho et al. 2012; Prasad et al. 1994; Prasad et al. 1999). P2 contains the most sequence diversity among noroviruses.

The recombinant expression of VP1 self-assembles into non-infectious virus-like particles (VLPs). They are typically 23 to 38 nm in size, depending on the number of copies of VP1 expressed, and recapitulate the antigenicity, structure, and immunogenicity of NoV native virions (Fields et al. 2013; Green et al. 1993; Jiang et al. 1992). Genogroup and strain specific immunogenic determinants can be engineered and expressed on the surface of recombinant VLPs. Expression of VLPs is only dependent on the NoV capsid protein sequence and can be

recombinantly expressed in insect, mammalian, or plants cells *in vitro* (Koho et al. 2012). VLPs also have the ability to stimulate a systemic and mucosal anti-NoV immune response, which has made them promising vaccine candidates (Richardson et al. 2013; Choi et al. 2008)

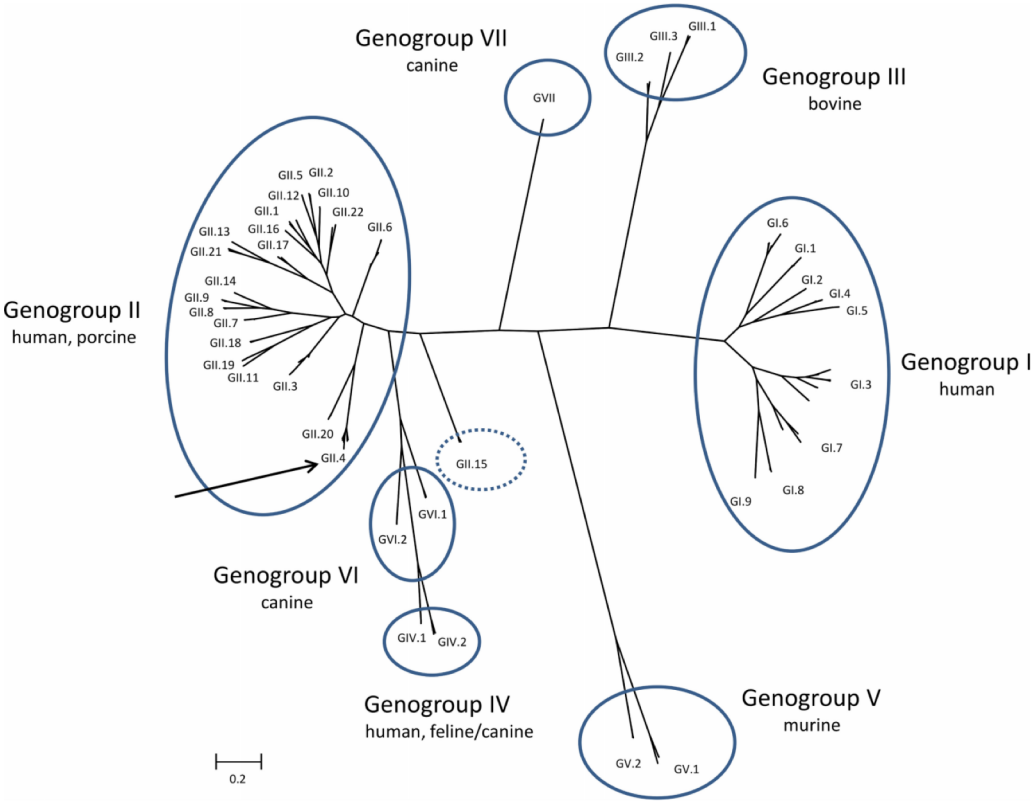

Figure 1-2. Noroviruses phylogenetically classified. The viruses are classified into seven genogroups based on the VP1 capsid protein amino acid sequence. Marked is GII.4 which has been responsible for the majority of outbreaks since the mid 1990s. From (Vinje et al. 2015).

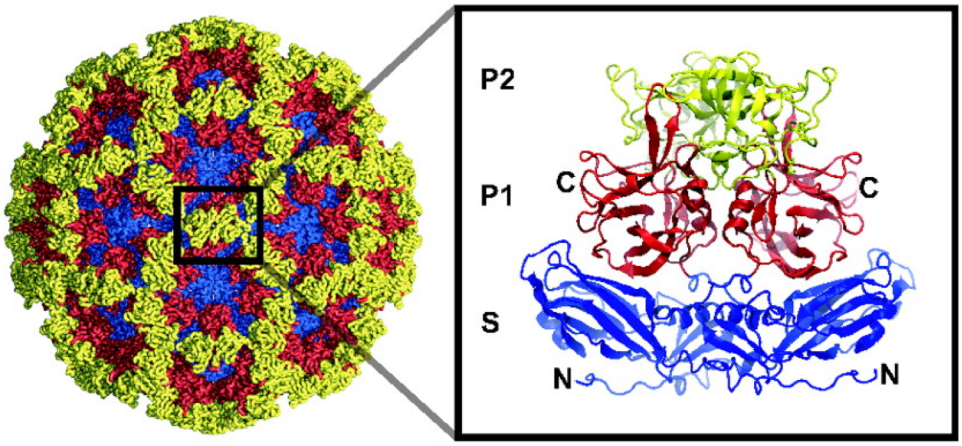

Figure 1-3. Three-dimensional ribbon representation of Norwalk virus. Enlarged is the major capsid protein separated in the shell and protruding domains. From (Choi et al. 2008)

Animal models and *in vitro* cultivation of human noroviruses

Human susceptibility to NoV infection can be genetically determined by the epithelial cell surface and mucosal expression of complex carbohydrate histoblood group antigens (HBGAs) (Reeck et al. 2010). HBGAs are a binding ligand and potential cell surface receptor for NoVs. Secretor status, or the synthesis of specific carbohydrate antigens, has been associated with susceptibility to specific strains (Lindesmith et al. 2003; Nordgren et al. 2016). An animal reservoir has yet to be identified for human NoVs and there still has not been any documentation of zoonotic transmission. This could be because NoVs are very specific to certain species. Instead, chronically infected immunocompromised patients are believed to be the reservoir of emergent NoV strains (Karst & Baric 2015).

Finding a suitable animal model to study human norovirus has been challenging. Scientist have made numerous attempts to induce infection using HuNoVs in gnotobiotic pigs and calves, non-human primates, guinea pigs and mice (Cheetham et al. 2006; Souza et al. 2008; Rockx et al. 2005). Some animals, such as gnotobiotic pigs and new born pigtail macaques develop a serological response, but only to specific strains of HuNoV and maintenance of these animals is extremely costly (Souza et al. 2007; Subekti et al. 2002). The use of gnotobiotic pigs and new born pigtail macaques as a disease model also has other limitations. For instance, pigtail macaques develop a NoV specific IgG and IgM response, but no IgAs, which is very different from humans. Gnotobiotic animals also lack microbiota leading to the lack of a developed immune system. Therefore, the need of an adequate norovirus disease animal model still remains.

For decades, there have been numerous failed attempts to try to establish an *in vitro* system for NoV replication. Initial studies using biopsies and histopathology from experimentally challenged volunteers showed damage to the proximal small intestine, which could suggest this is where the virus replicates (Schreiber et al. 1973). Various human and non-human cell lines, such as human gastric and duodenal cells, with varying cell culture conditions have been tested

to determine which cell lines and conditions can support viral growth (Duizer et al. 2004). Unfortunately, none of these combinations produced *in vitro* replication of HuNoV. Efficient cell culture systems to grow murine NoV have been achieved using murine macrophages and dendritic cells (Jones et al. 2014). Dendritic cells and macrophages from humans susceptible to NoV infection have also been tested, but were incapable of supporting HuNoV replication (Lay et al. 2010). Murine NoVs possess very distinct inherent biological characteristics when compared to HuNoVs. For instance, murine and human NoVs have different cell tropism and disease pathogenesis. B cells have also been identified as a cellular target for murine NoV (Jones et al. 2014). Replication of murine NoV in B cells *in vitro* was stimulated by commensal bacteria which served as a cofactor for replication. Similarly, attachment and infection of HuNoV to human B cells *in vitro* was suggested to also be enhanced by enteric bacteria, but this system was not consistently reproducible (Jones et al. 2014).

Due to these limitations, the development of VLPs has been a valuable asset for NoV research. Capitalizing on the *in vivo* interaction between NoVs and HBGAs, a surrogate neutralization assay was developed to evaluate VLP-HBGA binding or antibody-mediated neutralization of NoV VLPs *in vitro* (Harrington et al. 2002). Studies have also proven that the presence of blocking antibodies in human serum during infection correlates with protection from clinical gastroenteritis (Reeck et al. 2010).

Very recently a novel and successful culture system has been developed that involves the use of human intestinal enteroids (HIEs), which are derived from stem cells in intestinal crypts from human intestinal biopsies (Ettayebi et al. 2016; Costantini et al. 2018). HIEs are able to successfully recapitulate complex human intestinal physiology *in vitro* (Zachos et al. 2016). Interestingly, specific cofactors like bile were found to be necessary for strain specific NoV replication as well as appropriate HBGA expression on the intestinal cells. Most importantly, these studies have confirmed that human intestinal epithelium is a major site of HuNoV replication.

Human immune response to NoV infection

NoVs can be transmitted via fecal-oral route, which can happen by ingesting food or water that has been in contact with contaminated feces, by direct person-to-person contact or by exposure to contaminated fomites or aerosolized vomitus (Vajdy 2008). Following infection, symptoms typically last between 24-48 hours and are usually mild and self-limiting for healthy individuals. Symptoms usually include nausea, vomiting, diarrhea, fever, headaches, abdominal cramping, chills and general malaise. Viral shedding peaks anywhere from 1 to 3 days after the onset of symptoms. From challenge studies, we have learned that infected individuals can have prolonged viral shedding, even after symptoms have resolved, lasting anywhere from 12-56 days (Atmar et al. 2008).

Due to limitations with *in vitro* NoV studies, most of what is known about the human immune response to infection has come from serological studies. Unfortunately, many human challenge studies were conducted before there was knowledge of genetic factors that could predetermine susceptibility to NoV infection. From outbreak studies, we have learned that protective immunity to NoV can be separated in short or long-term immunity, with the latter being slightly controversial. Challenge studies have shown that short-term immunity, about 6 months or less, exists because patients who were re-challenged or re-exposed with the same NoV strain did not become ill (Wyatt et al. 1974). Protection from distinct strains could depend on the degree of antigenic similarity between the initial and subsequent strain of exposure. Other studies have shown that some individuals when re-challenged with the same strain three years later did not develop illness (Johnson et al. 1990). All of this research was also limited by the use of serum, where a mucosal antibody response could have depicted a more accurate representation of what is happening at the site of infection.

Numerous studies have noted the presence of a strong human polyclonal immune response to NoV infection, specifically an increase in immunoglobulin (Ig) alpha (IgA), gamma (IgG) and mu (IgM) antibodies in serum, with IgGs being the predominant isotype (Gray et al.

1994; Iritani et al. 2007; Lindesmith et al. 2015). NoV-specific IgAs have also been found in saliva and stool samples of infected patients (Erdman et al. 1989; Ramani et al. 2015). Antibodies are considered markers of NoV infection and therefore are used for laboratory diagnostic assays like immunoassays and immune electron microscopy.

The interaction between an antibody molecule and its specific antigen depends not only on the sequence and structure of an antigen but also on the sequence and specificity of an antibody. An immunoglobulin molecule consists of a heavy and light chain and each chain is further divided into variable (V) and constant (C) region (Dreyer & Bennett 1965). It was initially believed that each region had independent functions, where the V domain was responsible for affinity and specificity and the C domain determined the antibody isotype, class, half-life and provided effector functions such as complement fixation (Janeway 2001). However, studies with identical V region isotype switch variants have shown that antibody-antigen binding kinetics also are affected by the C region (Pritsch et al. 2000). In accordance with this notion, our own studies suggest that both binding affinity and blockade response to specific strains of NoV VLPs are influenced by the C region, or molecular size of an antibody (Sapparapu et al. 2016).

HuNoV VLPs have been vital in the study of HuNoV evolution and the emergence of new strains (Jiang et al. 1992; Lindesmith, Beltramello, et al. 2012). VLPs have also been used to isolate HuNoV specific antibodies from phage display libraries and murine monoclonal antibodies, but murine Abs do not provide any information regarding the human humoral immune response to infection (Kou et al. 2015; Crawford et al. 2015). The therapeutic potential of mouse monoclonal antibodies is also limited, since they have been shown to induce human anti-mouse antibody responses. On the other hand, when screening phage display Abs, they tend to be Ab fragments, like Fabs or single chain Fv, that bind antigen but do not mediate the function of a full-length Ab or isotype. These Ab fragments must also be converted to full-length Ig molecules which can involve a lot of work.

There has been little progress in understanding individual human NoV-specific

antibodies because of the difficulty in generating human monoclonal antibodies with functional activity. Our laboratory has developed a robust hybridoma platform technology using circulating B cells from convalescent patients to produce monoclonal antibodies. The approach generates hybridoma cell lines from circulating B cells that express naturally occurring and matched heavy and light chain genes. An additional benefit of using this hybridoma technology is that it does not involve the use of any laboratory animals to produce antibodies. Our laboratory has generated thousands of virus-specific B cell lines and mAbs to metapneumovirus, dengue, influenza, and Marburg and more recently to GI.1 and GII.4 NoVs (Alvarado et al. 2018; Sapparapu et al. 2016; Williams et al. 2007; Smith et al. 2013; Thornburg et al. 2013; He et al. 2015).

Norovirus therapeutics and vaccines

NoVs persistence is attributed to many factors, such as the infectious dose being less than 20 viral particles, high levels of shedding, and prolonged shedding even after symptoms have resolved (Teunis et al. 2008). There are currently no licensed vaccines or antiviral agents available to treat or prevent NoV infection. Developing an efficacious vaccine would be critical to reducing disease burden worldwide. NoV vaccine research remains challenging because of the difficulty in culturing the virus *in vitro* and the lack of an adequate small animal model to study this virus, but developing a vaccine would be essential to the prevention and control of NoV infection.

The antigenic and genetic diversity among NoVs also makes developing a broadly protective vaccine extremely difficult. Even though there are no commercially available NoV vaccines, there are several candidates currently under development using VLPs, protruding (P) particles and even a recombinant adenovirus expressing the NoV major capsid protein. One very promising intramuscularly administered bivalent VLP based vaccine candidate, which has been tested in humans and is now in Phase II clinical trials, is based on genotype GI.1 and a

multivalent consensus GII.4 (J. P. Ball et al. 2017). Work is being done to determine the chimeric VLP vaccines tolerability and immunogenicity (Atmar et al. 2016). VLP based vaccines are already in use for other viruses like human papillomavirus and hepatitis B and studies have shown that NoV VLP vaccines can also provide protection against illness and infection (Tegerstedt et al. 2006; Adkins & Wagstaff 1998; Atmar et al. 2011). The route of immunization can also play a vital role in the immune response elicited. Murine VLP immunization studies comparing intramuscular and intranasal immunization concluded that only intranasal immunization induced a mucosal IgA response with high blocking activity, suggesting there could be benefit to using a mucosal route of immunization (Tamminen et al. 2016). The adjuvants used in the vaccines could also enhance the NoV-specific immune response. For instance, in a study in which mice were orally administered VLPs combined with cholera toxin the adjuvant induced higher levels of NoV-specific serum IgG (J. M. Ball et al. 1998).

The NoV P particle based vaccine, which contains only recombinantly expressed NoV protruding domain, was used to immunize mice intranasally and proved to be highly immunogenic inducing antibodies that blocked the interaction between VLPs and HBGAs *in vitro*, but some suggest P particles do not display surface blockade epitopes the way VLPs do (Tan & Jiang 2012). Intranasally administered adenovirus vector-based NoV vaccines have been tested in mice and they induced a IgM, IgG and IgA NoV specific response in serum and in feces, intestinal and respiratory mucosa (Guo et al. 2008). We have also learned that prime-boost vaccination in mice using the adenovirus vector based prime and VLPs to boost enhances the immune response more than VLPs independently or VLP-prime adenovirus-boost combination (Guo et al. 2009). Various factors need to be taken into account as we decide which immunogen can be part of the best NoV vaccine such as cost of production, route of administration and the strain specificity of the elicited immune response.

There are currently no FDA approved therapeutics available to treat NoV infection other than supportive therapy, like oral rehydration, to prevent dehydration. Even though there are no

human NoV antiviral therapies available, viral polymerase inhibitor 2'-C-methylcytidine (2CMC) has been found to be an adequate prophylactic, preventing transmission of murine NoV in mice and can also work as a therapeutic preventing diarrhea and reducing viral shedding (Rocha-Pereira et al. 2016). Nitazoxanide, a broad spectrum antimicrobial agent, has been used in a randomized double-blind placebo controlled viral gastroenteritis clinical trial and it was shown to significantly reduce the time to resolution of symptoms for patients with norovirus (Rossignol & El-Gohary 2006). Nitazoxanides' mechanism of action against viruses remains to be elucidated as it is a thiazolide, drugs typically used against protozoa and anaerobic bacteria (Fox & Saravolatz 2005).

CHAPTER II

NOROVIRUS GI.1 BINDING AND BLOCKING HUMAN MONOCLONAL ANTIBODIES

Introduction

Even though Norwalk virus was initially identified over four decades ago, our knowledge of the human monoclonal antibody response to infection still remains limited. Human volunteer challenge studies have shown that the presence of NoV-specific antibodies in serum that can block VLPs from binding to HBGAs *in vitro* correlate with lower risk of illness (Reeck et al. 2010). More recent challenge studies have identified pre-challenge levels of NoV-specific salivary IgA and memory IgG B cells as a correlate of protection against gastroenteritis (Ramani et al. 2015). In July of 2015, a study determined that human serum IgA had GI cross-strain blockade potential (Lindesmith et al. 2015). Even though they concluded that Ab epitopes are more important in determining protection from infection than Ab titer or avidity, they did not map any Ab epitopes or determine whether Ab epitopes are influenced by Ab isotypes (Lindesmith et al. 2015). Soon after, a study found that human mucosal IgA titers correlated with protection from GI.1 infection (Ramani et al. 2015). A similar conclusion had been reached in 2003 by a group who suggested that an early post-exposure IgA response in patients who are genetically susceptible to Norwalk virus correlates with protection from infection (Lindesmith et al. 2003). Both studies suggest that IgAs may play an important role in protecting humans from HuNoV infection, but how isotype can influence mAb function or binding was yet to be determined.

In this chapter, I describe the isolation of a panel of fourteen human mAbs, seven dimeric IgAs (dIgAs) and seven IgGs, specific to NoV GI.1 VLPs. These mAbs were isolated using B cells from two otherwise healthy adults who participated in a GI.1 virus challenge study (Bidawid et al. 2003). Binding to GI.1 VLPs and the ability to block VLPs from binding to

synthetic glyans for each mAb was also tested. According to our binding assay, all the IgGs bound more avidly to the GI.1 VLPs in comparison to the IgAs. Surprisingly, when blocking $IC_{50,}$ half-maximal inhibitory concentration, and binding $EC_{50,}$ half-maximal effective concentration, for each mAb were evaluated together, meaning each blocking IC_{50} was divided by the corresponding mAb binding EC_{50}, the results suggested that dIgAs as a class blocked more effectively. To determine if this phenomenon was an isotype specific trend or instead dependent on the mAbs binding specificity, I recombinantly cloned and expressed isotype-switch variants for a selection of the initially isolated mAbs to test the effect of the constant domain on binding and blockade activities. These results were critical and allowed us to conclude that IgAs are more potent than IgGs in blocking GI.1 NoV VLPs from binding to histo-blood group antigens.

To obtain a clearer understanding of where the isolated mAbs could be binding a series of epitope mapping experiments were performed. All of the mAbs bound to nonlinear epitopes on the GI.1 major capsid protein and most of them bound to one major antigenic site. Using X-ray crystallography, one of the isolated dIgAs, 5I2, was crystallized as a Fab in complex with the GI.1 P domain. Three-dimensional characterization resulted in the discovery of a novel antigenic and neutralizing site on the GI.1 P domain.

I would like to acknowledge Dr. Gopal Sapparapu, one of our laboratory alumni, and Dr. Rita Czakó, from Dr. Mary Estes' group, for conducting initial binding, blockade and mapping experiments and Dr. Sreejesh Shanker, from Dr. V. Venkataram Prasad's group, for completing the three-dimensional characterization of NoV 5I2 IgA.

Isolation and characterization of anti-NoV GI.1 VLP human mAbs

Our first goal was to isolate IgGs and IgAs specific to GI.1 VLPs that could also inhibit GI.1 VLPs from binding to H3-PAA-glycans *in vitro*. To do so, we first isolated peripheral blood

mononuclear cells (PBMCs) from two donors who had been previously challenged with live GI.1 NoV. The PBMCs were transformed using Epstein-Barr virus (EBV) and the lymphoblastoid cell line (LCL) supernatants were screened for binding to GI.1 VLPs by enzyme-linked immunosorbent assay (ELISA) and blockade potential using a surrogate neutralization assay. Wells containing secreted IgG or IgAs Abs with binding and blockade activity were expanded. Binding and blockade activity was tested once again after expansion to obtain the frequency of IgGs or IgAs present in the LCLs. To determine the isotype of the mAbs tested, we used different polyclonal secondary antibodies, anti-IgG (γ-specific) or anti-IgA (α-specific). Of the antibodies that bound to the VLPs, a higher proportion of them were IgGs. However, the proportion of GI.1 VLP binding antibodies that also blocked the VLPs from binding to the synthetic glycan *in vitro* was higher for IgAs than IgGs (Figure 2-1). This data suggests that IgAs are highly over-represented in the repertoire of antibodies with GI.1 VLP blockade potential.

Wells containing binding and blocking antibodies were electro-fused with a human-mouse myeloma cell line to generate hybridoma clones. We were able to isolate a panel of fourteen monoclonal antibodies, seven IgGs (1A8, 2L8, 3I23, 4E7, 4I23, NV1 and NV48) and seven IgA (2J3, 3I3, 4B19, 4C10, 5I2, NV41and NV56), ten of the antibodies were from Donor 1 and four were from Donor 2. The isotype of each mAb was confirmed by ELISA. I resolved selected purified mAbs on a SDS-PAGE gel to verify their molecular weight, which confirmed that all IgAs were dimeric IgAs (Figure 2-2).

In order to appropriately compare binding and blockade function between the isolated dIgAs and IgGs, we normalized the concentration of antibodies used for each assay according to differences in molarity of binding sites. Graphed in Figure 2-3 are the binding and blockade absorbance values for each mAb. All of the isolated dIgA antibodies appear to have lower affinity for binding to the GI.1 VLPs when compared to the IgGs, but there was no isotype specific trend in the blockade assay. This distinction between the isotypes suggests that even

lower affinity IgAs can provide potent blockade activity.

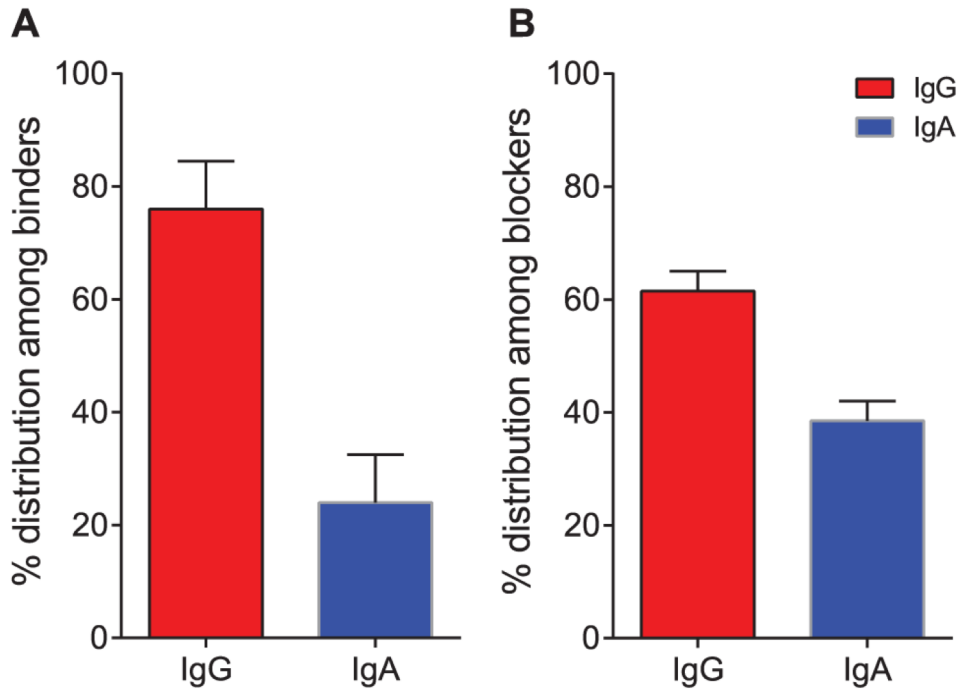

Figure 2-1. Distribution of binding and blocking antibodies by isotype. EBV-transformed B cell supernatants were screened from both donors. A) Total number of binding antibodies were compared IgGs or IgAs specifically. **B)** Of the number of total binding antibodies by isotype the percent distribution of blocking antibodies was calculated.

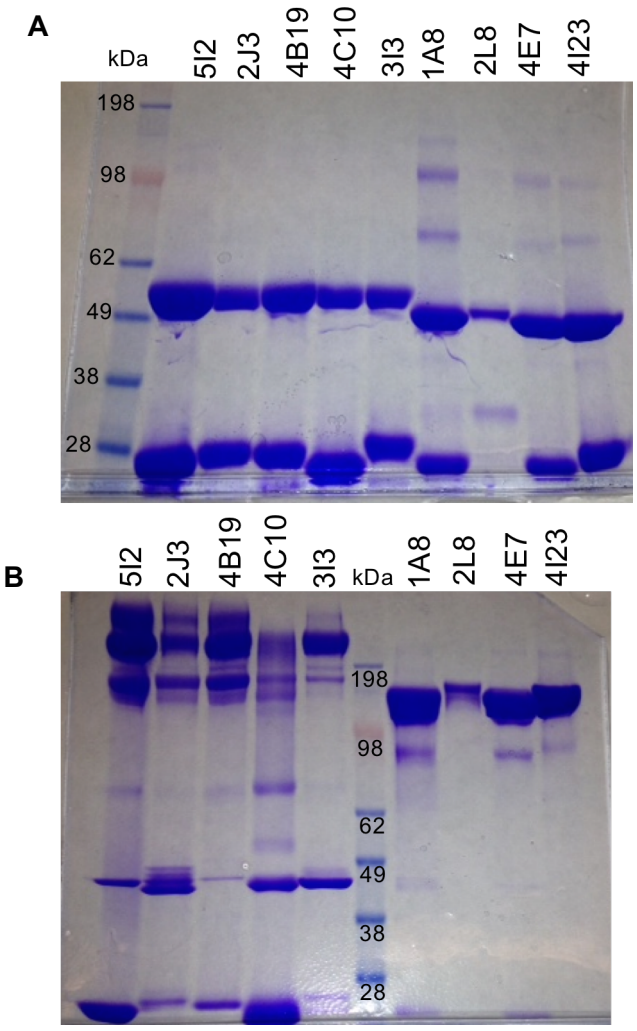

Figure 2-2. Verification of molecular assembly of Donor 1 hybridoma-derived mAbs. Antibodies were purified using affinity column chromatography and resolved on a SDS-PAGE gel under (Panel A) reducing, denaturing conditions or (Panel B) non-reducing conditions and stained with Coomassie Blue reagent.

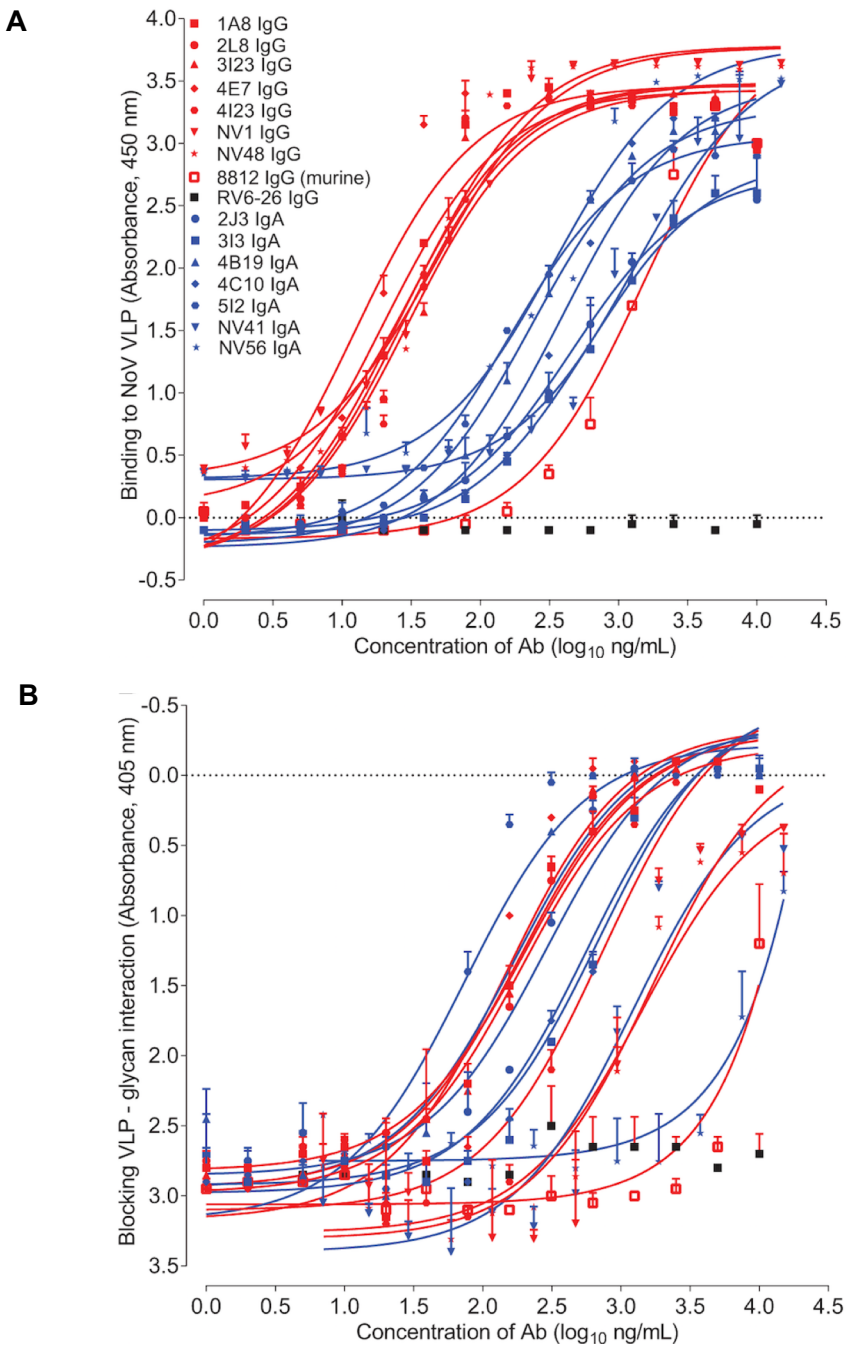

Figure 2-3. Binding and blockade activity of purified mAbs. Purified IgGs are graphed in red, purified IgAs are in blue and control murine mAbs in black. A) Binding was tested by indirect ELISA using GI.1 VLPs as an antigen. All of the IgGs had lower binding EC_{50}s compared to IgAs. **B)** Blockade function was tested using H3-PAA synthetic glycans and GI.1 VLPs.

Specificity and mapping of anti-NoV GI.1 VLP human mAbs

To determine the specificity of the isolated mAbs, VLPs for selected genogroup I, GI.2, GI.4, GI.6, GI.7, GI.8 in addition to GI.1, and a genogroup II, GII.4, NoV strain were used as antigen for an indirect ELISA. Antibodies 1A8, 2J3, 2L8, 3I3, 3I23, 4B19, 4C10, 4E7, 4I23 and 5I2 were all specific to GI.1 VLPs as is seen in Figure 2-4A. NoV GI.1 P domain dimers were also used as antigen to determine whether the mAbs bound to the protruding domain or shell domain which would be included on the complete VLP, but not the P domain dimer. Graphed in Figure 2-4B are the absorbance values for the ten mAbs when bound to GI.1 VLPs, GI.1 P domain dimers and two additional VLPs with a mutated VP1 to achieve either complete removal of the P domain, CT303, or a point mutation in the HBGA binding domain, W375A. All the isolated mAbs bound to the GI.1 P domain and therefore none bound to the CT303 mutant VLP. Antibodies 3I23 and 4I23 did not bind to the W375A VLP suggesting these residues could be essential for their binding. Three representative mAbs, 2L8, 4I23 and 5I2, were used to assess their specificity to block VLP binding to different glycans, H types 1, 2, 3, tri-A and Le(y). The tested mAbs all reduced GI.1 VLP binding to all of the tested glycans, except for 2L8 which had reduced blockade activity towards H type 3 tri-A and Le(y) (Figure 2-4C).

Identification of potential binding epitopes for the ten selected mAbs was first determined by comparing binding by western blot to nondenatured nonreduced or denatured reduced VLPs. Two antibodies previously mapped to linear or nonlinear epitopes, 3901 and 8812, were used as controls. All 10 mAbs and murine mAb 8812 bound to nondenatured nonreduced VLPs suggesting they bind to nonlinear epitopes on the major capsid protein of GI.1 NoV (Figure 2-5A). As expected only the control mAb 8812 bound to denatured reduced VLPs (Figure 2-5B).

The isolated mAbs were also competed in a pairwise manner against one another in a competition-binding ELISA to see if they were all binding to the same potential antigenic site on the major capsid protein. According to the binding data, most of the mAbs compete against each other and therefore could be binding to one major epitope. Two antibodies, 2L8 and 3I23,

still bound in the presence of capture antibodies 4B19, 4C10, 4I23 and 5I2 (Figure 2-5C). This could mean that all ten antibodies are likely binding to at least three distinct, but likely overlapping, epitopes on the major capsid protein.

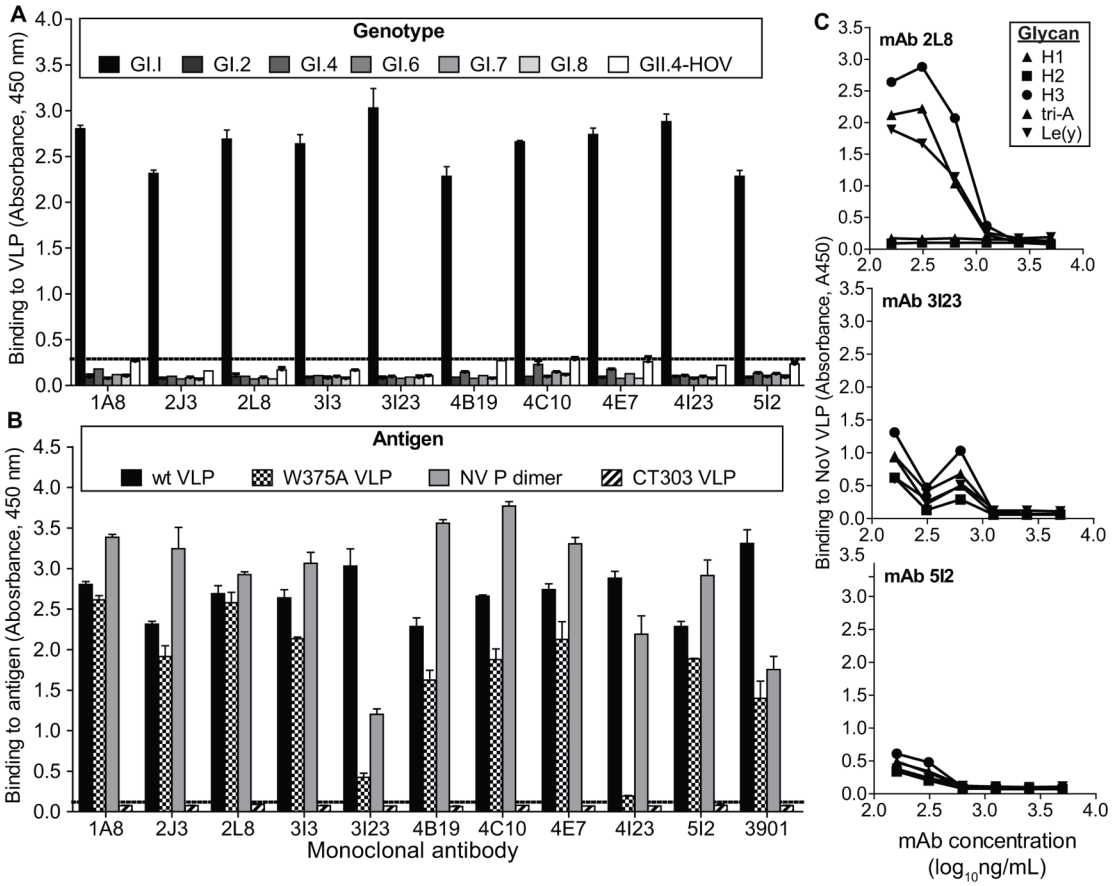

Figure 2-4. Specificity of isolated anti-GI.1 mAbs. All specificity was tested by ELISA with 20µg/mL of mAb. A) Binding to GI.1, GI.2, GI.4, GI.6, GI.7, GI.8 and GII.4-HOV. **B)** To specifify what subdomain the mAbs could be binding to a GI.1 P domain dimer was used, wt GI.1 VLP, a GI.1 mutatu VLP without the P domain (CT303) and GI.1 mutant with the HBGA binding domain ablated (W375A) were used as antigens. **C)** Different potential GI.1 VLP glycan ligands, H1, H2, H3, tri-A and Le(y) were used in vitro in independent blockade assays to determine the ligand specificity of the mAb-mediated inhibition of VLP binding.

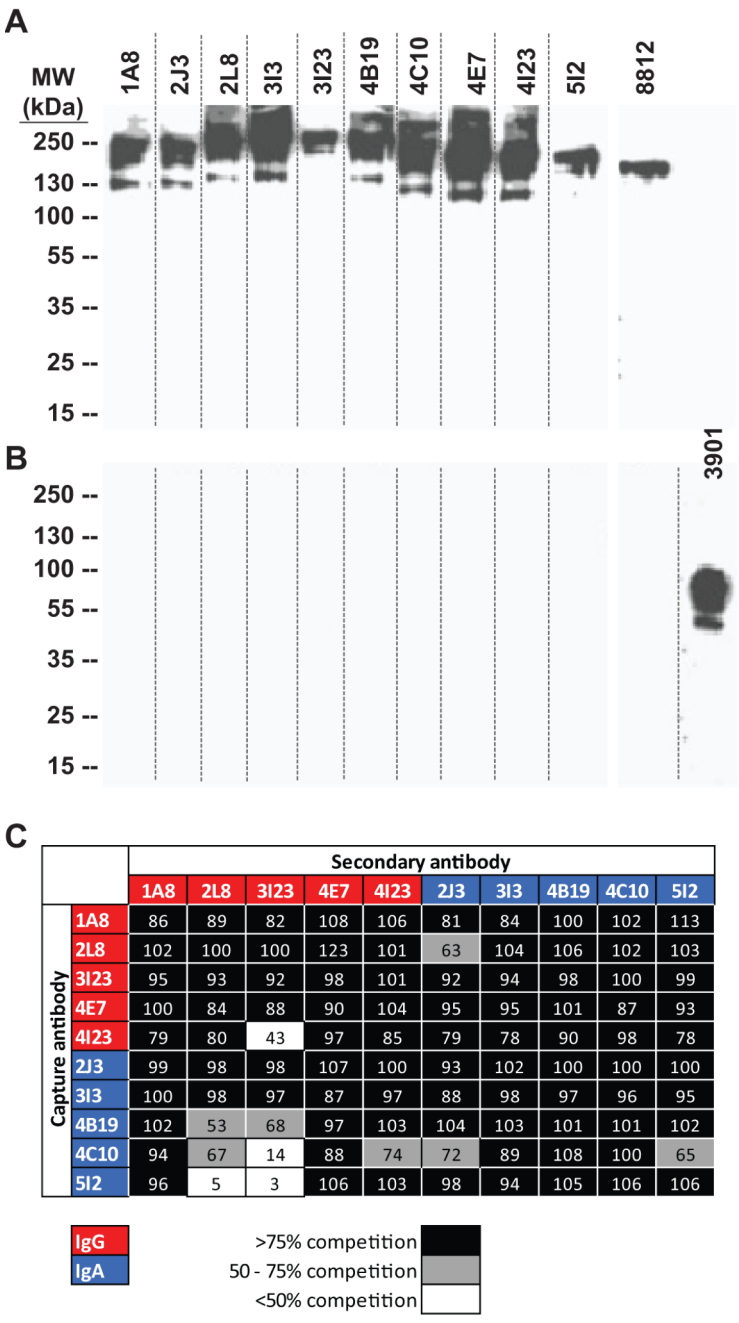

Figure 2-5. Eptiope recognition by anti-GI.1 mAbs. GI.1 VLPs were resolved on SDS-PAGE gel under either. A) nonreducing and non denaturing conditions or **B)** reducing and denaturing conditions. The gels were then transferred to membranes and probed with the individual anti-GI.1 mAbs, murine mAb 8812, a nonlinear eptiope control, and murine mAbs 3901, a linear epitope control. **C)** Eptiope binning by competition ELISA identify three potential binding groups for the isolated mAbs.

Structural basis of neutralization of NoV GI.1

In collaboration with Dr. B.V. Venkataram Prasad's laboratory, we also used X-ray crystallography for three-dimensional characterization of isolated IgA 5I2 Fab in complex with GI.1 P domain. I used the variable domain sequence of the 5I2 light and heavy chain and cloned them into recombinant expression Fab and kappa vectors for transfection and expression. Using BLI, biotinylated GI.1 P domain was immobilized on a streptavidin biosensor and titrated against serial dilutions of 5I2 Fab. The results showed that 5I2 Fab binds to the GI.1 P domain with an affinity constant K_D of 20.5 nM, and rate constants K_{on} of 2.04 x 10^5 M^1s^{-1} and K_{off} of 4.01 x 10^{-3} s^{-1} for association, which means there is a tight interaction between the P domain and 5I2 Fab. The crystals of complex GI.1 P domain and 5I2 Fab diffracted at ~2.3Å and the structure was determined by Dr. Sreejesh Shanker in the space group $P6_522$, with one P domain-Fab complex in the crystallographic asymmetric unit. The structure of the complex was determined using molecular replacement techniques and refined with a final R_{fac} and R_{free} values of 18% and 21%, respectively. The GI.1 P domains related by crystallographic 2-fold symmetry associate to form a dimer, as typically found on the NoV capsid and other NoV P domain available structures, with each of the dimeric subunits interacting independently with a 5I2 Fab antibody. The 5I2 Fab also appears to recognize and interact with a conformational epitope on the P2 subdomain of the major capsid protein (Figure 2-6A). Superposition of the unbound and Fab 5I2-bound P domain structures revealed that 5I2 Fab binding does not modify the overall structure of the P domain. The 5I2 Fab binding instead induces local conformation changes in some of the P domain loop regions. The structure also showed that the 5I2 Fab complementarity determining region (CDR) light chain 1 plays a leading role in antigen recognition.

Three surface exposed loops on the GI.1 P2 subdomain interact with 5I2 Fab. Two of the loops had been previously identified, T(377-386) and U(394-405), and a new loop identified by our studies, Q(345-354) form the conformational 5I2 binding epitope (Shanker et al. 2014;

Kubota et al. 2012) (Figure 2-6B). The 5I2 Fab paratope is made up of two of the light chain CDRs, CDRL1 and CDRL3, and a heavy chain, CDRH3. Binding of the 5I2 Fab also induces conformational changes in the GI.1 P domain U loop and a change in the orientation of the H381 sidechain (Figure 2-6C).

Structural studies revealed how 5I2 Fab inhibits GI.1 VLPs from binding to HBGAs. Comparison between the 5I2 Fab-P domain complex and HBGA bound to the P domain reveal that 5I2 Fab binds near the primary HBGA binding site on the P domain, but does not disrupt the structural integrity of the glycan binding site. Therefore, it can be concluded that 5I2 Fab neutralizes or blocks binding of the GI.1 VLPs to HBGA through steric hindrance. GI.1 P domain residues involved in binding to 5I2 Fab are also poorly conserved among other genogroup I strains, which could explain why 5I2 is specific to NoV GI.1.

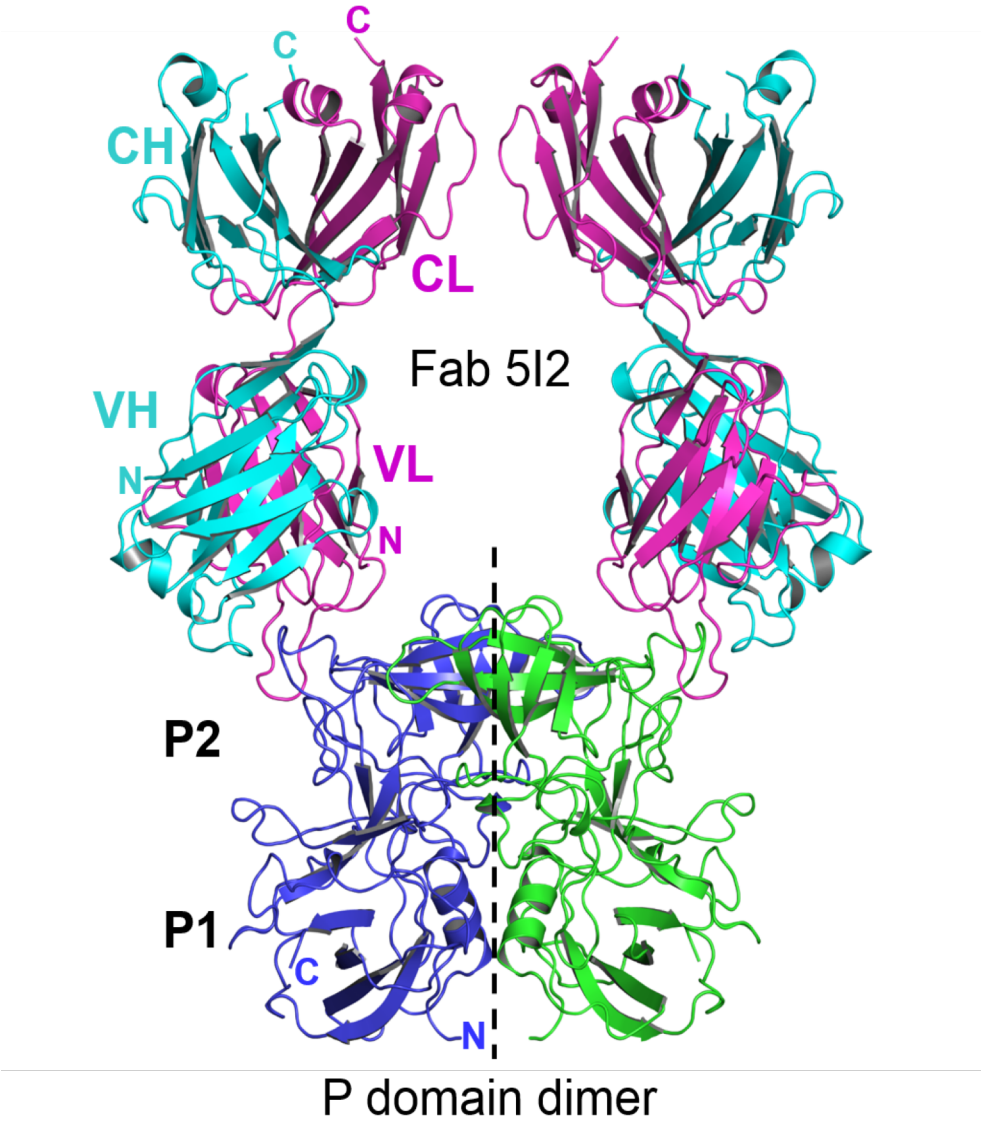

Figure 2-6. Ribbon diagram of human mAb 5I2 Fab bound to NoV GI.1 P2 subdomain. 5I2 Fab, depicted in cyan (heavy chain) and cyan (light chain), binds to a conformational epitope on the NoV GI.1 P2 subdomain, in blue and green. Two subunits are included in the diagram. The dashed black line indicated the the axis of symmetry. Figure credit: Sreejesh Shanker (Prasad laboratory)

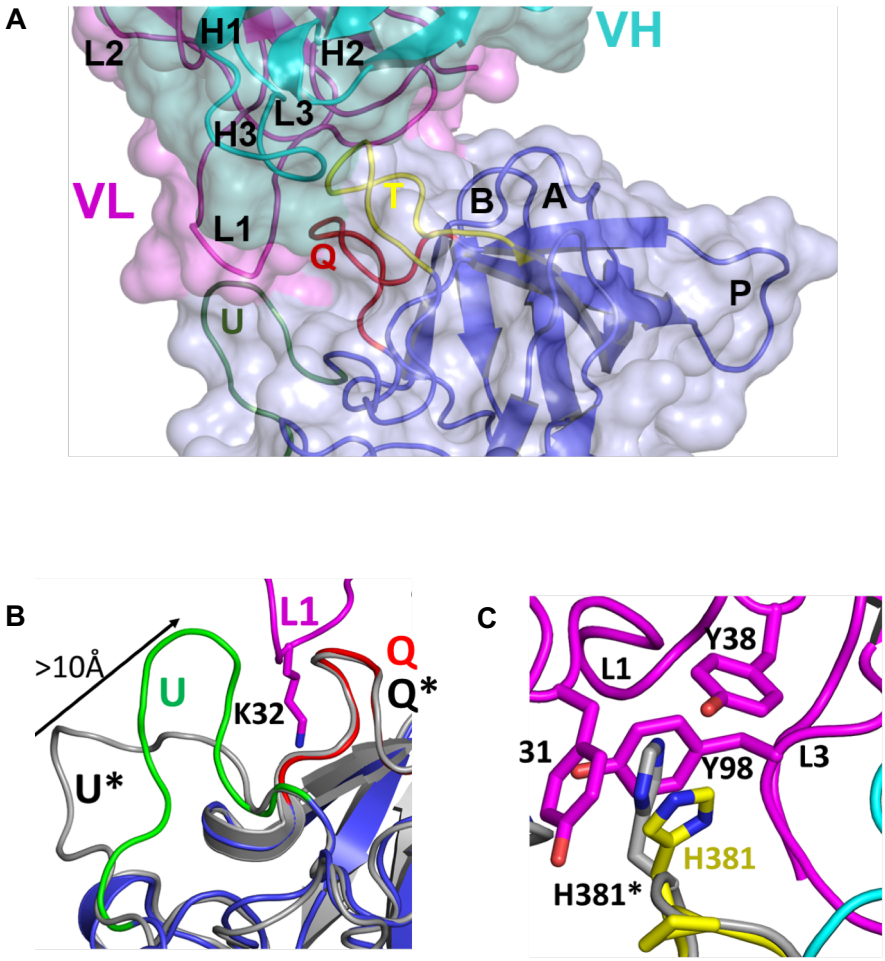

Figure 2-7. Close-up view of the interaction between 5I2 Fab and the NoV GI.1 P2 subdomain. A) Detailed view of 5I2 Fab, heavy chain in cyan and light chain in magenta, with heavy chain CDRs H1-H3 and light chain CDRs L1-L3. The six loops on the P domain, A, B, P, T and U, are also labeled. Three of the loops, T (yellow), Q (red) and U (green) interact with 5I2 Fab. **B)** Superposition of the 5I2 Fab in complex with GI.1 P2 domain and GI.1 VLP structure (PDB ID 1IHM; in grey). The Fab induces conformation changes on the U loop of the P2 subdomain. **C)** Binding of 5I2 Fab also induces a flip in the orientation of the side chain H381 (yellow) when compared to the GI.1 VLP structure (grey). Figure credit: Sreejesh Shanker (Prasad laboratory)

The role of antibody isotype in binding and blockade of GI.1 VLPs

Initial binding and blockade studies using the isolated panel of human mAbs identified dIgA mAbs as the more potent than IgGs in blocking the binding of GI.1 VLPs from binding to synthetic H3-PAA glycans *in vitro*. To verify if this observation was attributable to isotype or to the unique variable domain sequence of each mAb isolated, I engineered isotype-switch variants for each mAb. First, the variable heavy and light chain for each mAb was sequenced and then synthesized cDNAs encoding each variable domain was cloned into corresponding heavy and light immunoglobulin chain expression vectors for mammalian cell recombinant expression. All heavy chain variable sequences were cloned as α and γ chains and the light chains were cloned into λ or κ chains. To recombinantly express dimeric IgA, I co-expressed joining chain along with the heavy and light chains. I verified the molecular weight for recombinantly expressed IgGs, monomeric IgAs and dimeric IgAs and assembly of purified mAbs using electrophoresis on a SDS-PAGE gel under non-reducing conditions (Figure 2-8A). Following normalization according to molarity of the binding sites, I tested binding and blockade function of all recombinantly expressed mAbs. Representative blockade curves are included in Figure 2-9. I calculated the EC_{50} and IC_{50} at which binding or blocking occurred. To compare between the molecular forms of each antibody, I calculated the ratio of blocking IC_{50} to binding EC_{50} for each Ab (Figure 2-8B). If an antibody has a lower ratio, it suggests that less antibody is needed inhibit the VLPs from binding to their receptor. For the antibodies tested, both IgAs, in monomeric and dimeric form, had lower blocking-to-binding ratios in comparison to IgGs. Surprisingly, the ratio for the monomeric IgAs was lower than for IgGs, despite both antibodies having similar molecular weight. This could mean that IgAs might be better at blocking GI.1 VLPs from binding to glycans not only because of their potential to make larger polymeric antibodies with the ability to sterically hinder the VLPs, but also because of features that are also present on their monomeric form.

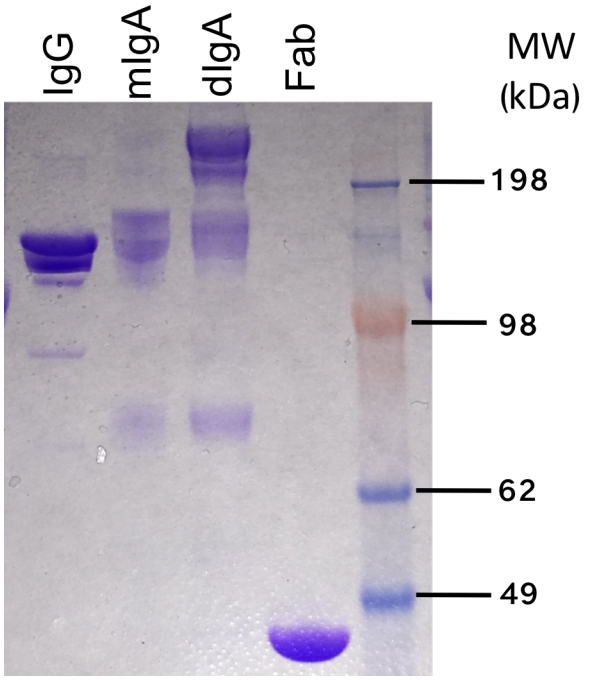

Figure 2-8. Verification of recombinant mAb expression binding and blockade activity for anti-Gl.1Abs. A) Recombinant mAbs were resolved on a SDS-PAGE gel by molecular weight under non-reducing conditions. A representative image of purified mAb 5I2 recombinant IgG, monomeric (mIgA) and dimeric (dIgA). **B)** Recombinantly expressed mIgA, dIgA and IgG forms were tested for 3I23, 4I23, 2J3, 4C10 and 5I2 antibodies. All recombinant antibodies were normalized by valency.

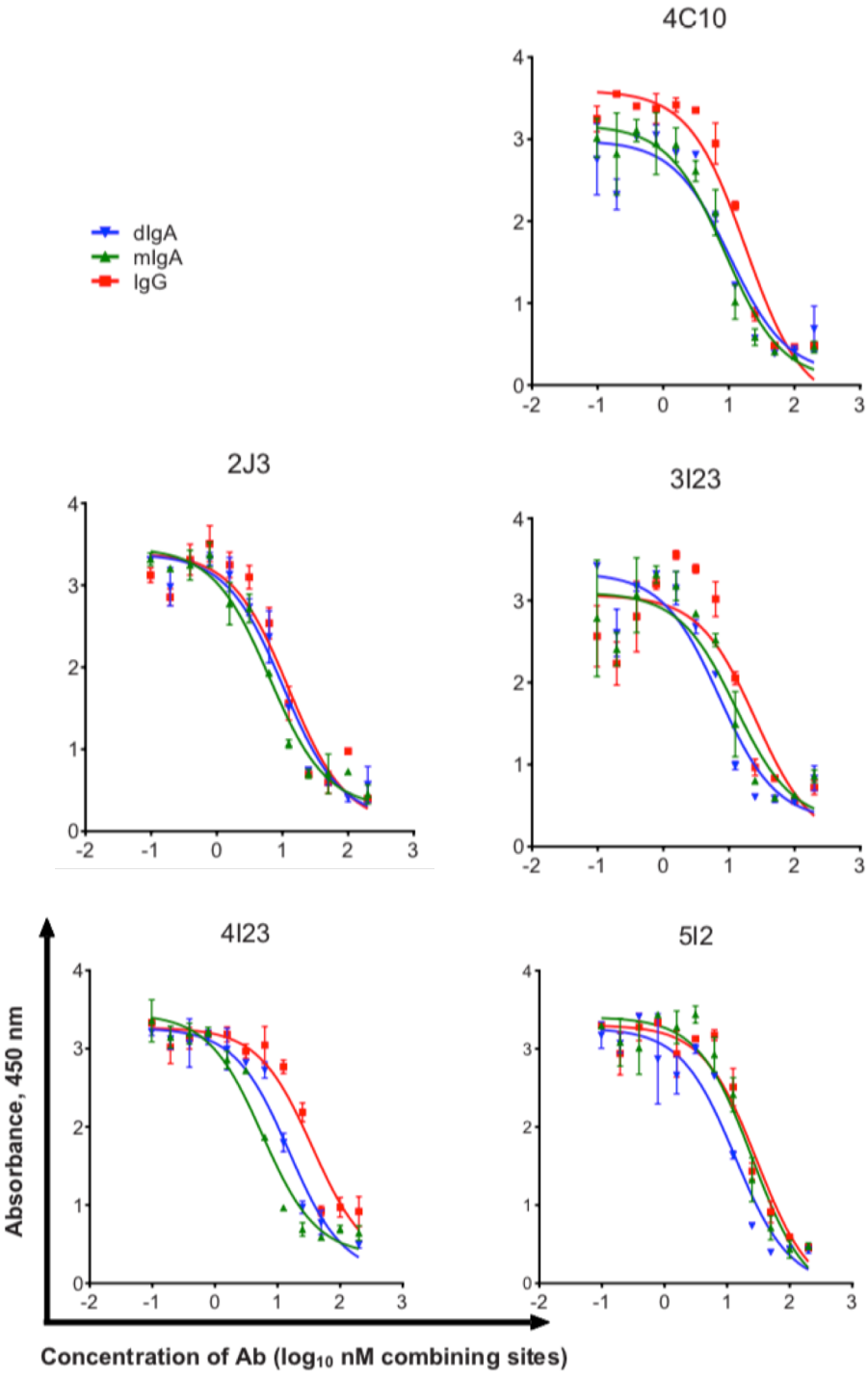

Figure 2-9. Representative blockade curves for recombinantly expressed isotype switch variants. Blockade activity for recombinantly expressed and purified IgG, monomeric (mIgA) or dimeric (dIgA) of GI.1 VLPs was tested.

Materials and methods

Donors

PBMCs were isolated from heparinized blood by density gradient centrifugation using Ficoll-Histopaque from two donors who had been orally challenged with live GI.1 norovirus 1-2 years before having their blood drawn for our study. Successful infection was determined by detection of viral genome and antigen in feces by RT-qPCR and ELISA, respectively. Donor serum was also tested and demonstrated a greater than four-fold increase in antibody levels as tested by ELISA and HBGA blocking activity.

Production and purification of NoV VLPs

VLPs were recombinantly expressed and purified representing different norovirus genogroups (GI and GII) and genotypes (GI.1, NC_001959; GI.2, FJ515294; GI.4, GQ413970; GI.6, KC998959; GI.7, JN005886; GI.8, GU299761; GII.4; EU310927) as previously described (Kou et al. 2015). Briefly, the major and minor capsid proteins, VP1 and VP2, sequences were cloned into recombinant baculovirus expression vectors and were expressed in SF9 insect cells. NoV VLPs were then purified from culture supernatants on a cesium chloride gradient (Jiang et al. 1992). VLPs were negatively stained (1.0% ammonium molybdenate (Sigma-Aldrich; St. Louis, MO), pH 6.0) on carbon coated grids and used in conjunction with electron microscopy to confirm the structural integrity and purity of the VLP preparations. Antigenicity of the VLPs was confirmed by Western blot. We also generated a GI.1 VLP mutants, which were designated as CT303, in which the P domain was deleted by mutagenesis of the VP1 gene construct (Bertolotti-Ciarlet et al. 2002). We prepared a second mutated GI.1 VLP with a point mutation, W375A, known to eliminate HBGA binding(Choi et al. 2008).

Generation of EBV-LCLs and hybridomas secreting NoV GI.1 specific mAbs

To transform B cells, we infected them with EBV that was released from a B95.8 cotton top tamarin lymphoblastoid cell line and plated into 384-well plates. Infection was done in the presence of 2.5 μg/mL CpG (phosphorothioate-modified oligodeoxynucleotide ZOEZOEZZZZZOEEZOEZZZT, Life Technologies), a TLR agonist, 10 μM Chk2 inhibitor [Chk2i] (Sigma), 10 μg/mL cyclosporine A (Sigma). After 7 days, cells from one 384-well culture plate were expanded into four 96-well culture plates containing CpG, Chk2i and irradiated heterologous human PBMCs to serve as feeder layers to stimulate the growth of LCL clusters. After an additional 3 days of culture, the supernatants were screened for binding to NoV GI.1 VLPs by ELISA or for the inhibition of binding to synthetic in a blockade assay.

Cells from wells with desired binding and blockade activity were electrofused with HMMA2.5 myeloma cells. The fused cells were then cultured in a selective medium using 100 μM hypoxanthine, 0.4 μM aminopterin, 16 μM thymidine (HAT Media Supplement, Sigma HO262), and 7 μg/mL ouabain (Sigma O3125) and incubated for 14–18 days before screening supernatants for antibody production by ELISA. Cells from the positive wells were biologically cloned by sorting single cells into 384-well plates using a FACSAria III fluorescence-activated cell sorter (Becton Dickinson), cultured for about 14 days and screened for antibody production once again.

VLP binding assay

To characterize the binding of LCL supernatants or purified mAbs we used ELISAs. Binding of LCLs was tested by using 5 μL of supernatant from each well of the 384-well plate of transformed B cell cultures and adding it to microplates (Nunc) that had been previously coated with 1 μg/mL NoV GI.1 VLPs at 4°C overnight and blocked with 5% nonfat dry milk 1XDPBS with 0.05% Tween-20 for 1 hour and 2% goat serum at room temperature. Purified mAbs were

serially diluted in 1XDPBS and added to the microplates. The bound antibodies were detected using alkaline phosphatase conjugated goat anti-human κ or λ chain antibodies (Southern Biotech). To compare binding between different classes of antibodies, IgGs in comparison to IgAs, the concentrations of antibodies were adjusted to normalize for the number of antigen binding sites (e.g. Fab = 1; IgG = 2; mIgA = 2 or dIgA = 4) before being used in ELISA. To determine the mAb genotype of each antibody, binding was determined by ELISA, as described above, with the following modifications: VLPs were coated at 10 µg/mL and antibodies were used at a concentration of 20 µg/mL. Plates were developed using ultra-TMB reagent (Pierce ThermoFisher; Rockford, IL), following the manufacturer's protocol, and optical density as read at 450 nm using a SpectraMax M5 plate reader.

VLP-carbohydrate binding antibody blockade assay

Due to the limitations with *in vitro* replication of live NoV, a surrogate system was devised to measure neutralization. This system measures the disruption of interaction between VLPs and HBGAs on microplates. Human monoclonal antibodies can be used to inhibit the VLP-HBGA interaction. Previous studies have also shown that pre-existing titer of HBGA blocking antibodies is correlated with protection from NoV gastroenteritis (Reeck et al. 2010; Atmar et al. 2011). In the blockade assay, biotin-polyacryamide (PAA)-blood group antigen conjugates (Glycotech, Rockville, MD) were first coated on neutravidin-coated plates (Thermo Scientific). For blockade studies with mAbs, VLPs were mixed with serial dilutions of each antibody, and the complexes were added to the glycan-coated microtiter plates. The relative amount of VLP bound to HBGAs was determined using rabbit anti-NoV antiserum followed by horseradish peroxidase-conjugated goat anti-rabbit (Southern Biotech). For blockade using LCL supernatants, 50 µL of 1:10 diluted supernatants were mixed with NoV GI.1 VLPs and the complexes were added to H3-PAA (Glycotech, Rockville, MD) immobilized on neutravidin-

coated plates. We tested mAbs for inhibition of binding of NoV GI.1 VLPs with a variety of biotin-PAA-HBGA ligands, including H type 1 (H1-PAA-biotin), H type 2 (H2-PAA-biotin), H type 3 (H3-PAA-biotin), A trisaccharide (tri-A-PAA-biotin), and Lewis(y) (Le(y)-PAA-biotin) (Glycotech, Rockville, MD). Plates were developed using ultra-TMB reagent (Pierce ThermoFisher; Rockford, IL), following the manufacturer's protocol, and optical density as read at 450 nm using a SpectraMax M5 plate reader.

NoV GI.1 P domain dimer binding assay

Recombinant P domain dimeric protein was prepared and purified as previously described (Choi et al. 2008). Briefly, a NoV GI.1 P domain construct was expressed in *E. coli* (Novagen) and purified by affinity chromatography, followed by size exclusion chromatography. We tested binding of each of the mAbs to the NoV GI.1 P domain dimer by ELISA, using the same protocol for the VLP binding assay.

P domain-Fab 5I2 complex formation and crystallization

Purified GI.1 P domain and recombinantly expressed 5I2 Fab were mixed in a 1:1 molar ratio in the P domain storage buffer and incubated for 2-4 hours at 4°C. The mixture was run through the S75pg 16/60 gel filtration column and the peak, believed to be corresponding to the complex, was collected. The complex eluted at a molecular weight of approximately 160 kDa corresponding to a NoV GI.1 P domain dimer bound to two 5I2 Fab molecules. The molecular weight was also confirmed on a SDS-PAGE gel. NoV GI.1 P domain-5I2 Fab complex crystallized in a buffer containing 0.2M sodium formate, 0.1M Bis Tris propane, pH 6.5 and 20% w/v PEG3350. The first crystals obtained were small and diffracted to ≥ 3.5Å. To obtain larger well diffracting crystals, crystallization conditions were optimized based on ionic strength, pH and precipitant concentrations, and microseeding technique. In 1- 2 weeks, crystals measuring 0.1-0.2 mm were obtained. The crystals were soaked in 20% glycerol as cryoprotectant followed

by flash freezing in liquid nitrogen.

Crystal diffraction, data collection and structure determination

Diffraction data for the NoV GI.1 P domain-5I2 Fab crystals were collected on the 5.0.1 beamline at Advance Light Source Berkeley. IMOSFLM was used to process diffraction data(Battye et al. 2011). Space group was confirmed using POINTLESS program incorporated in the PHENIX suite (Adams et al. 2002). An initial electron density map was obtained by molecular replacement using the previously published GI.1 P domain structure (PDB ID: 2ZL5) as the starting model using program PHASER in the CCP4i suite (McCoy et al. 2007) (Collaborative Computational Project, Number 4 1994). The solution from PHASER showed extra electron density for the bound Fab molecule. PHASER was then rerun using the P domain structure (PDB ID: 2ZL5) and an additional neutralizing Fab structure (PDB ID 4RQQ) as starting models to resolve the Fab density(Sok et al. 2014). This was followed by ab-initio automated model building and solvent addition using AUTOBUILD to reduce model bias (Terwilliger et al. 2008). Additional model building was carried out using iterative cycles of refinement and model building based on the F_O-F_C difference maps. The programs phenix.refine and Coot were used throughout structure determination and refinement (Emsley & Cowtan 2004). Program PyMOL was used for generating the final figures. NoV GI.1 P domain-5I2 Fab interactions were analyzed using COOT and LIGPLOT with donor to acceptor distances between 2.6 Å and 3.3 Å for hydrogen bonding interactions (Wallace et al. 1995). The buried surface area of the interaction was calculated using PISA server.

Sequence analysis of antibody variable region genes and molecular engineering of recombinant antibody variable gene domains

To amplify the genes encoding the heavy and light chain variable domain sequences we used the total RNA that was extracted from each individual hybridoma line. First-strand cDNA

synthesis and RT-PCR were done with gene-specific primers using the OneStep RT-PCR kit (Qiagen), according to the manufacturer's protocols. The following thermal cycling parameters were used: 50 °C for 30 min, 95 °C for 15 min, 39 cycles of (94 °C for 1 min, 55 °C for 1 min and 72 °C for 1 min) followed by a final extension step for 10 min at 72 °C. PCR products were purified using Agencourt AMPure XP magnetic beads (Beckman Coulter) and sequenced directly using an ABI3700 automated DNA sequencer. Heavy chain or light chain antibody variable region sequences were analyzed using the IMGT/V-Quest program (Brochet et al. 2008).

The nucleotide sequences of variable domains were optimized for mammalian expression and synthesized (Genscript) for expression and purification of recombinant forms of each antibody. The heavy chain fragments were cloned as EcoRI/HindIII fragments into pML-huCG1 or pML-huCA1 vectors for expression of γ1 or α1 chains, respectively (McLean et al. 2000). The light chains were cloned as BglII/NotI fragments into pML-huCk or pML-huCL vectors for κ or λ chains according to their corresponding hybridoma light chain.

Production and purification of antibodies

Hybridoma clone cells were cultured in serum-free medium, Hybridoma SFM (Life Technologies), for 21 days for antibody expression. Recombinant antibodies were expressed transiently in Expi293 F cells (Life Technologies), according to the manufacturer's protocol. I used a 1:1 ratio of antibody heavy and light chain DNA and ExpiFectamine 293 (Life Technologies) transfection reagents for transfections to generate recombinant IgG or monomeric IgA antibodies. For recombinant dimeric IgA, plasmids encoding cDNAs for the heavy chain, light chain and J chain DNA I mixed at 1:1:2 ratio as described (Aiyegbo et al. 2013). After 7 days of culture, the supernatants were centrifuged and filtered using 0.4-μm pore size filters. Antibodies were purified from the supernatants by affinity chromatography on HiTrap

KappaSelect or LambdaSelect columns (Life Technologies).

Antibodies eluted from affinity columns were concentrated using Amicon centrifugal filters (Millipore). I resolved purified antibodies under reducing or non-reducing denaturing conditions on polyacrylamide gels and stained them with Coomassie Blue reagent.

Discussion

The lack of a robust *in vitro* cell culture system to cultivate NoV has made it difficult to understand antibody-mediated mechanisms of neutralization. We do know the value of a neutralizing antibody response to infection since studies have shown that the presence of antibodies that disrupt the interaction between NoV VLPs and HBGAs in vitro is associated with protection against gastroenteritis (Atmar et al. 2011; Jiang et al. 1992). Research published by our collaborator, Dr. Mary Estes' laboratory, has shown that NoV specific serum IgA or memory IgG cells also correlate with protection (Ramani et al. 2015). Our knowledge of the human humoral response to NoV infection still remains limited. Therefore, the main goal of this study was to gain insight into the structural and functional determinants of neutralizing and their binding epitopes.

In this chapter, I present a panel of human mAbs, IgGs and dIgAs, specific to NoV GI.1 VLP and with blockade activity. The first objective was to try to define the molecular and structural basis of human mAb-mediated blocking of GI.1 NoV VLPs. To do so, human mAbs specific to GI.1 VLPs were isolated from two donors who were previously challenged with live GI.1 NoV. Human hybridoma technology was used to isolate a panel of fourteen mAbs, seven IgAs and seven IgGs. The EC_{50} values for each mAb in the panel were determined and isotype specific binding trend was noted. All seven IgG mAbs had lower EC_{50} values compared to the seven dIgAs, which suggests that IgGs bind more avidly than dIgAs to GI.1 VLPs.

In order to test the functional activity of our panel we used a surrogate system to test neutralization, an *in vitro* HBGA blockade assay. Using this system, we can assess how well an

antibody can block VLPs from binding to HBGAs, which are host susceptibility determinants of NoV infection and potential host cell receptors. We determined the IC_{50} of all fourteen mAbs, but did not note any isotype specific trend. But if blocking IC_{50} and binding EC_{50} are both evaluated together for each mAb, meaning if IC_{50} is divided by EC_{50} to understand how much binding is necessary to obtain a certain amount of blockade activity, we did note a pattern. Dimeric IgAs had lower blocking to binding IC_{50}/EC_{50} ratios in comparison to IgGs suggesting more efficient blockade activity. IgAs could block more efficiently because they are binding to different epitopes than IgGs, dIgAs, which are more than twice the molecular size of an IgG, could be exerting steric hindrance on the GI.1 VLPs, or the higher avidity of dIgAs could result in VLP aggregation, preventing VLPs from binding to HBGAs.

To determine why dIgAs were blocking VLPs from binding to HBGAs *in vitro* more efficiently, we first wanted to determine the effects of the constant domain on binding and blocking efficiency, I created IgG, monomeric IgA and dimeric IgA isotype switch variant recombinant Igs for five of the isolated mAb and assessed mAb binding and blocking. Using this system, I was able to test the differences in binding and blocking attributable to general differences between the isotypes themselves such as avidity or molecular size, or to distinctions in antibody specificity, as a result of variances in their variable domain sequences. All recombinant antibodies were resolved on SDS-polyacrylamide gels to verify their molecular weight. Both binding and blocking assays were repeated three times and then EC_{50} values were averaged for each Ab. Blocking IC_{50}/binding EC_{50} ratios for recombinant IgG mAbs were all higher than for mIgA and dIgA. Surprisingly, ratios for mIgAs, which are half the molecular weight and have half the number of antigen binding sites as a dIgA, blocked just as well and sometimes even better than dIgAs. These data imply that differences in blocking efficiency are likely due to differences in the CH1, CH2, CH3 domains. These findings suggest a new role for HuNoV-specific IgA antibodies and provide insight into neutralization of GI.1. This is a novel role for HuNoV-specific IgA immunoglobulins, but not for IgAs in general, as they have been

found to be better neutralizing antibodies compared to IgGs for viruses like human immunodeficiency virus and influenza (He et al. 2015; Tudor et al. 2012).

I expressed one of the mAbs we isolated, dIgA 5I2, as a recombinant Fab to be used in crystallographic studies with GI.1 P domain in complex. Our collaborators at the Baylor College of Medicine obtained a co-crystal complex and found that 512 Fab binds to a conformational epitope on two surface-exposed loop clusters on the GI.1 P domain. This mAb binds in the HBGA binding site, but did not cause any conformational changes in the P domain upon binding. Binding is highly mediated by the 512 CDR1. Identifying these important epitopes is critical information to understanding how norovirus evolves to escape immunity.

CHAPTER III

HUMAN MONOCLONAL ANTIBODIES THAT NEUTRALIZE PANDEMIC GII.4 NOROVIRUSES

Introduction

Since the mid-1990s, the majority of NoV outbreaks have been GII viral variants. GII.4 pandemic strains have emerged every 2-3 years displacing the previous predominantly circulating strain (Lindesmith, Beltramello, et al. 2012). In 2012, the GII.4 Sydney variant emerged and since then has been responsible for the majority of outbreaks in the U.S. (Leshem et al. 2013). The prevalence of GII.4 Sydney 2012 emphasizes the need to characterize the molecular basis for antibody-mediated recognition and antibody mediated neutralization of this virus.

In this chapter, I describe the isolation and characterization of a panel of human mAbs that bind to GII.4 Sydney 2012 VLPs. The majority of these antibodies also block receptor binding, as inferred by their ability to inhibit hemagglutination of human O+ red blood cells (RBCs) or the interaction between GII.4 Sydney 2012 VLPs and porcine gastric mucin (PGM). Both of these assays are surrogate systems for testing neutralization of HuNoV (Czako et al. 2012; Reeck et al. 2010).

For over 40 years there have been numerous documented attempts to cultivate HuNoVs *in vitro,* but previously none of them resulted in the establishment of a robust reproducible system of viral growth (Jones et al. 2014; Duizer et al. 2004; Herbst-Kralovetz et al. 2013). Recent breakthroughs in the development of an *in vitro* replication system using human intestinal organoid technology have now made it possible to cultivate HuNoV and to test inhibition of growth, or neutralization, using antibodies (Ettayebi et al. 2016; Costantini et al. 2018). In collaboration with Dr. Mary Estes' laboratory, we used a human jejunal monolayer culture system to identify antibodies that neutralize live GII.4 Sydney 2012 HuNoV.

Together, we identified the first human mAbs to reduce viral replication of live NoV. I also isolated panel of human anti-GII.4 Sydney 2012 VLP binding IgGs and the first anti-GII.4 human IgA molecules. Almost 70% of the mAbs I isolated exhibited a high level of potency, inhibiting GII.4 Sydney 2012 VLPs from binding to PGM at EC_{50} below 24 μg/mL. Using this panel, I also identified major antigenic sites on the GII.4 Sydney 2012 major capsid protein. These studies contribute new insights into natural human humoral immunity to HuNoVs and provide mAbs that have the potential to be used for diagnostic and therapeutic purposes.

I would like to acknowledge Dr. Mary Estes' group, specifically Dr. Khalil Ettayebi, for performing live NoV neutralization studies in human intestinal enteroids (HIE) *in vitro*.

Isolation of NoV GII.4 VLP-reactive human mAbs

To isolate naturally occurring human mAbs to GII.4 Sydney 2012 VLPs, I used PBMCs collected from subjects with previous history of laboratory-confirmed GII.4 Sydney 2012 virus infection. I transformed the PBMCs with EBV and later collected the supernatants from LCLs and screened by ELISA for binding to GII.4 Sydney 2012 VLPs. Recombinant expression of norovirus genome ORF2 and ORF3 in a baculovirus expression system were used to generate VLPs that are antigenically and morphologically indistinguishable from native virions (Jiang et al. 1992; Green et al. 1993). I detected antibodies that bound to VLPs using horseradish peroxidase conjugated anti-λ or -κ light chain secondary antibodies. I used an anti-light chain secondary antibody for detection in order to isolate antibodies of varying Ig heavy chain isotypes. Previous studies have noted the presence of diverse isotypes in the human polyclonal antibody response to infection, including an increase in IgA, IgG, and IgM antibodies in serum, and we have previously shown that human IgAs can be more potent than IgGs in blocking GI.1 VLPs from binding to histo-blood group antigens (HBGAs) (Iritani et al. 2007; Gray et al. 1994; Sapparapu et al. 2016). Transformed B cell lines corresponding to supernatants that contained

antibodies that bound to GII.4 VLPs were fused with myeloma cells to create human mAb-secreting hybridoma cells. I was able to isolate a panel of twenty-five hybridomas secreting VLP-reactive antibodies, twenty-one IgGs and four IgAs, from seven different donors (Figure 3-1).

Binding to and blockade of NoV GII.4 VLPs by human mAbs

Next, I wanted determine how well the antibodies bound to GII.4 Sydney 2012 antigens, and to identify if any blocked attachment of VLPs to surrogate receptor molecules. I used indirect ELISAs to determine the EC_{50} for the panel of GII.4 Sydney 2012 VLPs (Figure 3-1 and 3-2). For the twenty-one isolated IgGs, EC_{50} values ranged from 0.1 to 6.2 µg/mL. For the four isolated IgAs, EC_{50} values ranged from 0.1 to 0.4 µg/mL (Figure 3-1). I initially used a surrogate system to assess the neutralizing capacity of all twenty-five mAbs. To test blockade potential, I serially diluted the purified mAbs and pre-incubated them with GII.4 VLPs. I then added the VLP-antibody complexes to microtiter plates that had been previously coated with porcine PGM III (Reeck et al. 2010). Previous studies have validated PGM as a reliable substrate to be used in VLP blockade assays (Lindesmith, Beltramello, et al. 2012). I determined EC_{50} values for the four IgAs and thirteen IgGs, which ranged between 2.4 to 23.9 µg/mL (Figure 3-3A and 3-4). Blockade activity was not detected for eight of the IgGs when using antibody concentrations as high as 100 µg/mL. We determined the antibody variable gene heavy and light chain sequences for seventeen of the twenty-five isolated mAbs. All seventeen mAbs, both mAbs that did and did not inhibit GII.4 VLP binding to PGM, had distinct variable gene sequences, suggesting that blockade response is not restricted to a specific genetic sequence motif in antibody repertoires.

Hemagglutination inhibition assay confirms mAb blockade activity

I used a second functional assay to confirm the activity I observed in the blockade assay. Previous studies have shown that an additional surrogate system to determine mAb neutralization is HAI, and that HAI serum antibody levels correlate with protection from symptomatic infection (Czako et al. 2012; Lindesmith, Beltramello, et al. 2012). I used serial dilutions of the isolated mAbs and pre-incubated them with GII.4 Sydney 2012 VLPs. VLP-antibody complexes were then added to human type O+ RBCs. HAI activity was assessed visually, and HAI titers were determined (Figure 3-3A). The majority of the mAbs, about 84%, had HAI activity similar to that of the measured blockade activity. Four mAbs differed in these measures, having either a greater than 2-fold difference in activities or exhibiting only HAI activity or only blockade activity.

Isotype	NORO-mAb clone	Light chain	EC_{50} (µg/mL)
IgG	115	K	0.1
	313.1	K	0.1
	246A	λ	0.2
	250B	λ	0.2
	279A	λ	0.2
	329A	λ	0.2
	118	λ	0.3
	316	λ	0.3
	202A.1	λ	0.4
	312A	λ	0.4
	317	λ	0.4
	303	λ	0.5
	263	λ	0.6
	296A	λ	0.6
	327A	λ	0.6
	315B	λ	0.7
	251A	λ	0.9
	256A	λ	0.9
	278	λ	4.0
	123	λ	5.4
	310A	K	6.2
IgA	318	K	0.1
	320	K	0.1
	273A	K	0.2
	232A.2	K	0.3

Figure 3-1. Isotype, light chain and ELISA binding characterization of GII.4 Sydney 2012 VLP-specific human mAbs. Listed are the half-maximal concentrations (EC_{50}) at which half-maximal binding was obtained when tested by ELISA using VLPs as the antigen. MAbs are organized by isotype (IgG or IgA) and arranged in order from lowest to highest EC_{50} value when binding to GII.4 VLPs.

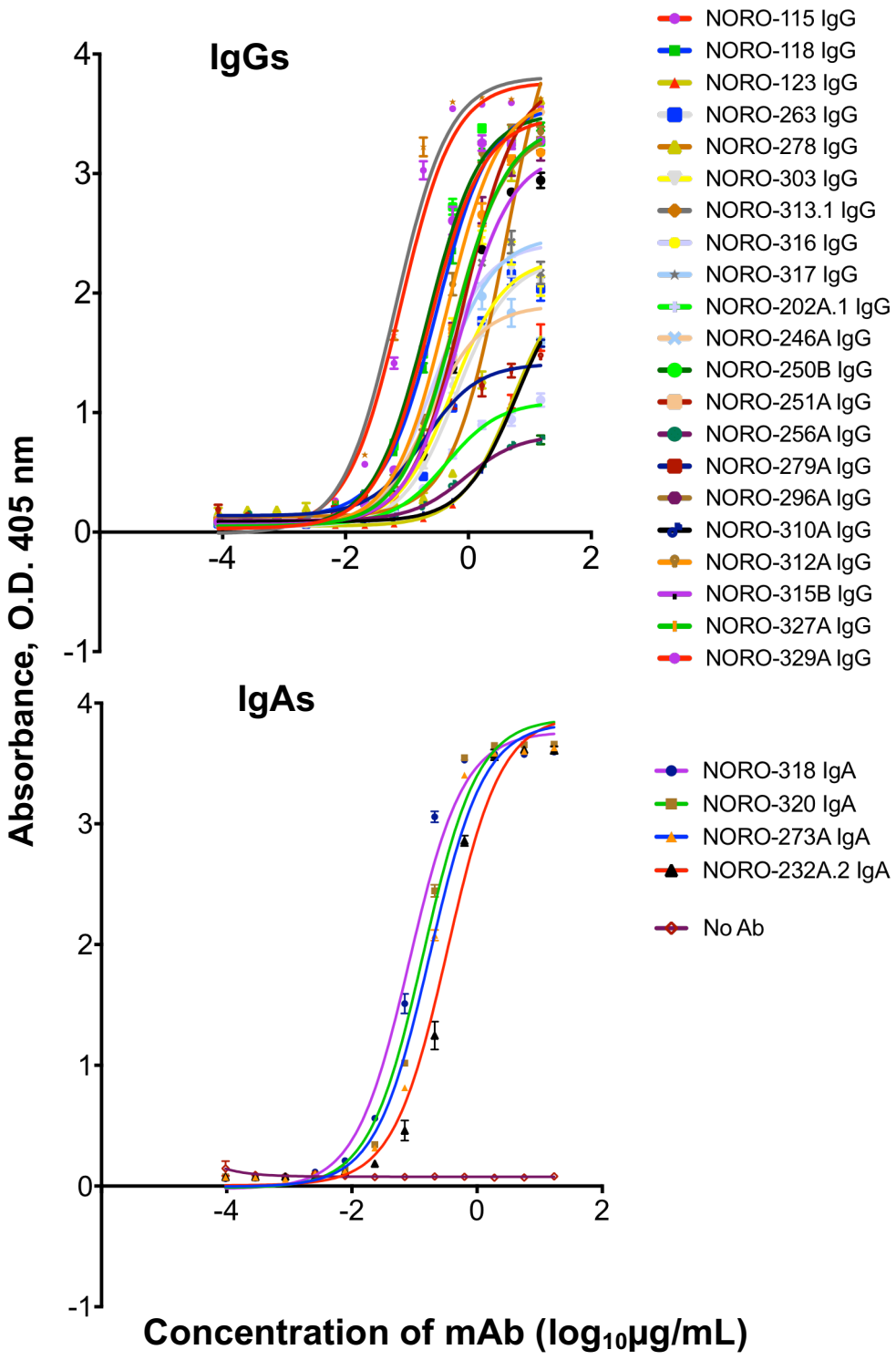

Figure 3-2. Characterization of human mAbs binding to GII.4 Sydney 2012 VLPs. Reactivity of serially diluted mAbs or a no-antibody control for GII.4 Sydney 2012 tested by ELISA.

A

Isotype	NORO mAb clone	Blockade EC_{50} (µg/mL)	HAI titer (µg/mL)
IgG	115	2.8	1.7
	313.1	7.6	15.0
	246A	7.4	5.0
	250B	2.4	5.0
	279A	>	>
	329A	5.6	5.0
	118	>	5.0
	316	2.5	5.0
	202A.1	>	>
	312A	7.2	5.0
	317	5.3	3.4
	303	>	>
	263	9.7	>
	296A	8.3	5.0
	327A	5.0	5.0
	315B	2.7	3.4
	251A	>	>
	256A	>	>
	278	>	>
	123	23.9	10.0
	310A	>	>
IgA	318	3.7	1.7
	320	3.1	5.0
	273A	3.6	5.0
	232A.2	4.4	15.0

B

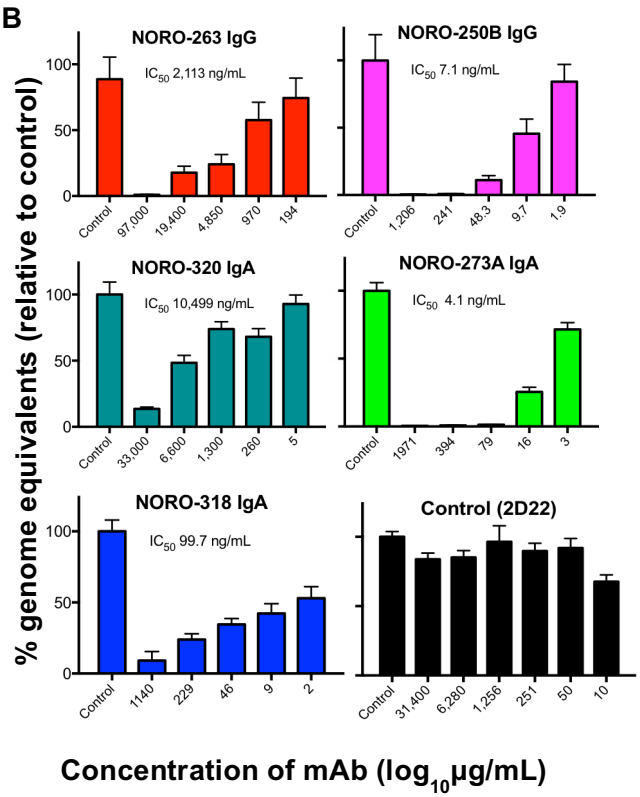

Figure 3-3. Neutralization for GII.4 Sydney 2012 VLPs or live virus. A) EC_{50} values for all isolated IgGs and IgAs using a VLP blockade assay, and the antibody concentration at which hemagglutination was inhibited when using VLPs and O+ red blood cells. > symbols indicate blockade EC_{50} values >100 µg/mL for IgGs or >113 µg/mL for IgAs, or HAI titers > 15 µg/mL. **B)** Inhibition of replication of GII.4 Sydney 2012 virus using selected IgGs, IgAs and a non-specific mAb were tested in a human intestinal enteroid system. An additional control for each experiment was virus incubated without a mAb. The IC_{50} values for each mAb is indicated in each individual graph. The data presented is an average of two independent experiments. The number of genome equivalents for each concentration tested for each mAb including the no antibody control was the average of 6 replicates tested.

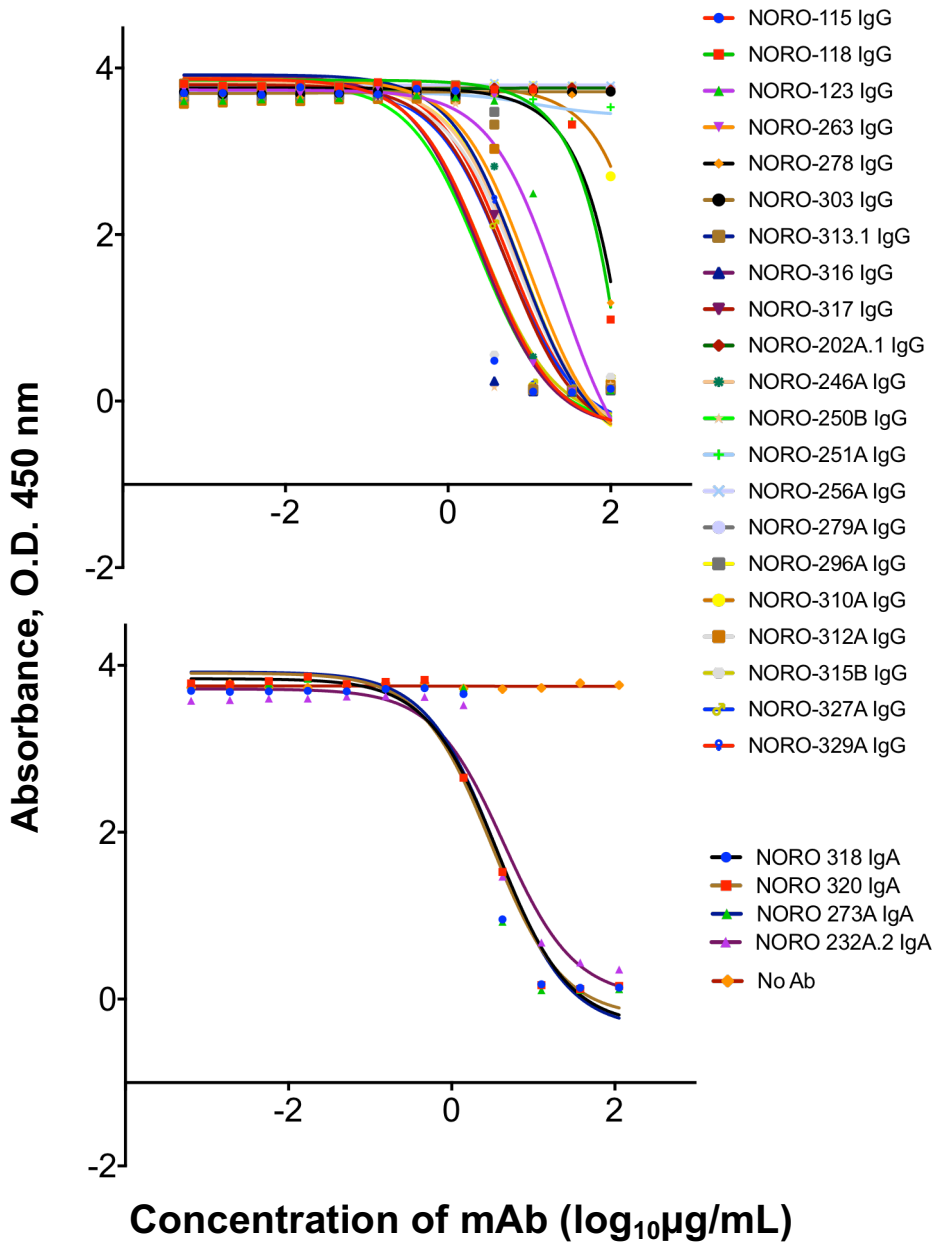

Figure 3-4. Characterization of blockade activity of GII.4 Sydney 2012 VLPs using isolated mAbs. Blockade potential of serially diluted mAbs or a no-antibody control for GII.4 Sydney 2012 VLP binding to porcine gastric mucin was measured.

Neutralization of NoV GII.4 virus using stem-cell derived enteroids

Inhibition of replication of GII.4 Sydney 2012 virus by mAbs NORO-250B, -263, -320, -273A, -318 and a non-GII.4 VLP binding control antibody, 2D22, were tested using an intestinal epithelial stem-cell derived *in vitro* cultivation system. I selected two IgGs, NORO-263 and -250B and three IgAs, NORO-320, -273A and -318. These five mAbs were chosen so that we could test neutralization by representative mAbs belonging to the three major antigenic sites we identified on the GII.4 Sydney 2012 P domain and to test at least two mAbs belonging to each isotype (Figure 3-4). I measured neutralization by comparing the percent reduction of genome equivalents when compared to a no-antibody control within each assay using RT-qPCR (Figure 3-3B). A no-antibody control was used in each assay to normalize for any variability between experiments. Variability was noted due to the high sensitivity when using genome equivalents to measure replication. To account for these differences, we used six replicates for each mAb concentration tested within each assay and for the no-antibody control. We then averaged the genome equivalents from two separate assays for each antibody to obtain an IC_{50} value. To verify that equal amounts of virus were added to each monolayer, each assay was performed in duplicate and RNA was collected from one assay at 1 hours post-infection (HPI) and from the other at 24 HPI. Four of the five antibodies tested, NORO-250B, -263, -273A and -318, had approximately 5 to 883-fold lower IC_{50} values compared to blockade EC_{50} values, or between 17 and 1,227-fold lower than HAI titers (Figure 3-3A and 3C). NORO-320 had a higher IC_{50} in comparison to its blockade EC_{50} or HAI titer. The dengue virus mAb 2D22 used as a similarly prepared negative control did not exhibit concentration-dependent inhibit of replication of GII.4 Sydney 2012 virus. Previous studies with polyclonal serum have shown that neutralization IC_{50} values of GII.4 and GII.3 noroviruses are lower in comparison to blockade EC_{50} values (Ettayebi et al. 2016). These studies, as well as our data suggest that the HIE neutralization assay is likely more sensitive than the HBGA blockade or HAI assays.

Binding studies using GII.4 protruding domain dimers and shell domain

I then wanted to determine where the antibodies might potentially be binding, specifically if they were binding to the protruding (P) or shell (S) domains of the major capsid protein VP1. I expressed glutathione S-transferase (GST)-tagged recombinant GII.4 Sydney 2012 P domain dimers and purified them using affinity column chromatography, as previously described (Choi et al. 2008). To determine if the twenty-five isolated mAbs were specific to the P or S domain of the GII.4 major capsid protein VP1, I used P domain dimers or recombinantly expressed S domains as antigen for an indirect ELISA assay with serial dilutions of each mAb. The VP1 region is divided into the S domain, which is not expressed on the recombinant GST-GII.4 P domain dimers, and the P1 and P2 subdomains that are expressed in the dimers. The P domain is the surface-exposed protruding region of the norovirus virion and also believed to include determinants for host cell attachment and antibody binding epitopes (Debbink, Donaldson, et al. 2012 ; Lindesmith, Debbink, et al. 2012; Lochridge et al. 2005). The S domain is connected to the P domain by a flexible hinge region and forms the interior core of the viral capsid. The S domain has the highest degree of genetic sequence conservation of any protein domain in diverse norovirus strains (Parra et al. 2013). When I tested binding by ELISA, twenty of the twenty-five isolated mAbs bound to the GST-GII.4 P domain (Figure 3-5). The five mAbs that did not bind to the P domain did bind to the S domain. NORO- 329A, -312A, -296A and -232A.2, bound to both the P and S domain proteins, indicating that these antibodies likely bind to a quaternary epitope on the GII.4 Sydney 2012 major capsid protein. I also used the Isolated mAbs and GII.4 P domain dimers for competition-binding studies. I used a real-time bio-layer interferometry biosensor system to identify potential major antigenic sites recognized by the GII.4 Sydney 2012 P domain binding mAbs. Neutralizing mAbs and mAbs that did or did not block GII.4 Sydney 2012 VLPs from binding to PGM were classified into three major competition-binding groups, with some overlap between two groups (Figure 3-6). Despite multiple attempts, I was not able to detect binding using bio-layer interferometry for two of the

twenty mAbs that bound to the GII.4 Sydney 2012 P domain by ELISA. Competition-binding studies were performed using the Octet® RED96 and Octet® HTX systems, which are both instruments that can measure biomolecular interactions. The HTX system is a high-throughput system that has the ability to compete all eighteen P domain binding mAbs within the same experiment. The RED96 system was only able to compete mAbs in groups of eight. Using data from the RED or HTX experiments, we noted three major competition-binding groups on the GST-GII.4 Sydney 2012 P domain. By using both instruments, in two independent laboratories, we were able to validate the reproducibility of the results.

The emergence of new GII.4 strains has been associated with the evolution of the GII.4 major capsid protein and antigenic variation (Karst & Baric 2015). To measure the reactivity of my panel of mAbs for another GII.4 strain, I tested binding reactivity and blockade activity to a GII.4 Houston 2002 (ABY27560.1) variant. About 93% of the amino acid sequence of the major capsid protein is conserved between GII.4 Houston 2002 and Sydney 2012, but there are remarkable differences among predicted GII.4 blockade epitopes (Figure 3-7). All twenty-five mAbs exhibited binding reactivity to GII.4 Houston 2002 antigen (Figure 3-8). Only three mAbs, NORO-115, -329A, and -318 had a greater than 10-fold higher binding EC_{50} value when compared to GII.4 Sydney 2012 VLPs. The eighteen mAbs that either blocked with EC_{50} values <100 µg/mL or had HAI titers < 15 µg/mL all blocked GII.4 Houston 2002 VLPs from binding to PGM. GII.4 Houston 2002 and Sydney 2012 had different amino acid sequences in four of the five predicted blockade epitopes, these results suggest the potential existence of additional blockade epitopes or the use of Epitope B, which was conserved among both strains (Figure 3-7).

Isotype	NORO-mAb clone	Protruding domain EC_{50} (µg/mL)	Shell domain EC_{50} (µg/mL)
IgG	115	0.1	>
	313.1	0.8	>
	246A	0.9	>
	250B	0.1	>
	279A	>	0.4
	329A	0.2	35.8
	118	0.4	>
	316	0.2	>
	202A.1	>	0.2
	312A	0.2	9.9
	317	0.2	>
	303	6.8	>
	263	0.9	>
	296A	0.4	12.5
	327A	0.5	>
	315B	0.3	>
	251A	>	4.1
	256A	>	0.4
	278	68.5	>
	123	6.1	>
	310A	>	1.8
IgA	318	0.2	>
	320	0.6	>
	273A	0.2	>
	232A.2	0.4	38.1

*Shell domain reactive

Figure 3-5. Half-maximal binding concentrations of purified mAbs to GII.4 Sydney 2012 protruding or shell domain. EC_{50} value indicates the concentration at which half-maximal binding was obtained when tested by ELISA using either recombinantly expressed P domain or shell domain as antigen. MAbs are organized by isotype, IgG or IgA, and arranged in order from lowest to highest EC_{50} value when binding to GII.4 VLPs. The > symbol for IgGs indicates EC_{50} binding value >150 µg/mL or >172 µg/mL for IgAs. Grey boxes indicate mAbs that exclusively bind to the GII.4 Sydney 2012 shell domain.

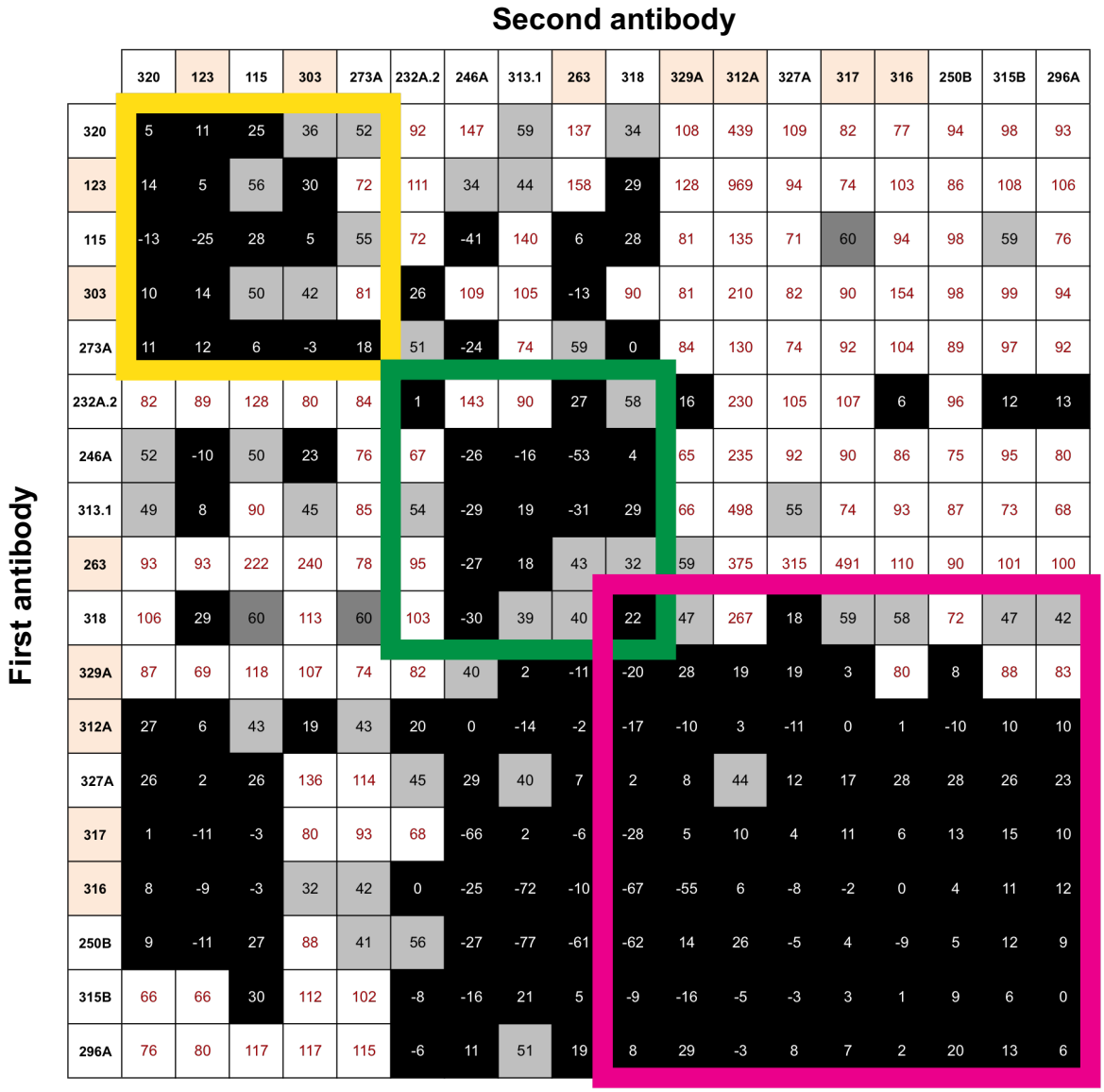

Color	Interpretation	% of max uncompeted signal
	First Ab blocks the binding of the second mAb	≤33%
	First Ab partially blocking the binding of second mAb	34-66%
	First Ab does not block the binding of the second mAb	>66%

	Block GII.4 Sydney VLPs from binding to HBGAs *in vitro*

Figure 3-6. Competition binding of GII.4 specific mAbs on GII.4 Sydney 2012 P domain with the Octet® Red96 system. Epitope binning was performed using biolayer interferometry. GST-tagged GII.4 Sydney 2012 P domain was loaded onto anti-GST tips, then the first antibody was loaded followed by loading of the second antibody. The numerical data indicate percent binding of the second antibody in the presence of the first antibody. Yellow, green, and magenta boxes indicate potential binding groups.

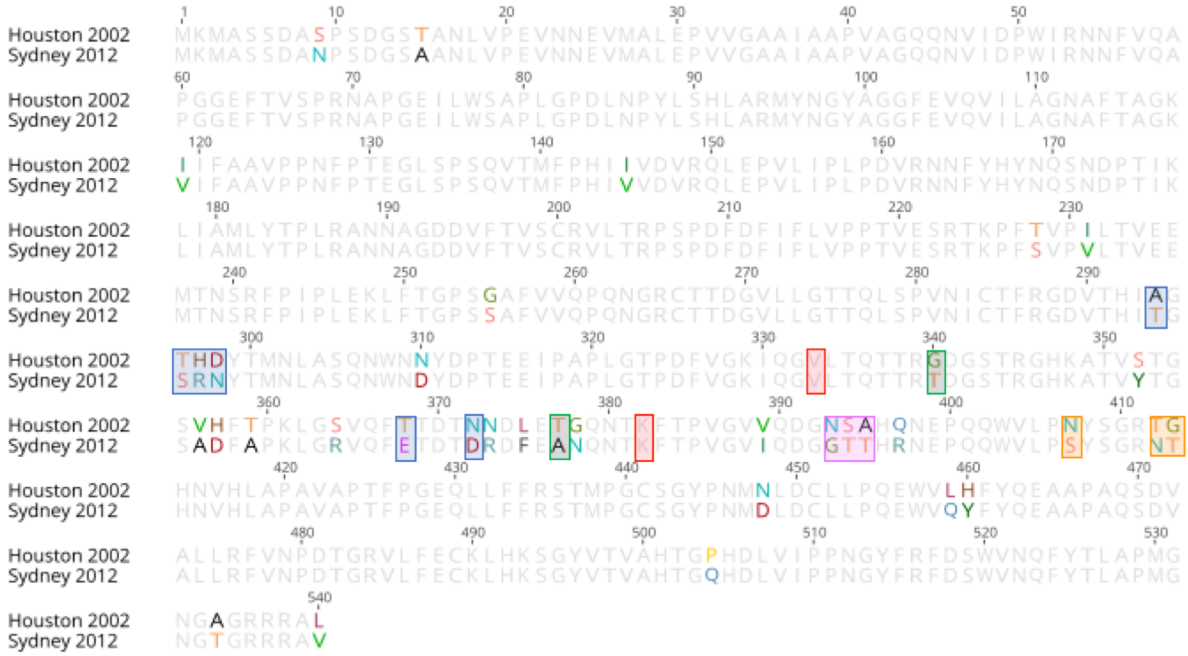

FIGURE 3-7. Predicted blockade epitopes on amino acid sequence alignment of GII.4 Houston 2002 and Sydney 2012. Amino acid sequence alignment of the major capsid protein of GII.4 Houston 2002 and Sydney 2012 noroviruses. Boxes indicate predicted blockade epitopes AS previously described (Lindesmith et al., 2012). Epitope A is amino acids 294, 296-298, 368 and 372. Epitope B is amino acids 333 and 382. Epitope C is amino acids 340 and 376. Epitope D is amino acids 393 and 395. Epitope E is amino acids 407, 412 and 413.

Isotype	NORO mAb clone	Binding EC_{50} (µg/mL)	Blockade EC_{50} (µg/mL)
IgG	115	1.1	2.3
	313.1	0.1	2.1
	246A	0.2	2.1
	250B	0.1	17.9
	279A	0.3	>
	329A	5.5	3.0
	118	0.4	9.5
	316	0.6	2.1
	202A.1	0.1	>
	312A	0.6	3.0
	317	0.7	2.0
	303	0.5	>
	263	0.5	2.1
	296A	0.1	3.2
	327A	0.3	2.2
	315B	0.5	2.2
	251A	0.3	>
	256A	0.4	>
	278	0.5	>
	123	0.6	2.5
	310A	0.6	>
IgA	318	4.5	3.5
	320	0.3	3.3
	273A	0.2	5.2
	232A.2	0.2	5.4

Figure 3-8. Half-maximal binding and blockade concentrations (EC_{50}) of purified mAbs to GII.4 Houston 2002 VLPs. Listed are the EC_{50} of each mAb for binding or blockade activity using GII.4 Houston VLPs. The > symbols indicate blockade EC_{50} values >100 µg/mL.

Materials and methods

Expression of GII.4 Virus-like particles

I produced and purified GII.4 Sydney 2012 VLPs, based on strain AFV08795.1, as previously described (Kou et al. 2015). Briefly, VP1 and VP2 capsid protein sequences were cloned into the transfer vector pVL1392 (Epoch Life Sciences, Inc.). The vector was co-transfected with a bacmid vector into Sf9 insect cells. Recombinant virus then was used to inoculate Sf9 cells. VLPs were purified from the culture supernatant using a cesium chloride cushion gradient. I verified GII.4 VLP assembly visually using electron microscopy, and antigenicity was tested by western blot.

GII.4 VLP binding assay

I tested antibody reactivity to GII.4 VLPs using indirect ELISAs. Microtiter plates were coated with 1 µg/mL of GII.4 VLPs in PBS at 4°C overnight. Wells then were blocked with 5% nonfat dry milk in PBS with 0.05% Tween-20 for 1 hour at room temperature. I diluted purified antibodies serially in 1XDPBS and then added them to VLP-coated plates for 1 hour at room temperature. Microtiter plates were washed 3 times with PBS-0.05% Tween-20 in between each step. Antibodies that bound to VLPs were detected using horseradish peroxidase tagged anti-κ or -λ chain secondary antibodies (Southern Biotech) for 1 hour at room temperature. Plates were developed using the ultra-TMB reagent (Pierce ThermoFisher) and stopped using sulfuric acid. Absorbance was measured at 450 nm using a BioTek Synergy HT Microplate Reader.

VLP-carbohydrate binding antibody blockade assay

Microtiter plates were coated with 10 µg/mL of pig gastric mucin (PGM) Type III (Sigma) in PBS for 4 hours at room temperature, and then were blocked overnight at 4°C in 5% nonfat

dry milk in PBS with 0.05% Tween-20. I pretreated GII.4 Sydney 2012 VLPs (0.5 μg/mL) with each mAb applied in serial 3-fold dilutions with decreasing concentrations. Complexes then were applied to PGM-coated plates for 1 hour at room temperature. In between each step, I washed the microtiter plates three times with PBS-0.05% Tween-20. Bound VLPs were detected using guinea pig serum containing anti-GII.4 Sydney 2012 polyclonal antibodies, followed by an alkaline phosphatase-conjugated anti-guinea pig IgG. Optical density was measured at 405 nm using a Synergy HT Microplate Reader (BioTek).

Hemagglutination inhibition assay

Human type O+ RBCs were purchased from Rockland Immunochemicals, Inc. Cells were pelleted at 500 x *g* for 10 minutes at 4°C and washed twice with PBS without Ca^{2+} or Mg^{2+}. I pretreated GII.4 Sydney 2012 VLPs (3.5 μg/mL) with decreasing concentrations of each mAb, from 15 to 0.007 μg/mL, in PBS pH 5.5 and incubated at room temperature for 30 minutes. I then added VLP-mAb complexes to an equal volume of 0.5% washed red blood cells in PBS pH 6.2 and incubated for 2 hours at 4°C in a 96-well V-bottom microtiter plate. The HAI titer was determined as the lowest concentration of antibody that completely inhibited hemagglutination.

Human subjects

We studied otherwise healthy adult subjects with a history of acute gastroenteritis contracted during a HuNoV outbreak in North Carolina between February 27 and March 1, 2013. The cause of the outbreak was determined by the Orange County, NC health department to be a GII.4 Sydney 2012 norovirus strain. Subjects were recruited after recovery to donate a one-time peripheral blood sample. The research study was approved by the Vanderbilt University Medical Center Institutional Review Board; all subjects provided written informed consent prior to participation.

PBMC isolation and hybridoma generation

We obtained PBMCs from heparinized blood by density gradient centrifugation using Ficoll-Histopaque from seven donors who had recovered recently from natural infection with HuNoV. B cells were transformed with EBV substrain B95.8 in the presence of 2.5 µg/mL of CpG10103, 10 µg/mL of cyclosporine A, and 10 µM Chk2 inhibitor. Approximately 10^7 PBMCs were plated into a 384-well plate in transformation medium, and a week later were expanded into four 96-well plates containing irradiated human PBMCs as a feeder layer. After an additional seven days of culture, I screened the supernatants by indirect ELISA for the presence of antibodies that bound to GII.4 Sydney 2012 VLPs. Antibodies that bound to GII.4 Sydney 2012 VLPs were detected using horseradish peroxidase tagged anti-human IgA or IgG secondary antibodies (Southern Biotech). Wells containing transformed B cells secreting anti-GII.4 Sydney 2012 VLP antibodies were fused with HMMA2.5 myeloma cells using a CytoPulse Sciences Generator. After fusion, I plated hybridomas in selection medium containing 100 µM hypoxanthine, 0.4 µM aminopterin, 16 µM thymidine and 7 µg/mL ouabain. After two weeks, hybridomas were screened for production of human antibodies reacting with GII.4 Sydney 2012 VLPs and then cloned biologically using single cell sorting on a FACSAria III flow cytometer in the Vanderbilt Flow Cytometry Shared Resource.

Competition-binding assay

To identify groups of antibodies binding to similar antigenic sites on norovirus GII.4 Sydney 2012, we performed bio-layer interferometry using an Octet® Red96 or Octet® HTX biosensor system (FortéBio). The Octet® HTX is a high-throughput biosensor system that was used to validate results obtained from the Octet® Red96 system. With both biosensor systems, antibodies and antigen were diluted in 1X kinetic buffer (FortéBio 18-5032). GST-tagged GII.4 Sydney 2012 P domain dimers were immobilized onto anti-GST biosensor tips (FortéBio 18-

5096). The P domain dimers were coated onto the biosensor tip by immersing the tip in a solution containing dimers at a concentration of 5 µg/mL. The biosensor tip with the bound P domains was washed and then submerged into a well containing 50 µg/mL of the first antibody and then dipped into another well containing 50 µg/mL of the second antibody. If binding of the first antibody still resulted in greater than 66% of binding of the second antibody, there is believed to be no competition between both antibodies. If binding of the second antibody was between 34-66% in the presence of the first antibody, there is believed to be partial competition. If 33% or less binding of the second antibody is noted in the presence of the first, both antibodies are believed to be in competition with each other. Antibodies then were clustered based on their binding patterns.

Use of stool filtrates from infected patients for NoV isolation

To prepare 10% stool filtrates, 4.5 mL of sterile PBS was added to 0.5 g of GII.4 Sydney 2012 positive stool sample. The stool suspension was sonicated using a cup horn sonicator and centrifuged at 1,500 x *g* for 10 minutes at 4°C. Supernatant was collected and transferred to a new tube and centrifuged once again at 1,500 x *g*, for 10 minutes at 4°C. The resulting supernatant then was passed serially through 5 µm, 1.2 µm, 0.8 µm, 0.45 µm and 0.22 µm filters, and aliquoted and frozen at -80°C.

Expression and purification of GST-GII.4 Sydney 2012 P domain

P1 and P2 domain sequences of GII.4 Sydney 2012, AFV08795.1, VP1 were cloned into the pGEX-4T-1 expression vector with a GST tag and thrombin cleavage site. I expressed the P domain in *Escherichia coli* BL-21 cells and purified using standard column chromatography techniques with a prepacked Glutathione Sepharose Fast Flow column (GE Healthcare). GST-tagged proteins were eluted using 50 mM Tris-HCl, 10 mM reduced glutathione, pH 8.0 and stored at 4°C.

GII.4 Sydney 2012 virus neutralization assay

HIEs were generated and cultured as described previously (Ettayebi et al. 2016). Briefly, HIEs were grown as three-dimensional cultures in Matrigel (Corning) for 5 days and then plated as cell monolayer cultures in 96-well plates. Before plating, 96-well plates were pre-coated with collagen IV (Sigma) at 33 µg/mL in sterile cold water for 1.5 hours at 37°C. Three-dimensional HIEs were collected in 0.5 mM ethylenediaminetetraacetic acid diluted in ice-cold Dulbecco's PBS, no calcium, no magnesium (Life Technologies, Cat# 14190-144) and spun down at 200 x *g* for 5 minutes at 4°C in a swinging bucket rotor. The pellet then was suspended in 0.05% trypsin/0.5 mL ethylenediaminetetraacetic acid and incubated at 37°C for 4 minutes. Trypsin then was inactivated with complete medium without growth factors [CMGF(-)] supplemented with 10% fetal bovine serum (FBS). The resulting pellet was suspended and passed through a 0.4 µm cell strainer and spun down at 400 x *g* at room temperature for 5 minutes. The pellet then was suspended in complete medium with growth factors [CMGF(+)] containing 10 µM Y-27632 (Sigma-Aldrich; Y0503) and seeded into a 96-well plate. After 24 hours, the culture medium was removed and replaced with differentiation medium. Cells were differentiated for 5 days. HuNoV GII.4 Sydney 2012 (TCH12-580) (Ettayebi et al. 2016) stool filtrate (2 x 10^7 genome equivalents/µL) was used to test neutralization. Serial dilutions of the mAbs were prepared in CMGF(-) medium and each dilution was pre-incubated with 2.5 x 10^5 genome equivalents of GII.4 Sydney 2012 at 37°C for 1 hour. Samples were diluted with equal volume of CMGF(-) medium supplemented with 1000 µM sodium glycochenodeoxycholate. Monolayers then were inoculated with pre-incubated samples. At 1 hour post-infection (HPI), monolayers were washed twice and incubated with differentiation medium supplemented with 500 µM glycochenodeoxycholate. After 1 and 24 HPI, cells and medium were collected and RNA was extracted using KingFisher Flex Purification System and MagMax Viral RNA Isolation kit. For RT-qPCR, a primer pair (COG2R /QNIF2d) and probe (QNIFS) (Loisy et al. 2005) (Kageyama et al. 2003) were used with qScript XLT One-Step RT-qPCR ToughMix reagent with ROX

(Quanta Biosciences). Reactions were performed on an Applied Biosystem StepOne Plus thermocycler. A recombinant HuNoV RNA transcript was provided by Dr. Estes' laboratory and used to create a standard curve to quantitate viral genome equivalents in new RNA samples.

Discussion

In this chapter, I present the first instance of neutralization of HuNoV by mAbs and describe a large panel of human mAbs that neutralize the pandemic GII.4 Sydney 2012 strain. Previously it was not possible to test norovirus neutralization directly because of the lack of a reliable *in vitro* culture system for norovirus replication. A surrogate system to predict neutralization was devised and used to study inhibition of the interaction between VLPs and HBGAs. The presence of blocking antibodies in serum correlates with protection from clinical gastroenteritis induced by HuNoV infections, and therefore the HBGA blocking assay has been considered a surrogate system for HuNoV neutralization (Reeck et al. 2010). Recently, our collaborator Dr. Estes group developed an *in vitro* system using human enteroids to replicate multiple HuNoV strains (Ettayebi et al. 2016). Here, we used that system to identify the first norovirus human mAbs with demonstrated virus neutralizing activity. Of the twenty-five human mAbs isolated in this study, seventeen of them blocked GII.4 Sydney 2012 VLPs from binding to PGM at concentrations as low as 2.4 μg/mL. The eighteen mAbs that blocked GII.4 Houston 2002 from binding to PGM at concentrations as low as 2 μg/mL, also either blocked GII.4 Sydney 2012 VLPs from binding to PGM or inhibited hemagglutination at the concentrations tested. Interestingly, thirteen of the fourteen IgGs that blocked GII.4 Houston 2002 VLPs from binding to PGM did so at a lower EC_{50} value in comparison to blockade EC_{50} values for GII.4 Sydney 2012. This could indicate that our donors had prior exposure to an earlier norovirus variant similar to GII.4 Houston 2002. This panel also contains the first reported human IgA mAbs that bind to GII.4 Sydney 2012 VLPs and also inhibit receptor binding. We tested neutralization of live GII.4 Sydney 2012 HuNoV using the mAbs NORO-263, -320, -250B, -273A

and -318. These antibodies were selected for testing so that we could investigate differences in neutralizing activity between mAbs of differing isotypes, those which belong to different competition-binding groups, and those with different binding and blockade EC_{50} values. NORO-250B, -263, -273A and -318, had lower neutralization IC_{50} values in comparison to blockade EC_{50} values and HAI titers. Surprisingly, NORO-320 had an IC_{50} value about 2-fold higher than its HAI titer and about 3-fold higher than its blockade EC_{50} value. Some of our previous studies, as I discussed in Chapter 2, have noted differences in blockade potency of GI.1 VLPs among human IgG and IgA mAbs with blockade potency being enhanced for IgAs (Sapparapu et al. 2016). To draw a similar conclusion for GII.4 Sydney 2012 neutralizing human antibodies, it would be essential to test mAbs binding to different epitopes with identical variable domain sequences and distinct isotypes. Such studies could determine if isotype plays a critical role in neutralization of GII.4 Sydney 2012 by human mAbs.

HuNoV-specific antibodies have been described previously, but these were antibody fragments derived from phage display libraries (Huang et al. 2014), murine mAbs from infected mice (Crawford et al. 2015), nanobodies from alpacas immunized with VLPs (Koromyslova & Hansman 2017), or mAbs isolated from patient PBMCs with an unknown norovirus history of exposure (Lindesmith, Beltramello, et al. 2012). Such antibodies do not provide direct information about the physiologic human humoral immune response to HuNoV infection. The therapeutic potential of mouse mAbs is limited, since they have been shown to induce human anti-mouse antibody responses. There has been little progress in understanding individual HuNoV-specific antibodies in the past because of the difficulty in generating human mAbs with functional activity. To isolate NoV GII.4 specific human mAbs, I used hybridoma technology (Smith & Crowe 2015) and circulating B cells from convalescent patients to produce human mAbs. This approach generates hybridoma cell lines from circulating B cells that express naturally occurring and matched heavy and light chain genes. An additional benefit of using this approach is that it does not involve the use of any laboratory animals to produce antibodies.

Using this method, I isolated twenty-five GII.4 Sydney 2012 VLP-reactive mAbs. The majority of these antibodies were neutralizing when tested in a surrogate system for neutralization and all five of the mAbs tested also inhibited replication of live GII.4 Sydney 2012 virus by direct neutralization *in vitro*. Neutralizing human mAbs have potential for use in prophylactic, therapeutic or diagnostic applications. We currently do not have any drugs available to treat or prevent HuNoV infection, so our panel of neutralizing mAbs now have the high potential to impact the design of improved diagnostic and therapeutic measures for HuNoVs.

Since the mid-1990s, new antigenically diverse GII.4 pandemic viral strains have emerged continuously every 2 to 5 years, and today these strains continue to be the predominant cause of norovirus outbreaks. In 2012, the epidemic GII.4 Sydney variant emerged in Australia and began spreading globally. Even though blockade epitopes among some contemporary GII.4 strains have been predicted or identified, we have limited information about the neutralization determinants on GII.4 Sydney 2012 viruses (Lindesmith, Beltramello, et al. 2012; Debbink et al. 2013). Here, I determined that there are at least three major antigenic and neutralizing sites on the P domain of GII.4 Sydney 2012 viruses. In the future, defining neutralization epitopes in high resolution with neutralizing antibodies could contribute valuable insights for rational structure-based vaccine design efforts.

HuNoV is one of the leading causes of severe acute gastroenteritis, therefore the global burden of norovirus infection is extremely high in both developed and developing countries. Unfortunately, there is currently no licensed vaccine to prevent norovirus infection. Efforts to design a vaccine have been hindered by the lack of a small animal model or tissue culture model to test neutralization or infection, the antigenic heterogeneity among noroviruses, and uncertainty about the durability of protective immunity (Debbink, Lindesmith & Baric 2014). Vaccine efforts have focused on the use of monovalent GI.1 or bivalent GI.1/GII.4 virus-like particles or P particle subunits (El-Kamary et al. 2010; Bernstein et al. 2015; Tan et al. 2011). Clinical trials have shown that norovirus VLP vaccines are immunogenic and without frequent

serious adverse events (Ramirez et al. 2012; Leroux-Roels et al. 2018). We now have developed a reliable *in vitro* system to test the replication or inhibition of replication of live noroviruses. Mapping the neutralization or blockade epitopes using the panel of mAbs we isolated against this circulating pandemic strain of norovirus will provide critical information that can be used for the design of future VLP vaccines that can elicit a protective immune response.

CHAPTER IV

BROADLY BINDING AND NEUTRALIZING HUMAN MONOCLONAL ANTIBODIES TO GI AND GII NOROVIRUSES

Introduction

In 2010, there were 1.8 billion cases of diarrheal disease worldwide and a large number of cases, about 18%, were due to norovirus (Pires et al. 2015). In the United States, the Center for Disease Control estimates that there are approximately 19 to 21 million annual cases of acute gastroenteritis caused by norovirus (Hall et al. 2014). This evidence suggests that there is a substantial global disease burden caused by NoVs and highlights the need for therapeutics and an efficacious vaccine could alleviate some of this burden. Unfortunately, creating a broadly protective vaccine has been extremely challenging due to the antigenic and genetic diversity among circulating strains of human norovirus.

When I began my thesis project in the summer of 2013, Calicinet, the U.S. national NoV outbreak surveillance network, reported that from September 2013 to February 2015 GII.4 Sydney, GII.6, GII.13, GI.3, and GI.2 were responsible for the majority of NoV outbreaks. Calicinet's latest genotype distribution of NoV outbreaks, reported in August of 2018, attributes 61% of outbreaks to GII.4 and GII.6 variants. Between genogroups, the genomic nucleotide sequence of structural proteins can differ by more than 50% (Pletneva et al. 2001). Genetic diversity in strain structural proteins also causes changes in antigenic properties. It is imperative to understand the antigenic diversity and identify conserved cross-reactive epitopes on circulating strains of NoV to develop an effective vaccine option.

Antibody-mediated neutralization of a virus occurs when a specific antibody recognizes a viral epitope and inhibits viral entry or infection. This can be achieved by preventing the virus from binding to a receptor, blocking internalization into a cell, or even by causing aggregation of

virus particles. The intricacies of human antibody-mediated NoV cross-reactivity and neutralization remain to be elucidated. Numerous studies have assessed the presence of a human polyclonal immune response to NoV (Hale et al. 1998; Czako et al. 2015; Lindesmith et al. 2005; Treanor et al. 1993). We hypothesized that broadly neutralizing human antibodies and cross-reactive immunogenic epitopes exist. To test our hypothesis, I would attempt to isolate broadly neutralizing human mAbs from patients who were previously infected with a GII NoV using a panel of VLPs that mimic the major circulating strains of NoV. These broadly neutralizing human mAbs could then be used in competition assays and three-dimensional structural analysis to pinpoint cross-reactive epitopes.

These studies can define novel mechanisms of NoV neutralization, antigenic and neutralizing epitopes, antibody paratopes, and any structural changes on the major capsid protein during neutralization. Isolated human mAbs could also be directly used as a prophylactic, therapeutic, or a reagent for diagnosis. In the past, broadly cross-reactive murine mAbs have been isolated from mice immunized with GII.3 VLPs (Parra et al. 2013). Cross-reactive inter- and intra-genogroup murine Abs have been isolated by the laboratories of our collaborators Dr. Estes and Dr. Atmar, but none of these mAbs inhibited replication of live NoV or blocked VLPs from binding to glycan *in vitro*. A murine Ab response to a human infection offers little information about the actual human response. Therefore, my main objective was to isolate cross-reactive human broadly blocking monoclonal antibodies and to map their corresponding epitopes. The information we gather will also be useful when reformulating multivalent VLPs for HuNoV vaccine trials, since the goal of a vaccine is to elicit a protective response against more than one circulating strain of HuNoV.

I present in this chapter a panel of fourteen mAbs, five IgMs, seven IgGs and two dIgAs, with cross-reactive binding activity within a genogroup or to strains within more than one genogroup. Ten of the mAbs also inhibit at least one NoV strain VLP from binding to glycans *in vitro*. I have also conducted initial antigenic mapping studies using strain specific P vs S domain

binding. As expected some of the most cross-reactive mAbs bind to the highly conserved shell domain on the strains tested. Three-dimensional X-ray crystallography studies of NORO-320, a GII specific mAb, in complex with GII.4 P domain suggest NORO-320 does not neutralize by directly inhibiting receptor binding. Blockade studies using different molecular forms of NORO-320 revealed that NORO-320 could be neutralizing GII.4 NoV through steric hindrance.

I would like to acknowledge Dr. Prasad's group, specifically Wilhelm Salmen, for providing three-dimensional structural characterization of NORO-320 in complex with GII.4 P domain.

Isolation of broadly binding anti-NoV human mAbs

To isolate cross-reactive NoV human mAbs, I used PBMCs that had been collected form patients who were overall healthy with a previous history of acute gastroenteritis. As previously described, I transformed the PBMCs using EBV. A week later, I tested the supernatants by ELISA to screen for the expression of mAbs that bound to more than one NoV VLP. The VLPs used to screen were NoV GI.1, GI.2, GI.3, GII.3, GII.4, GII.6, GII.13 and GII.17. Each VLP was individually coated and blocked on a microtiter plate before screening. The bound antibodies were detected using alkaline phosphatase conjugated goat anti-human κ or λ chain secondary antibodies. I used this secondary antibody so I could capture binding activity from any isotype. Since my goal was to isolate cross-reactive mAbs, I expanded the wells that contained transformed B cells expressing mAbs that recognized at least more than one VLP. To create anti-NoV mAb secreting hybridomas, I electrofused these cells B cells with HMMA 2.5 cells, a myeloma cell line. The hybridoma cells were ultimately cloned using single cell-sorting.

Binding and blockade activity of cross-reactive mAbs to NoV GI and GII VLPs

I isolated a panel of fourteen cross-reactive mAbs, five IgMs, seven IgGs and two IgA (Figure 4-1). The binding and ability to block or neutralize GII.4 Sydney was previously

characterized for six of the mAbs, NORO-279A, -310A, -202A.1, -251A, -232A.2 and -320. I normalized each mAb according to the number of antigen binding sites and tested binding starting at concentration of 500 nM followed by eleven serial dilutions. Every concentration was tested in duplicate and the complete experiment was repeated three times. I used these data to determine the EC_{50} value of each mAb when binding to NoV GI.1, GI.2, GI.3, GII.3, GII.4, GII.6, GII.13 and GII.17 VLPs (Figure 4-1). NORO-168.2, -156.3, -170.5, all IgMs, and NORO-251A, an IgG, all exhibited the most breadth by binding to all eight VLPs tested. Both IgAs, NORO-232A.2 and -320, as well as NORO-167.3, an IgG, maintained breadth only to GII variants.

To determine if any of the isolated cross-reactive mAbs had functional activity I used a surrogate system to analyze neutralization. PGM which has been purified from porcine stomach mucosa contains both H and Lewis antigen, α-1,2- fucose and α-1,4-fucose respectively (Lindesmith et al. 2008; Lindesmith, Debbink, et al. 2012; Tian et al. 2010). The use of PGM in blockade assays has been previously validated (Lindesmith, Beltramello, et al. 2012). I first tested if GI.1, GI.2, GI.3, GII.3, GII.4, GII.6, GII.13 and GII.17 VLPs could bind to the glycans present in PGM. All the mAbs were normalized before testing blockade ability and tested at concentrations beginning at 1000 nM and then serially diluted (Figure 4-2). Blockade studies were also repeated three times. Unfortunately, only GI.3, GII.4, GII.6 and GII.17 were able to bind to PGM. NORO-161.2, -155.5, -170.5, all IgMs, and -167.3, an IgG, were not able to inhibit GI.3, GII.4, GII.6 or GII.17 VLPs from binding to PGM *in vitro*. Surprisingly, NORO-251A blocked GI.3, GII.4, GII.6 and GII.17 VLPs from binding to PGM. In previous studies, NORO-251A did not block GII.4 VLPs from binding to PGM when tested at similar concentrations. This difference could potentially be attributable to the variation is glycans present in the PGM. Ten of the fourteen mAbs isolated were able to block at least one of the four VLPs tested.

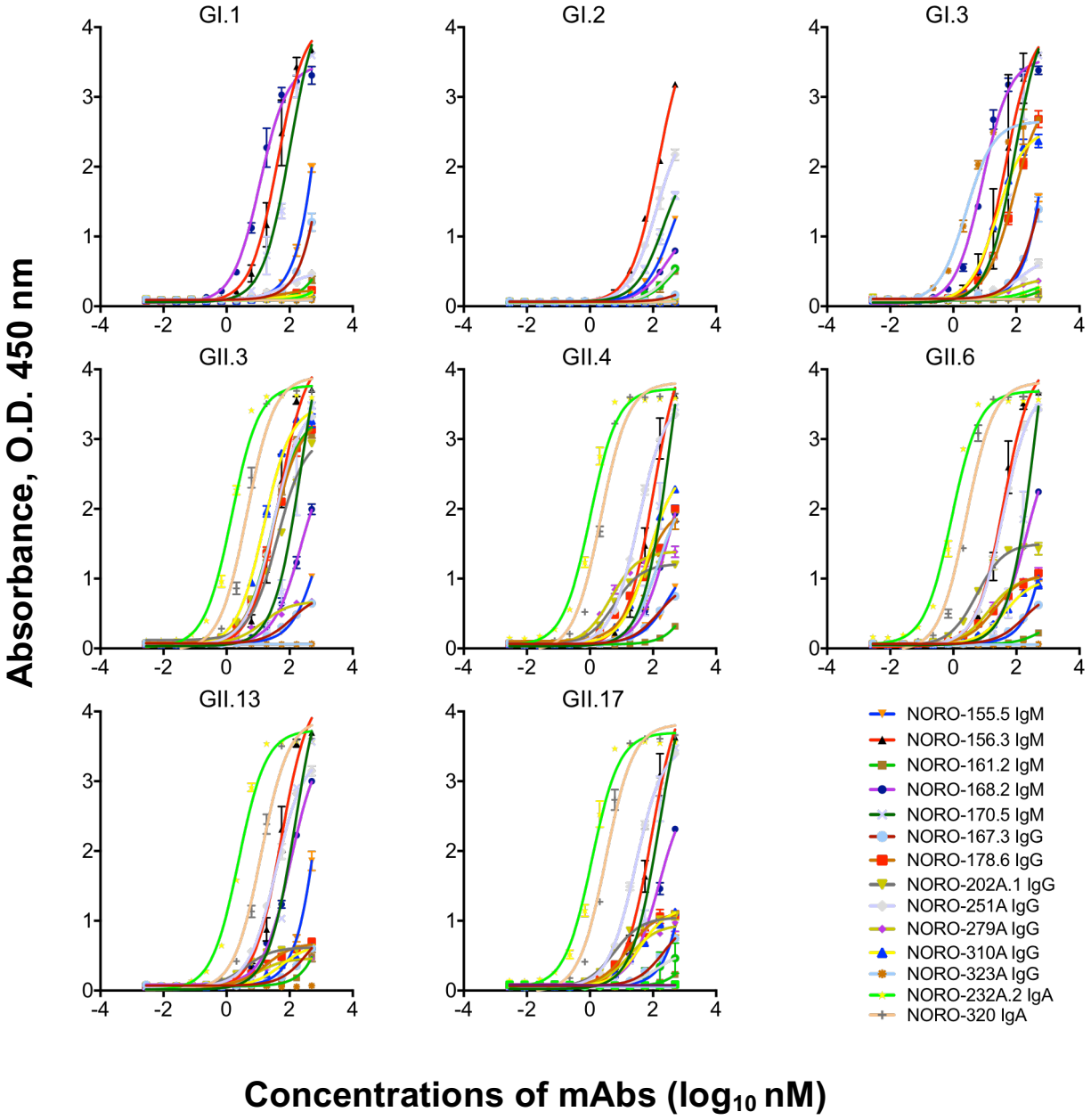

Figure 4-1. Binding activity of cross-reactive human mAbs to GI and GII VLPs. Indirect ELISA was used to assess binding activity of serially diluted fourteen isolated human mAbs to GI.1, GI.2, GI.3, GII.3, GII.4, GII.6, GII.13 and GII.17 VLPs.

			EC_{50} (nM)							
			Genogroup I			Genogroup II				
Isotype	NORO-	κ / λ	GI.1	GI.2	GI.3	GII.3	GII.4	GII.6	GII.13	GII.17
IgM	155.5	κ	>	415	>	>	332	>	>	>
	156.3	κ	42	175	47	46	106	39	54	90
	161.2	λ	>	>	>	27	>	>	>	>
	168.2	κ	11	265	8	224	285	198	107	153
	170.5	κ	104	209	90	233	366	474	154	158
IgG	167.3	λ	>	>	>	115	152	176	383	226
	178.6	λ	>	>	83	29	49	20	18	16
	202A.1	λ	>	>	>	41	6	6	4	6
	251A	λ	68	129	124	31	35	37	37	28
	279A	λ	>	>	70	14	5	14	10	18
	310A	κ	>	>	24	15	72	44	53	40
	323A	λ	>	>	3	>	146	>	>	>
IgA	232A.2	κ	>	>	>	1	1	1	2	1
	320	κ	>	>	>	4	2	3	12	3

Figure 4-2. Half-maximal effective concentrations (EC_{50}) for binding of cross-reactive human mAbs to GI and GII VLPs. Listed are the isotype, light chain and EC_{50} value to GI.1, GI.2, GI.3, GII.3, GII.4, GII.6, GII.13 and GII.17 VLPs. The > indicates binding EC_{50} greater than 500 nm. Greater EC_{50} values are in the lightest shade of orange and lowest EC_{50} values are in the darkest shade of orange.

A

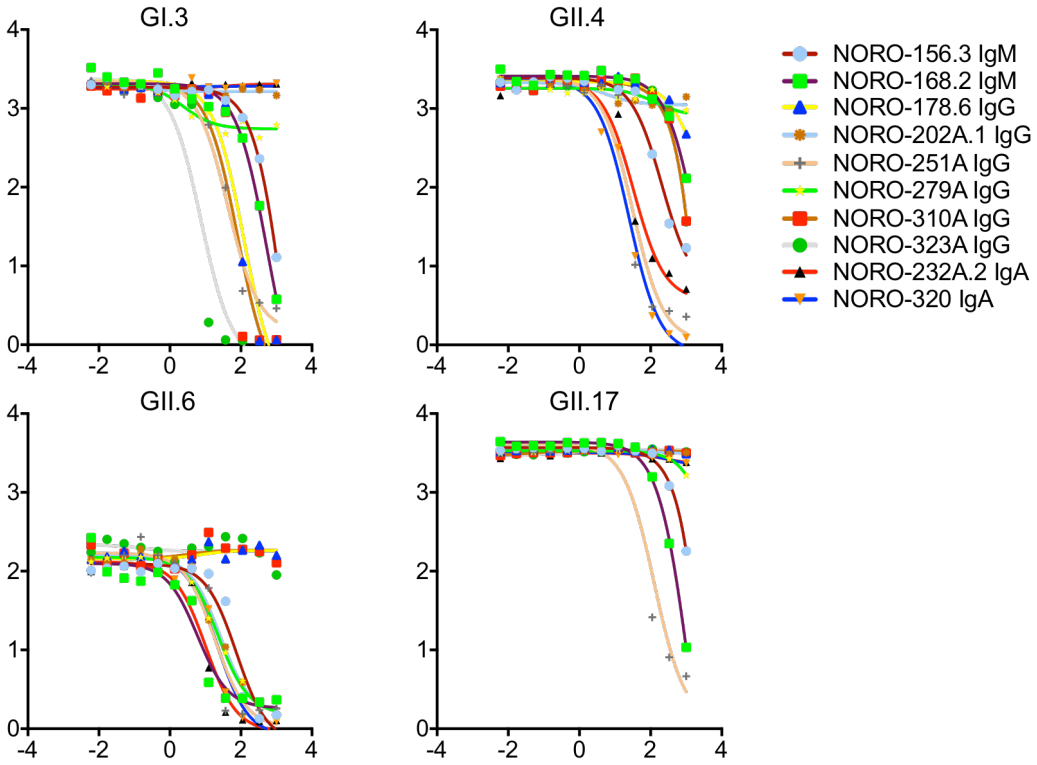

B

		EC_{50} (nM)			
Isotype	**NORO-**	**GI.3**	**GII.4**	**GII.6**	**GII.17**
IgM	156.3	678	>	355	>
	168.2	>	>	7	>
IgG	178.6	470	>	>	>
	202A.1	>	>	47	>
	251A	40	93	23	135
	279A	>	>	32	>
	310A	192	>	>	>
	323A	15	>	>	>
IgA	232A.2	>	115	20	>
	320	>	73	36	>

Figure 4-3. Blockade activity of cross-reactive human mAbs to GI and GII VLPs. A) A surrogate system to test neutralization of GI.1, GI.2, GI.3, GII.3, GII.4, GII.6, GII.13 and GII.17 VLPs using the isolated human mAbs. Blockade activity was tested using serial dilutions of each mAb. **B)** Half-maximal effective concentrations (EC_{50}) for cross-reactive mAbs when blocking GI and GII VLPs from binding to PGM. The > symbol indicates binding EC_{50} greater than 1000 nm.

Binding to GI.3, GII.4, GII.6 or GII.17 variant protruding vs shell domains

The major capsid protein, VP1, which is expressed on VLPs, is divided into a shell and protruding domain. To begin mapping where the cross-reactive mAbs could be binding, I decided to first recombinantly express the shell and protruding domains each independently for GI.3, GIII.4, GII.6 and GII.17. This way, both domains could be independently used as individual antigens in an ELISA and compared to binding results using a complete VLP, expressing both the protruding and shell domain together. GST-tagged recombinant P domains were expressed in *Escherichia coli* and purified using affinity column chromatography, as has been previously described (Choi et al. 2008). S domain sequences were cloned into pVL1392 and expressed using a baculovirus expression system and purified using a sucrose and cesium chloride cushion gradient. P and S domain recombinant proteins were coated at equal concentrations of 2 µg/mL on microtiter plated and blocked with 5% nonfat dry milk 1X DPBS with 0.05% Tween-20. Before adding the mAbs to plates, I normalized each mAb according to the number of antigen binding sites. I tested binding starting at concentration of 500 nM followed by eleven serial dilutions of each mAb to obtain the half-maximal binding concentrations. Both IgAs, NORO-232A.2 and -320, appear to be specific to the GI.3, GII.4, GII.6 and GII.17 P domain (Figure 4-4). Cross-reactive murine mAbs have also been mapped to the NoV protruding domain (Parker et al. 2005). NORO-168.2 bound to both the P and S domain of GI.3, GII.4, GII.6 and GII.17, but in all instances had a lower EC_{50} value when bound to the S domain. NORO-251A, one of the mAbs with the most binding and neutralizing breath, bound exclusively to the S domain of GI.3, GII.4 and GII.17. This was an unexpected result because typically very broad mAbs that bind to the shell domain lack any neutralizing activity (Parra et al. 2013). In rare instances, S domain binding mAbs have partially inhibited binding to carbohydrates *in vitro* (Parra et al. 2012). Some mAbs like NORO-156.3 did not bind to any of the P or S domains tested. This could be due to differences in the expression of the antigens, either bacterial or insect cells, or the need for a necessary conformational interaction between the shell and

protruding domain to achieve Ab binding.

		EC_{50} (nM)							
		GI.3		GII.4		GII.6		GII.17	
Isotype	NORO-	GST P	Shell	GST P	Shell	GST P	Shell	GST P	Shell
IgM	168.2	143	37	238	78	135	162	390	183
	161.2	>	>	>	>	>	>	>	>
	156.3	>	>	>	>	>	>	>	>
	155.5	>	>	>	>	>	>	>	>
	170.5	>	385	>	>	>	304	>	255
IgG	279A	>	>	>	3	>	>	>	>
	178.6	336	>	>	8	>	>	>	>
	310A	60	>	219	19	>	>	>	>
	202A.1	>	>	>	3	>	>	>	>
	251A	>	89	>	27	>	>	>	102
	323A	7	>	172	>	>	>	>	>
	167.3	>	>	>	90	>	>	>	>
IgA	232A.2	>	>	3	>	2	>	2	>
	320	>	>	2	>	3	>	3	>

Figure 4-4. Half-maximal effective concentrations (EC_{50}) for cross-reactive human mAbs when binding to protruding or shell domain. GI.3, GII.4, GII.6 and GII.17 NoV strain protruding or shell domain were used as antigen n an indirect ELISA. The > symbol indicates binding EC_{50} greater than 500 nm.

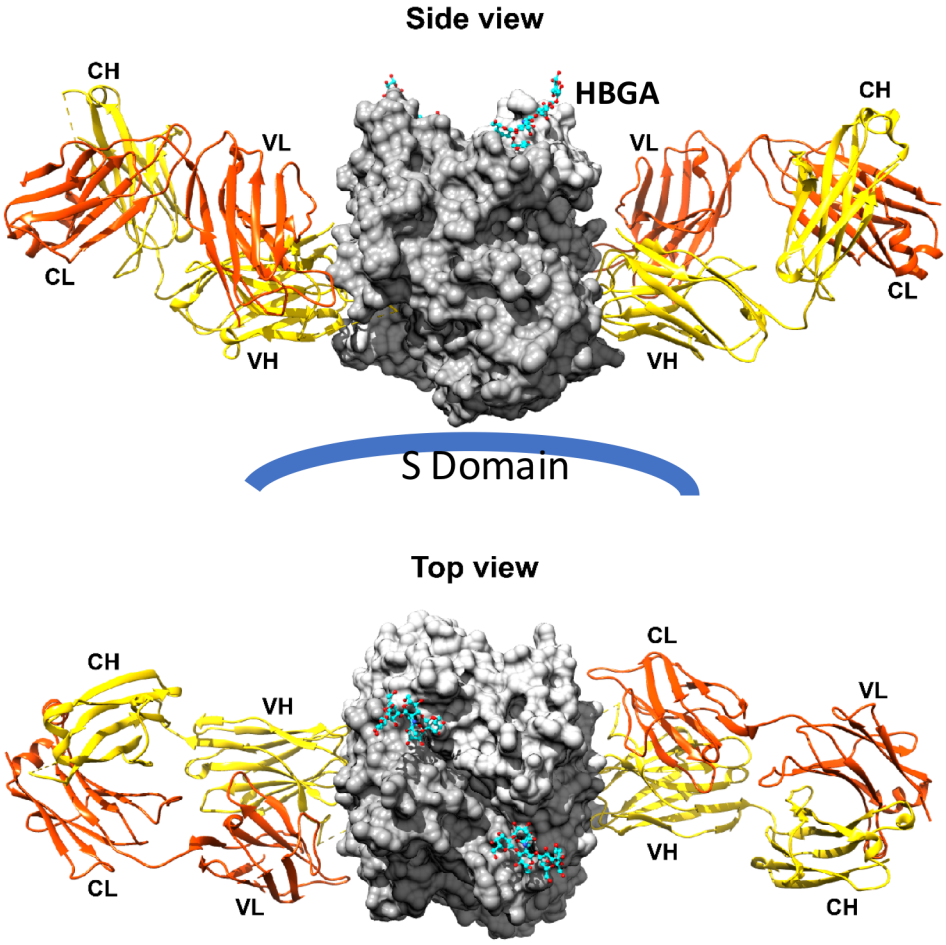

Figure 4-5. NORO-320 Fab in complex with GII.4 P domain. X-ray crystal structure of a GII.4 P domain dimer (grey) with two molecules of NORO-320 Fab (yellow-heavy chain and red-light chain) and two molecules of glycan bound. Depicted are a side and top view of the complex. Figure credit: Wilhelm Salmen (Prasad laboratory)

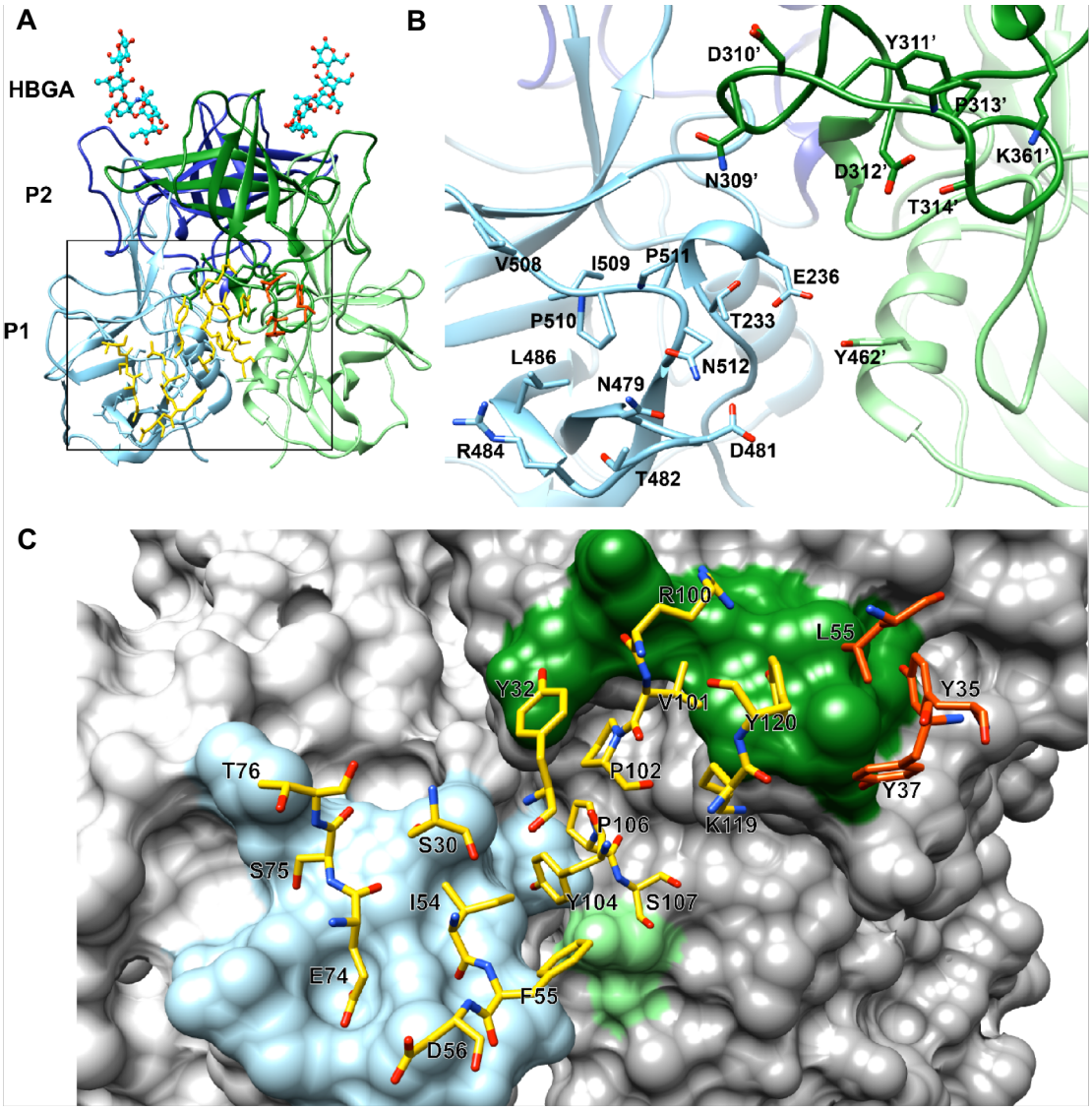

Figure 4-6. Close-up view of NORO-320 in complex with GII.4 P domain. A) GII.4 P domain dimer (light and dark blue as well as light and dark green) with one NORO-320 Fab (yellow-variable heavy chain and red-variable light chain)) molecule and 2 HBGA molecules bound. **B)** Included are the GII.4 P domain amino acid residues that interact with NORO-320 Fab. **C)** Residues on the variable heavy and light chain that interact with the GII.4 P domain. Figure credit: Wilhelm Salmen (Prasad laboratory)

Mechanism of neutralization of NoV by broad human mAb

To identify the potential mechanisms of neutralization for my broadly binding and neutralizing mAbs, we collaborated with Dr. Prasad at the Baylor College of Medicine. We decided to start with NORO-320, a dIgA, with broadly binding potential, across NoV GII.3, GII.4, GII.6, GII.13 and GII.17 VLPs, and the ability to block GII.4, GII.6 and GII.17 from binding to PGM. In our previous studies, we learned that NORO-320 not only neutralizes via a surrogate system established to test neutralization, but also inhibits replication of live GII.4 Sydney 2012 virus (Alvarado et al. 2018). I provided Dr. Prasad's laboratory with recombinantly expressed NORO-320 Fab and they obtained a 2.4 Å resolution of NORO-320 Fab in complex with GII.4 P domain. According to the crystal structure, NORO-320 Fab binds perpendicular to the P domain dimer and binds near a region close to the shell domain (Figure 4-5). This means NORO-320 Fab does not bind directly to the HBGA binding site to inhibit GII.4 VLP-carbohydrate binding or replication of GII.4 Sydney 2012 virus. We also learned that upon binding, NORO-320 Fab does not cause and conformational changes on the GII.4 P domain. We hypothesized that neutralization of GII.4 by NORO-320 could be a result of steric hindrance, since full-length NORO-320 is originally a dimeric IgA.

To determine if NORO-320 is neutralizing GII.4 because it is sterically hindering binding to glycans, I wanted to test if blockade activity was influenced by the molecular weight, or size, of NORO-320. In order to obtain varying forms of NORO-320, I recombinantly expressed the sequence of the variable domain into Fab and IgG recombinant expression vectors. The light chain variable sequence was also cloned into a kappa recombinant expression vector. Corresponding heavy and light chains were transfected using Chinese hamster ovary (CHO) cells with a ExpiCHO^{TM} expression system. To verify the molecular weight of the original hybridoma and all recombinantly expressed mAbs, I resolved 4 µg of each mAb, along with a set of control mAbs of known molecular weight, on a SDS-PAGE gel under non-reducing conditions (Figure 4-6A). All the mAbs were of expected molecular weight, dIgA ~350 kDa, IgG

~150 kDa and Fab ~50 kDa. I then tested NORO-320 IgA, recombinant IgG, recombinant Fab and a no mAb control for their ability to inhibit GII.4 Sydney 2012 VLPs from binding to PGM *in vitro*. As hypothesized, NORO-320 IgA had the lowest EC_{50} value followed by NORO-320 recombinant IgG (Figure 4-6B). Recombinant NORO-320 Fab did not block GII.4 Sydney 2012 VLPs from binding to PGM at concentrations as high as 1000 nM.

Materials and methods

Generation of NoV virus-like particles

VLPs based on norovirus strains GI.1 (M87661), GI.2 (AF435807), GI.3 (AF439267), GII.3 (TCH02-104), GII.4 (AFV08795.1), GII.6 (AF414410), GII.13 (JN899242) and GII.17 (AB983218) were recombinantly expressed and purified as previously described (Jiang et al. 1992). Briefly, I used a baculovirus recombinant protein expression system for VLP production. We cloned the VP1 and VP2, major and minor, protein capsid sequence from each strain into the transfer vector pVL1392 (Epoch Life Science, Inc). Sf9 insect cells were co-transfected with a transfer vector corresponding to a specific strain and with a bacmid vector. Recombinant baculovirus was isolated and expanded. I then purified the VLPs from cell culture supernatants using a sucrose and cesium chloride gradient. VLP formation was verified using electron microscopy.

A)

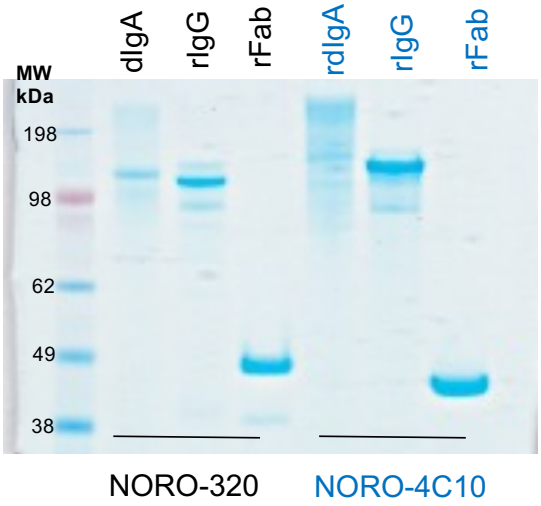

B)

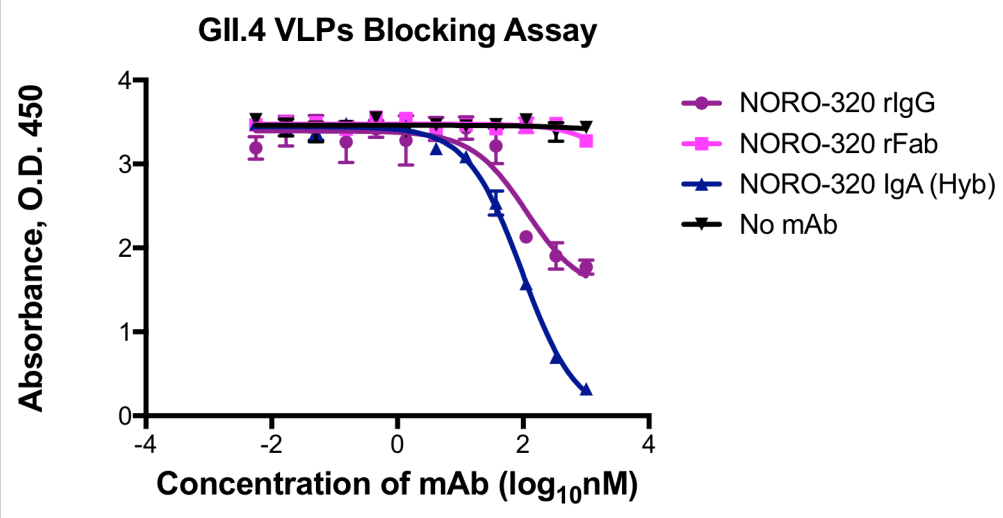

NORO-320	GII.4 VLP EC_{50} (nM)
rIgG	113
rFab	>
dIgA	96
No mAb	N/A

Figure 4-7. Recombinantly expressed NORO-320 variants and GII.4 VLP blockade ability. A) NORO-320 dIgA and recombinantly expressed IgG and Fab were resolved under non-reducing conditions on a SDS-PAGE gel. NORO-4C10 recombinant dIgA, IgG and Fab were used as controls**. B)** Blockade function of NORO-320 dIgA and recombinant IgG and Fab was tested with GII.4 Sydney 2012 VLPs. Blockade half-maximal effective concentrations (EC_{50}) values are also noted. The > symbol indicates EC_{50} values greater than 1000 nM.

Reactivity to NoV VLPs by ELISA

To determine the binding potential of all isolated human mAbs to VLPs I used indirect ELISAs. Each VLP was coated individually at 1 μg/mL on 384-well microtiter plates at 4°C overnight. Plates then were blocked for one hour at room temperature using 5% nonfat dry milk 1XDPBS with 0.05% Tween-20. For screening and EC_{50} analysis, antibody reactivity to VLPs was detected using horseradish peroxidase (HRP) tagged anti-κ or -λ chain secondary antibodies (Southern Biotech). 1-Step™ Ultra-TMB Substrate Solution (Pierce ThermoFisher) was used to detest HRP activity.

Human subjects

The Vanderbilt University Medical Center Institutional Review Board approved of the participation of the six adult subjects used in this study. All participants also provided written informed consent before we obtained their blood samples. The subjects were healthy with a previous history of acute gastroenteritis.

Human hybridoma generation

Human hybridomas secreting human mAbs were generated as previously described (Alvarado et al. 2018). Briefly, PBMCs were isolated from human subject blood samples using Ficoll-Histopaque and density gradient centrifugation and then cryopreserved. Later, cells were thawed, transformed using Epstein-Barr virus, CpG10103, cyclosporine A and a Chk2 inhibitor and plated in a 384-well plate. Transformed cells were incubated at 37°C for 7 days, and then expanded into 96-well plates containing irradiated human PBMCs. Four days later, cell supernatants were screened by indirect ELISA for the presence of anti-norovirus VLP cross-reactive mAbs. B cells secreting cross-reactive mAbs were electrofused to HMMA2.5 myeloma cells and plated in medium containing hypoxanthine, aminopterin, thymidine and ouabain.

Hybridoma cell lines were incubated at 37°C for 14 days, and then supernatants were screened by indirect ELISA for productions of cross-reactive mAbs. Cell lines expressing cross-reactive mAbs then were cloned biologically using single-cell fluorescence activated cell sorting.

Purification of cross-reactive mAbs

To purify mAbs I first biologically cloned the hybridomas using single-cell sorting. Hybridoma cell lines producing cross-reactive mAbs were then expanded gradually from 48-well plates to 12-well plates, T-25, T-75 and eventually to four T-225 flasks for each cell line. Supernatant from each cell line also was screened by ELISA to determine the corresponding light chain for each clone. Following 4-weeks of incubation at 37°C, supernatant from the four T-225 flasks was harvested and filtered through a 0.4-µm filter. The supernatant was filtered using column chromatography, specifically HiTrap KappaSelect and Lambda FabSelect affinity resins (GE Healthcare Life Sciences).

VLP-carbohydrate mAb blockade assay

To test the ability of each mAbs to inhibit the interaction between the selected VLPs and glycans *in vitro* I used a blockade assay. As previously described, I coated microtiter plates with 10 µg/mL of pig gastric mucin Type III (Sigma) for 4 hours at room temperature. Plates were then blocked overnight at 4°C in 5% nonfat dry milk. VLPs at 0.5 µg/mL were pretreated with serially diluted concentrations of each mAb for 1 hour at room temperature. VLP-mAb complexes were added to the PGM-coated and blocked microtiter plates. After 1 hour of incubation, the plates were washed 3 times with PBST and the same was done in between each step. Bound VLPs were tested using murine serum containing anti-GI.3, GII.4, GII.6 or GII.17 polyclonal antibodies, followed by a HRP conjugated goat anti-mouse IgG human adsorbed antibody. Optical density was measured at 450 nm using a Synergy HT Microplate Reader

(BioTek).

Expression and purification of protruding and shell domain for selected NoV strains to be used in Ab binding studies

In order to begin mapping the isolated cross-reactive mAbs I first recombinantly expressed P1 and P2 domain sequences or shell domain of GI.3 (AF439267), GII.4 (AFV08795.1), GII.6 (AF414410), GII.13 and GII.17 (AB983218). P domain sequences were cloned into the pGEX-4T-1 expression vector with a GST tag and thrombin cleavage site. The P domain was then expressed in *Escherichia coli* BL-21 cells and purified using a Glutathione Sepharose Fast Flow Column (GE Healthcare) and column chromatography.
The S domain sequences into pVL1392 and co-transfected with a bacmid vector into Sf9 insect cells. Recombinant baculovirus particles were then harvested and used to inoculate Sf9 cells. S domain particles were then purified from the inoculated Sf9 cell culture supernatant using a sucrose and a cesium chloride cushion gradient.

Expression, purification and crystallization of GII.4 P domain and NORO-320 Fab

The GII.4 P domain used in the crystallography studies was expressed, purified and crystallized with NORO-320 Fab by Dr. Prasad's laboratory. I provided Dr. Prasad's laboratory with recombinant NORO-320 Fab. The sequence for the GII.4 protruding domain was cloned into the expression vector pMal-C2E (New England BioLabs). The expression vector includes a N-terminal His_6-maltose binding protein (MBP) tag and a tobacco etch virus (TEV) protease cleavage site between the MBP and P domain sequence. The P domain was expressed in *Escherichia coli* BL21(DE3) and purified using an Affipure Ni-NTA agarose bead column (GenDepot). The His-MBP tag was then removed using TEV protease and separated from the P domain by purifying it once again using His-Trap (GE Healthcare), MBPTrap (GE Healthcare) affinity columns and size exclusion chromatography. Finally, the purified P domain was

concentrated and stored in 20 mM Tris-HCl buffer (pH 7.2) containing 150 mM NaCl, and 2.5 mM $MgCl_2$.

The nucleotide sequences of the variable domain of NORO-320 was optimized for mammalian expression and synthesized (Genscript) for expression and purification of recombinant Fab. The heavy chain fragment was cloned into a vector for expression of recombinant human Fabs (McLean et al. 2000). The light chain was cloned into a vector for κ light chain. Each vector was independently transformed into *Escherichia coli* cells and DNA was then purified. Both the heavy and light chain were transfected into CHO cells using an ExpiCHO™ expression system. Cell supernatant was collected, centrifuged and filtered using a 0.45 µm filter. NORO-320 Fab was purified by affinity chromatography using a KappaSelect (GE Healthcare).

Purified GII.4 P domain and NORO-320 Fab were combined in a 1:1.5 molar ration and incubated for 1 hour at 4 °C. The mixture was run through an S75pg 16/60 gel filtration column, and the peak corresponding to the complex was collected. The size of the complex and presence of both protein was validated on a SDS-PAGE gel. The peak fractions were then pooled and concentrated to 10 mg/mL for crystallization trials. Crystallization screening using hanging-drop vapor diffusion method at 20 °C was set up by a Mosquito nanoliter handling system (TTP LabTech) with commercially available crystal screens, and crystals were visualized by using a Rock Imager (Formulatrix). The GII.4 P domain–NORO-320 Fab complex crystallized in a buffer containing 0.1 M BIS-TRIS prop 8.5 pH, 0.2 M KSCN, 20% w/v PEG 3350. Crystals diffracted to 2.25Å resolution.

Discussion

The genetic and antigenic diversity across NoVs makes the generation of a broadly immunogenic vaccine extremely difficult. Identification of conserved antigenic epitopes on circulating strains of NoV would be useful information that could potentially be used to guide vaccine design. Cross-reactive and broadly neutralizing human mAbs could potentially be used to identify these conserved sites among circulating strains of NoV.

The primary goal of this study was to define the molecular and structural determinants of cross-reactive binding and blocking, or neutralizing, human mAbs to circulating strains of HuNoV. Previous studies have characterized the antigenic landscape of specific HuNoV strains, but with the rapid emergence of new genetically diverse strains there is still the need to map new immunogenic epitopes. This new information can also build upon previous studies to help track the evolution of HuNoV. Identification of antigenic epitopes using human mAbs also will provide insight into the immunogenicity of NoV proteins in humans.

In this chapter, I describe the isolation of fourteen NoV cross-reactive human monoclonal mAbs, seven IgGs, two IgAs and five IgMs, from patients with a previous history of acute gastroenteritis. To isolate human cross-reactive and broadly blocking mAbs, I obtained de-identified PBMCs and transformed them with EBV. To screen for robust antibody secretion, supernatants from wells containing EBV-transformed LCLs were used for an indirect ELISA while using NoV GI.1, GI.2, GI.3, GII.3, GII.4, GII.6, GII.13 and GII.17 VLPs each independently as antigen. LCLs then were fused with myeloma cells to form human hybridomas. The hybridoma cells then were screened for anti-HuNoV antibody production to at least two of the VLPs tested and the positive wells were expanded and single-cell sorted using a fluorescence-activated cell sorter. Single hybridoma cells were given time to proliferate and supernatants with secreted antibodies were once again screened for binding reactivity.

To determine the functional activity of the isolated mAbs, I used a surrogate blockade assay that measures the inhibition of VLPs from binding to glycans *in vitro*. Unfortunately, not all

eight VLPs bind to the same glycan, so I was only able to test the inhibition of binding for NoV VLPs GI.3, GII.4, GII.6 and GII.17. Of the fourteen mAbs isolated, ten mAbs blocked at least one of four VLPs testing from binding to PGM with EC_{50} values less than 1000 nM. Interestingly, one of the isolated IgGs broadly bound and blocked NoV VLPs GI.3, GII.3, GII.6 and GII.17. NORO-168.2, an IgM, was able to block GI.3 and GII.6. Meanwhile, the blockade ability of eight of the fourteen mAbs remained specific to either GI or GII strains.

I hypothesized that cross-reactive and neutralizing human antibodies isolated will bind to the P subdomain of the circulating strains, similar to the findings for cross-reactive murine Abs (Crawford et al. 2015). The P domain has more surface exposure on a live virion and should therefore be more accessible than the S domain. To begin mapping where these cross-reactive broadly blocking mAbs could be binding, I used an indirect ELISA with protruding or shell domain recombinant proteins as antigen. All fourteen mAbs were tested for binding to GI.3, GII.4, GII.6 and GII.17 P or S domain proteins. NORO-251A, a mAb that bound to GI.1, GI.2, GI.3, GII.3, GII.4, GII.6, GII.13 and GII.17 VLPs bound specifically to the GI.3, GII.4 and GII.17 shell domain. GII specific mAbs like NORO-232A.2, -320, bound to the GII.4, GII.6 and GII.17 P domain.

Three-dimensional characterization using X-ray crystallography of NORO-320 bound to GII.4 Sydney 2012 P domain also showed that the NORO-320 Fab binds perpendicular to the GII.4 P domain. Even though NORO-320 does not directly bind to the receptor binding domain, as 5I2 bound to GI.1 P domain (Shanker et al. 2014), it still inhibits GII.4 VLPs from binding to glycans *in vitro* and inhibits viral replication of GII.4 Sydney 2012 virus (Alvarado et al. 2018). There was no change in structural conformation of the GII.4 P domain noted when NORO-320 Fab bound to it. We hypothesized that NORO-320, originally isolated as a dIgA, could be mediating neutralization of GII.4 through steric hindrance. To determine if the molecular size of the mAb was influencing neutralization, I created two recombinant variants, IgG of ~150 kDa and Fab of ~50 kDa, to compare with the original IgA of about ~320 kDa in size. Blocking

potential increased with the increase in molecular size of the NORO-320 variants tested. This study identifies a new method of neutralization for GII.4 NoV.

Amino acids believed to be critical to the interaction between GII.4 and NORO-320 also appear to be conserved among GI.3, GII.6 and GII.17 which could indicate that they are neutralized similarly. To test if a similar binding method is used by VLPs that do not bind to PGM, we will also attempt to co-crystallize NORO-320 with GII.6. Our studies will provide a thorough analysis of the nature of cross-reactive human anti-NoV mAbs. In collaboration with Dr. Estes' laboratory we also plan on verifying neutralization with our broadest mAbs with a HIE system.

CHAPTER V

SUMMARY AND FUTURE DIRECTIONS

Thesis summary

Human noroviruses, also known as Norwalk-like viruses, are the leading cause of sporadic and epidemic gastroenteritis in humans (Glass et al. 2009). The U.S. Center for Disease Control estimated that annually on average, NoV causes nearly 71,000 hospitalizations and 570 to 800 deaths (Hall et al. 2013). Outbreaks of NoV most frequently occur in closed crowded environments like nursing homes, schools, hospitals, and cruise ships. NoV is transmitted via the fecal-oral route and is highly infectious (Heijne et al. 2009). Over 40 strains of NoV exist and it is believed that immune selection pressures have driven strain evolution (Vinjé 2015; Karst & Baric 2015).

NoV research has been hindered by the lack of a robust *in vitro* cell culture system or small animal model that resembles human disease. There are no vaccines, therapeutics, or prophylactics available to prevent or treat NoV infection. Little is known about the human humoral immune response to NoV infection. To design a vaccine that elicits broad protective immunity, we must have a solid understanding of the NoV-mediated human antibody response to infection and antigenic sites recognized by human antibodies, so a critical area of human norovirus research has become the identification of type specific and cross-genotype and genogroup epitopes.

My general hypothesis was that in response to NoV infection, humans produce cross-reactive neutralizing antibodies. The primary goal of my dissertation research was to define the molecular and structural determinants of strain specific or broadly neutralizing human mAbs and to improve our understanding of mechanism guiding neutralization. We decided to take an approach that would include the high efficiency isolation of human mAbs from patients

previously infected with NoV coupled with three-dimensional structural analysis to comprehend mechanisms of antibody mediated neutralization of NoV. This information is extremely valuable to the NoV field because it can aid in the development of vaccines and therapeutics. Our studies were also expected to generate a panel of fully human mAbs that could be directly used to prevent and treat NoV infection. To accomplish our goals, we recruited the help of Dr. Mary Estes and Dr. B.V. Venkataram Prasad and their laboratories who are experts in virology and structural biology.

NoV GI.1, also known as Norwalk virus, is considered the prototype of human NoVs and was first identified in 1972 as the causative agent of acute infectious nonbacterial gastroenteritis (Kapikian et al. 1972). Today, it continues to be a threat to human health. Using hybridoma technology, we were able to isolate a panel of fourteen human mAbs, seven IgGs and seven dIgAs, from two donors who were previously challenged with live GI.1 NoV. We then proceeded to functionally characterize ten mAbs, five IgGs and five dIgAs, from Donor 1. Antibody reactivity to GI.1 Norwalk VLPs was assessed using indirect ELISA. According to the EC_{50} values from our panel of mAbs, IgG mAbs were more potent binders than dIgAs. To analyze neutralization capabilities of the ten mAbs isolated from Donor 1, we used an *in vitro* HBGA blocking assay. This blocking assay was previously validated and it was concluded that it may be used as a surrogate method for measuring virus neutralization (Reeck et al. 2010). Unlike binding activity, no clear isotype dependent blocking pattern emerged from the antibodies tested. Interestingly, if blocking IC_{50} and binding EC_{50} for each mAb were evaluated together, meaning each blocking IC_{50} was divided by the corresponding mAb binding EC_{50}, the results suggested that IgAs as a class blocked more effectively.

To determine the effects of antibody isotype, specifically the constant domain, on binding and blocking efficiency, I engineered and expressed IgG, mIgA and dIgA isotype switch variant recombinant Igs for five of the ten GI.1 VLP specific hybridoma mAbs and assessed mAb binding and blockade activity of GI.1 VLPs. To analyze disruption of interaction between

the VLPs and host cell attachment factors *in vitro*, I once again used a surrogate neutralization assay. Using switch variant recombinant mAbs would allow me to test whether the differences in binding and blocking were attributable to general differences between the isotypes themselves such as avidity or molecular size, or to distinctions in antibody specificity, as a result of variances in their variable domain sequences. From these studies, I was able to conclude that in fact the IgA forms of each antibody blocked GI.1 VLPs from binding to host cell attachment factors *in vitro* more potently than IgGs. Surprisingly, ratios for mIgAs, which are half the molecular weight and have half the number of antigen binding sites as a dIgA, blocked just as well and sometimes even better than dIgAs. This data implies that differences in blocking efficiency are likely due to differences in the CH1, CH2 or CH3 domain.

In collaboration with B.V. Venkataram Prasad at the Baylor College of Medicine, we used X-ray crystallography to define antigenic epitopes on the major capsid protein of GI.1 and elucidate the mechanism behind human mAb mediated neutralization. A crystal structure was obtained with 5I2 Fab in complex with the GI.1 VP1 protein. The structural data shows the 5I2 Fab CDR1 light chain binding to a loop located on the top of the P2 subdomain of VP1. There also were not any conformational changes in the VP1 protein when the Fab fragment is bound to the P2 subdomain. The 5I2 binding site also appears to be relatively close to the HBGA binding site, so it could be neutralizing the GI.1 VLPs by blocking access to HBGAs. These findings suggest a new role for IgA antibodies against norovirus and provide insight into neutralization of GI.1 NoV.

NoV GI.1 is only one of many circulating strains of human NoV. From September 2013 to February 2015, CaliciNet, the U.S. national NoV outbreak surveillance network, reported that GII.4 Sydney, GII.6, GII.13, GI.3, and GI.2 were responsible for the majority of NoV outbreaks. GII.4 Sydney was the predominant strain causing more than half of the outbreaks. In 2012, GII.4 Sydney emerged as the predominant norovirus strain and to this day still continues to be responsible for the majority of outbreaks. Limited information is known on the antigenicity and

potential neutralization of live virus GII.4 Sydney 2012. Therefore, I decided to isolate and characterize human mAbs that bind and neutralize GII.4 Sydney 2012.

I isolated a panel of twenty-five human mAbs, twenty-one IgGs and four dIgAs, that bind to GII.4 Sydney VLPs. To characterize GII.4 Sydney 2012 binding mAbs, I sequenced each hydridoma line, determined the EC_{50} values for binding to GII.4 Sydney VLPs and for inhibition of binding of the VLPs to glycans *in vitro*. Of the panel of twenty-five mAbs, I was able to sequence both the heavy and light chain sequences of seventeen mAbs. All seventeen appear to be different mAbs because they all had unique HCDR3 sequences. Using indirect ELISA, we determined binding EC_{50} values for the twenty-one IgG and four dIgAs. To evaluate the mAb potential blockade response, I used a HBGA blocking assay and a hemagglutination inhibition assay. Approximately 32% of the mAbs did not block GII.4 Sydney VLPs from binding to PGM at mAb concentrations as high as 40 µg/mL. Similarly, 32% of the mAbs also did not inhibit hemagglutination of O+ red blood cells at concentrations at high as 15 µg/mL. The majority of the mAbs had similar HAI to blockade activity, within about a two-fold mAb concentration difference, except for four mAbs, which either had a greater than two-fold difference or had HAI activity when they did not have blockade activity or vice versa. In collaboration with Dr. Mary Estes' laboratory, we used human enteroids to test neutralization of live GII.4 Sydney 2012 virus using NORO-263, -250B, -320, -273A and -318A. All 5 of the mAbs tested inhibited replication of NoV GII.4 Only NORO-320 had a higher IC_{50} value than blockade or HAI EC_{50} values. Which suggests, that at times the HIE neutralization assay is more sensitive than the HBGA blockade or HAI assays. One reason why the HIE neutralization assay could be more sensitive than the surrogate systems is because the surrogate system mainly measures the ability of mAbs to neutralize NoV by blocking attachment to glycan receptors. Meanwhile, the HIE could be measuring other methods of neutralization by mAbs such as blocking uptake into a cell or preventing genome uncoating.

To identify potential binding epitopes on GII.4 Sydney, I recombinantly expressed GST-

GII.4 Sydney P domain dimers and used it in conjunction with recombinantly expressed S domain provided by Dr. Prasad's laboratory and used them both as individual antigens in an indirect ELISA assay. If binding was drastically reduced when using the P domain dimer or S domain I could conclude that binding was specific to the opposing domain. Five mAbs did not bind to P domain, but did bind to S domain. Using Bio-layer Interferometry, I also performed a competition-binding assay and identified three potential competition groups on the GII.4 Sydney P domain.

Using human monoclonal antibodies, I also wanted to define the determinants of molecular cross-reactivity and broad blockade to eight of the major circulating strains of human NoV, GI.1, GI.2, GI.3, GII.3, GII.4, GII.6, GII.13 and GII.17. Specifically, I was interested in isolating cross-reactive broadly blocking, or neutralizing, mAbs and identifying their epitopes. This information would be useful when reformulating multivalent VLPs for HuNoV vaccine trials, since the goal of a vaccine is to elicit a protective response against more than one circulating strain of HuNoV. We hypothesized that human broadly neutralizing antibodies to eight current major circulating strains of NoV exist. NoV is an enteric pathogen, so I decided to isolate dIgAs and IgMs in addition to IgGs, since both IgAs and IgMs play a critical role in intestinal immunity.

I have a panel of fourteen different inter or intra-genogroup cross-reactive independent mAbs. Six of the fourteen mAbs were previously included in the panel of GII.4 Sydney 2012 reactive mAbs. Three of the mAbs tested were also reactive to all the VLPs tested. The majority of the mAbs, about ten mAbs, were able to block at least one strain, of four NoV strains tested, from blocking to PGM *in vitro*. I only tested blockade of NoV GI.3, GII.4, GII.6 and GII.17 VLPs, strains capable of binding to PGM.

To begin identifying cross-reactive and blockade epitopes, I tested reactivity of the fourteen isolated mAbs to NoV GI.3, GII.4, GII.6 and GII.17 recombinantly expressed P and S domains. As expected, a couple of mAbs with the most breadth, NORO-168.2 and -251A had some specificity towards the shell domain. Surprisingly, NORO-232A.2 and -320, mAbs that

broadly bound to GII strains, were specific to the P domain. We also collaborated with Dr. Prasad's group to study NORO-320 Fab in complex with GII.4 P domain using X-ray crystallography. We were able to obtain a 2.4 Å resolution crystal structure that revealed that NORO-320 Fab binds perpendicular to the GII.4 P domain. To our surprise, this GII.4 neutralizing mAbs does not inhibit binding to the P domain by binding to or near the HBGA binding site. We hypothesized that NORO-320 dIgA could be neutralizing GII.4 as a result of steric hindrance. To test this hypothesis, I recombinantly expressed NORO-320 as a Fab and IgG and tested their blockade efficiency compared to a dIgA. We noticed that with a reduction of molecular size of the tested mAb that blockade efficiency also decreased implying that neutralization could be due to steric hindrance.

The cross-reactive or strain specific mAbs I have isolated to GI.1, GI.2, GI.3, GII.3, GII.4, GII.6, GII.13 and GII.17 can potentially be used as a prophylactic, therapeutic, or a reagent for diagnosis. Antigenic epitopes identified on any of these strains will also be useful when reformulating multivalent VLPs for HuNoV vaccine trials, since the goal of a vaccine is to elicit a protective response against more than one circulating strain of HuNoV. We also currently have the first neutralizing human monoclonal antibodies to human norovirus.

Future directions: therapeutics, vaccines and diagnostics

Significant strides have been made in NoV research within the past decade. We now have a better understanding of viral evolution, approaches to vaccine development, *in vitro* replication and the human antibody response to infection. Below, I propose ways in which we can build upon the findings gathered during my dissertation research to address some of the most critical problems that remain in areas of disease diagnosis, prevention and treatment in the NoV field.

In immunocompetent individuals, symptoms due to NoV infection are typically acute and self-limiting. However, for immunocompromised patients symptomatic infection and viral

shedding can be extensive. We know that antigenically and genetically diverse strains of NoV periodically emerge and replace older variants as the dominant strain, but how and where these strains might be originating it still unknown. Transmission of NoVs between animals and humans is thought to be unlikely due to the viruses' high species specificity. Instead, chronically infected immunocompromised patients are believed to be the reservoir of NoV strain diversity (Vega et al. 2014). This emphasizes the need for effective therapies to treat NoV infection. Previous studies have reported that immunocompromised patients benefited from oral human immunoglobulin treatment. Patients had a reduction of stool volume, increase in stool consistency, symptoms improved faster and had a decrease in length of hospital stay (Florescu et al. 2008). We also know that mice genetically deficient in B cells are not able to clear murine NoV infection as well as mice with B cell (Chachu et al. 2008). Furthermore, from this same study we also learned that passive immune transfer of anti-murine NoV polyclonal serum or anti-murine NoV mAbs can reduce systemic and intestinal infection. Therefore, I propose developing some of my post potent and broadly neutralizing mAbs as therapeutics. First, I recommend testing neutralization of the viruses that can replicate in human enteroids such as GI.1, GII.3, GII.4 and GII.17 HuNoV strains. Unfortunately, there is no ideal animal model to test neutralization efficiency i*n vivo* but there are some models available with some strengths. For instance, gnotobiotic pigs can be orally infected by GII.4 or GII.12 strains of HuNoV and can develop symptomatic infection with fecal shedding (Souza et al. 2007; Cheetham et al. 2006). Human mAbs with the lowest neutralization IC_{50} values to GII.4 could then be tested in gnotobiotic pigs. We should also determine the best route of administration, antibody half-life in the gastroentestinal system, appropriate dosage as well as efficacy and potency.

There are currently no licensed vaccines available to prevent NoV infection. The antigenic variation among circulating strains and rapid emergence of novel variants makes designing a vaccine that induces broad immunoprotection particularly challenging. Efficacious therapeutics and vaccines require a solid understanding of virus mediated immunological

responses. Fortunately, clinical trials have shown that VLP-based vaccines are well tolerated and capable of eliciting a robust immune response (Atmar et al. 2016) (Atmar et al. 2011). The VLP vaccine would require the periodic reformulation to account for emerging strains of NoV. The panel of fourteen human cross-reactive mAbs I have isolated to GI and GII NoV strains should be mapped to identify common neutralizing epitopes among circulating strains, so these epitopes can be taken into account for the reformulation of new NoV multivalent VLP vaccines. I have begun mapping studies using recombinantly expressed S and P domain. Inhibition of replication using live virus, HIEs and the isolated mAbs should also be tested and compared to the results I obtained using the surrogate system to test neutralization. Isolated mAbs can then be competed against each other using bio-layer interferometry or competition ELISA to identity potential binding and neutralizing groups on the S or P domain. Fortunately, our studies have already identified at least one neutralizing epitope using NORO-320. Antibodies with the lowest neutralizing IC_{50} values and broadest binding and neutralizing activity should then be crystalized in complex with strains they bind to identify, on a molecular level, the location of where they are binding. Newly identified capsid binding sequences can then be merged and included into new chimeric consensus GI and GII VLPs. Previous studies have shown that NoV GII.4 capsid chimeric vaccines can induce a broadly blocking immune response in mice. The broad response was even similar to that induced by multivalent vaccine formulations (Debbink, Lindesmith, Donaldson, et al. 2014). Reformulated chimeric VLPs with our new cross-reactive neutralizing epitopes should also be used to immunize mice. Serum can then be isolated from these mice and used *in vitro* in a surrogate neutralization to measure the presence of blocking antibodies. Our efforts have provided much needed information regarding the identification and characterization of emerging antigenic site of circulating strains of NoV and should be taken into consideration when designing new NoV vaccines.

Most viral infections are diagnosed by culturing the virus, nucleic acid detection antigen detection or serology (Storch 2000). The lack of an *in vitro* replication system or small animal

has made human NoV difficult to study. Initial identification of the virus in 1972 required the use of a novel method of visualization, immune electron microscopy, to circumvent the limitations at the time (Kapikian et al. 1972). Today, we still do not have a standard for laboratory detection of NoV infection. Diagnosis of NoV infection is usually based on symptoms due to the lack of sensitive methods of detections. Current methods available to detect NoV infection include electron microscopy (EM), immunoassays and nucleic acid-based detection (Pang & Lee 2015). Unfortunately, methods like EM and nucleic acid-based detection are costly, at times too sensitive making them prone to false positive results and requiring special instruments. The currently available immunoassays are also only able to detect a limited number of strains of HuNoV due to the absence of cross-reactive antibodies.

Using antigen detection as a method to test for the presence of a viruses with widespread antigenic heterogeneity can be difficult because of the lack of cross-reactive reagents. There are some advantages to antigen detection techniques such as rapid results, virus in specimen does not need to be viable, they are inexpensive, they do not require the use of equipment like a thermocycler or cull culture equipment and do not require the use of highly trained personnel to perform assays. The NoV strain specific and cross-reactive panel I have isolated could be useful for the creation of improved enzyme immune assays to detect NoV in stool samples.

In 2011, the Food and Drug Administration approved the marketing of Ridascreen® a 3rd generation NoV antigen enzyme immunoassay (EIA) that can screen for the presence of selected GI and GII NoV strains in fecal specimens. It is a solid phase sandwich-type EIA in which microwell strips are coated with a mixture of GI and GII specific mAbs. Fecal suspensions are then added to the strips and detected with biotinylated NoV specific mAbs. IDEIA Norovirus™ EIA by Oxoid is a similar system, but it has been reported that both assay lack sensitivity against particular circulating strains, like GII.17 Kawasaki 2014 (Chan et al. 2016).

There are also rapid immunochromatographic assays, or lateral flow assays, like Rida®quick Norovirus and SD Bioline Norovirus for the detection of GI and GII strains. Both assays significantly reduce the amount of time to complete testing from 90-105 mins to about 15 minutes compared to IDEIA and Ridascreen.

To determine if our isolated mAbs can improve current detection methods I recommend first testing the reactivity of all the anti-NoV mAbs we have isolated. Once we have gathered the specificity of each mAbs then it can be compared to the GI and GII strains currently advertised to be detectable by the current EIAs available. We currently have access to a series of different circulating GI and GII NoV VLPs, such as GI.1 GI.2, GI.3, GII.3, GII.4, GII.6, GII.13 and GII.17. The CDC has identified new circulating strains, so we can also use the major capsid protein of these new variants to recombinantly express new VLPs. At the same time, we can start engineering recombinant IgGs of the broadest mAbs to normalize the mAbs that will be used in each assay. We should also once again screen reactivity of recombinant forms of mAbs since we have noted some reactivity differences in switch variants. These results can then be compared to the sensitivity offered by available EIAs. For a lateral flow assay, we should attempt to biotinylated and gold-label the mAbs we plan to use in the assay. Assuming our panel, can contribute some improvement to current EIAs then we can begin to optimize factors that might influence assay conditions such as the diluent used for ant-NoV mAbs and concentration necessary for conjugated and capture mAbs.

LIST OF PUBLICATIONS RELEVANT TO DISSERTATION

1. Alvarado, G., Ettayebi, K., Atmar, R., Bombardi, R., Kose, N., Prasad, B.V.V., Estes, M., Crowe, J., (2018) *Isolation and characterization of human GI and GII cross-reactive and neutralizing human antibodies.* Gastroenterology. 2018.

2. Shanker, S., Czako, R., Sapparapu, G., Alvarado, G., Viskovska, M., Sankaran, B., Atmar, R., Crowe, J., Estes, M., Prasad, B.V.V., (2016) *Structural basis for norovirus neutralization by an HBGA blocking human IgA antibody.* Proceedings of the National Academy of Sciences U.S.A. 2016; 113:E5830-E5837.

3. Sapparapu, G.*, Czakó, R.*, Alvarado, G.*, Shanker, S., Prasad, B.V.V., Atmar, R., Estes, M., Crowe, J. Jr. (2016). *Frequent use of the IgA isotype in human B cells encoding potent norovirus-specific monoclonal antibodies that block HBGA binding.* Public Library of Science Pathogens. 2016; 12:e1005719

[* Co-first authors]

ADDITIONAL PUBLICATIONS FROM GRADUATE STUDIES

1. Manzanillo, P., Mouchess, M., Naruhisa, O., Bingbing, D., Ichikawa, R., Wuster, A., Haley, B., Alvarado, G., Kwon, Y., Caothien, R., Roose-Girma, M., Waming, S., McKenzie, B., Keir, M., Scherf, A., Ouyang, W., Tangsheng, Y. (2018) *Inflammatory bowel disease susceptibility gene C1ORF106 regulated intestinal epithelial permeability*. ImmunoHorizons. 2018; 2(5) 164-171

2. Mousa, J., Binshtein, E., Human, S., Fong, R., Alvarado, G., Doranz, B., Moore, M., Ohi, M., Crowe, J. (2018) *Human Antibody recognition of antigenic site IV on Pneumovirus fusion proteins*. Public Library of Science Pathogens. 2018; 14(2): e1006837

3. Mousa, J., Sauer, M., Sevy, A., Finn, J., Bates, J., Alvarado, G., King, H., Loerinc, L., Fong, R., Doranz, B., Correia, B., Kalyuzhniy, O., Wen, X., Jardetzky, T., Schief, W., Ohi, M., Meiler, J., Crowe, J. (2016) *Structural basis for nonneutralizing antibody competition at antigenic site II of the respiratory syncytial virus fusion protein*. Proceedings of the National Academy of Sciences U.S.A.. 2016; 113; E6849-E6858

4. Alvarado G., Crowe, J.E. Jr. (2016) *Development of human monoclonal antibodies against respiratory syncytial virus using a high efficiency human hybridoma technique.* Methods in Molecular Biology. 2016; 1442:63-76.

5. Guo, F., Ding, Y., Caberoy, N., Alvarado, G., Liu,R., Shen, C., Yu, J., Zhou, Y., Salero, E., LeBlanc, M., Wang, W., Li, W. (2015). *Lyar is a new ligand for retinal pigment epithelial phagocytosis*. Journal of Cellular Biochemistry. 2015; 116:2177-87

6. Guo, F., Ding, Y., Caberoy, N., Alvarado, G., Wang, F., Chen, R., Li, W. (2015). *ABCF1 extrinsically regulates retinal pigment epithelial cell phagocytosis*. Molecular Biology of the Cell. 2015; 26:2311-20

7. Knowles, B. C., Weis, V., Yu, S., Roland, J., Williams, J., Alvarado, G., Lapierre, L., Shub, M., Gao, N., Goldenring, J. (2015). *Rab11a regulates Syntaxin 3 localization and microvillus assembly in enterocytes*. Journal of Cell Science. 2015; 128:1617-26

8. LeBlanc, M.E., Wang, W., Caberoy, N.B., Chen, X., Guo, F., Alvarado, G., Shen, C., Wang, F., Wang, H., Chen, R., Liu, Z.J., Webster, K., Li, W. (2015). *Hepatoma-derived growth factor-related protein-3 is a novel angiogenic factor*. Public Library of Science One. 2015; 10:e01279

BIBLIOGRAPHY

Adams, P.D. et al., 2002. PHENIX: building new software for automated crystallographic structure determination. *Acta crystallographica. Section D, Biological crystallography*, 58(Pt 11), pp.1948–1954.

Adkins, J.C. & Wagstaff, A.J., 1998. Recombinant hepatitis B vaccine: a review of its immunogenicity and protective efficacy against hepatitis B. *BioDrugs : clinical immunotherapeutics, biopharmaceuticals and gene therapy*, 10(2), pp.137–158.

Aiyegbo, M.S. et al., 2013. Human rotavirus VP6-specific antibodies mediate intracellular neutralization by binding to a quaternary structure in the transcriptional pore. D. X. Liu, ed. *PloS one*, 8(5), p.e61101.

Alvarado, G. et al., 2018. Human Monoclonal Antibodies That Neutralize Pandemic GII.4 Noroviruses. *Gastroenterology*.

Atmar, R.L. et al., 2011. Norovirus vaccine against experimental human Norwalk Virus illness. *The New England journal of medicine*, 365(23), pp.2178–2187.

Atmar, R.L. et al., 2008. Norwalk virus shedding after experimental human infection. *Emerging infectious diseases*, 14(10), pp.1553–1557.

Atmar, R.L. et al., 2016. Rapid Responses to 2 Virus-Like Particle Norovirus Vaccine Candidate Formulations in Healthy Adults: A Randomized Controlled Trial. *The Journal of infectious diseases*, 214(6), pp.845–853.

Ball, J.M. et al., 1998. Oral immunization with recombinant Norwalk virus-like particles induces a systemic and mucosal immune response in mice. *Journal of virology*, 72(2), pp.1345–1353.

Ball, J.P. et al., 2017. Intranasal delivery of a bivalent norovirus vaccine formulated in an in situ gelling dry powder. Z. Xing, ed. *PloS one*, 12(5), p.e0177310.

Bartsch, S.M. et al., 2016. Global Economic Burden of Norovirus Gastroenteritis. D. R. Olson, ed. *PloS one*, 11(4), p.e0151219.

Battye, T.G.G. et al., 2011. iMOSFLM: a new graphical interface for diffraction-image processing with MOSFLM. *Acta crystallographica. Section D, Biological crystallography*, 67(Pt 4), pp.271–281.

Bernstein, D.I. et al., 2015. Norovirus vaccine against experimental human GII.4 virus illness: a challenge study in healthy adults. *The Journal of infectious diseases*, 211(6), pp.870–878.

Bertolotti-Ciarlet, A. et al., 2002. Structural requirements for the assembly of Norwalk virus-like particles. *Journal of virology*, 76(8), pp.4044–4055.

Bidawid, S. et al., 2003. A feline kidney cell line-based plaque assay for feline calicivirus, a surrogate for Norwalk virus. *Journal of virological methods*, 107(2), pp.163–167.

Bok, K. & Green, K.Y., 2012. Norovirus gastroenteritis in immunocompromised patients. *The New England journal of medicine*, 367(22), pp.2126–2132.

Brochet, X., Lefranc, M.-P. & Giudicelli, V., 2008. IMGT/V-QUEST: the highly customized and integrated system for IG and TR standardized V-J and V-D-J sequence analysis. *Nucleic acids research*, 36(Web Server issue), pp.W503–8.

Chachu, K.A. et al., 2008. Antibody is critical for the clearance of murine norovirus infection. *Journal of virology*, 82(13), pp.6610–6617.

Chan, M.C.W. et al., 2016. Reduced Diagnostic Performance of Two Norovirus Antigen Enzyme Immunoassays for the Emergent Genogroup II Genotype 17 Kawasaki 2014 Variant. A. J. McAdam, ed. *Journal of clinical microbiology*, 54(6), pp.1650–1652.

Cheetham, S. et al., 2006. Pathogenesis of a genogroup II human norovirus in gnotobiotic pigs. *Journal of virology*, 80(21), pp.10372–10381.

Choi, J.-M. et al., 2008. Atomic resolution structural characterization of recognition of histo-blood group antigens by Norwalk virus. *Proceedings of the National Academy of Sciences of the United States of America*, 105(27), pp.9175–9180.

Collaborative Computational Project, Number 4, 1994. The CCP4 suite: programs for protein crystallography. *Acta crystallographica. Section D, Biological crystallography*, 50(Pt 5), pp.760–763.

Costantini, V. et al., 2018. Human Norovirus Replication in Human Intestinal Enteroids as Model to Evaluate Virus Inactivation. *Emerging infectious diseases*, 24(8), pp.1453–1464.

Crawford, S.E. et al., 2015. Mapping broadly reactive norovirus genogroup I and II monoclonal antibodies. R. L. Hodinka, ed. *Clinical and vaccine immunology : CVI*, 22(2), pp.168–177.

Czako, R. et al., 2015. Experimental human infection with Norwalk virus elicits a surrogate

neutralizing antibody response with cross-genogroup activity. R. L. Hodinka, ed. *Clinical and vaccine immunology : CVI*, 22(2), pp.221–228.

Czako, R. et al., 2012. Serum hemagglutination inhibition activity correlates with protection from gastroenteritis in persons infected with Norwalk virus. *Clinical and vaccine immunology : CVI*, 19(2), pp.284–287.

Debbink, K. et al., 2013. Emergence of new pandemic GII.4 Sydney norovirus strain correlates with escape from herd immunity. *The Journal of infectious diseases*, 208(11), pp.1877–1887.

Debbink, K., Donaldson, E.F., et al., 2012. Genetic mapping of a highly variable norovirus GII.4 blockade epitope: potential role in escape from human herd immunity. *Journal of virology*, 86(2), pp.1214–1226.

Debbink, K., Lindesmith, L.C. & Baric, R.S., 2014. The state of norovirus vaccines. *Clinical infectious diseases : an official publication of the Infectious Diseases Society of America*, 58(12), pp.1746–1752.

Debbink, K., Lindesmith, L.C., Donaldson, E.F., et al., 2014. Chimeric GII.4 norovirus virus-like-particle-based vaccines induce broadly blocking immune responses. *Journal of virology*, 88(13), pp.7256–7266.

Debbink, K., Lindesmith, L.C., et al., 2012. Norovirus immunity and the great escape. R. C. Condit, ed. *PLoS pathogens*, 8(10), p.e1002921.

Dreyer, W.J. & Bennett, J.C., 1965. The molecular basis of antibody formation: a paradox. *Proceedings of the National Academy of Sciences of the United States of America*, 54(3), pp.864–869.

Duizer, E. et al., 2004. Laboratory efforts to cultivate noroviruses. *The Journal of general virology*, 85(Pt 1), pp.79–87.

El-Kamary, S.S. et al., 2010. Adjuvanted intranasal Norwalk virus-like particle vaccine elicits antibodies and antibody-secreting cells that express homing receptors for mucosal and peripheral lymphoid tissues. *The Journal of infectious diseases*, 202(11), pp.1649–1658.

Emsley, P. & Cowtan, K., 2004. Coot: model-building tools for molecular graphics. *Acta crystallographica. Section D, Biological crystallography*, 60(Pt 12 Pt 1), pp.2126–2132.

Erdman, D.D., Gary, G.W. & Anderson, L.J., 1989. Serum immunoglobulin A response to Norwalk virus infection. *Journal of clinical microbiology*, 27(6), pp.1417–1418.

Ettayebi, K. et al., 2016. Replication of human noroviruses in stem cell-derived human enteroids. *Science*, 353(6306), pp.1387–1393.

Fields, B.N., Knipe, D.M. & Howley, P.M., 2013. *Fields Virology*, Lippincott Williams & Wilkins.

Florescu, D.F. et al., 2008. Two cases of Norwalk virus enteritis following small bowel transplantation treated with oral human serum immunoglobulin. *Pediatric transplantation*, 12(3), pp.372–375.

Fox, L.M. & Saravolatz, L.D., 2005. Nitazoxanide: a new thiazolide antiparasitic agent. *Clinical infectious diseases : an official publication of the Infectious Diseases Society of America*, 40(8), pp.1173–1180.

Glass, R.I., Parashar, U.D. & Estes, M.K., 2009. Norovirus gastroenteritis. *The New England journal of medicine*, 361(18), pp.1776–1785.

Gray, J.J. et al., 1994. Detection of immunoglobulin M (IgM), IgA, and IgG Norwalk virus-specific antibodies by indirect enzyme-linked immunosorbent assay with baculovirus-expressed Norwalk virus capsid antigen in adult volunteers challenged with Norwalk virus. *Journal of clinical microbiology*, 32(12), pp.3059–3063.

Green, K.Y. et al., 1993. Comparison of the reactivities of baculovirus-expressed recombinant Norwalk virus capsid antigen with those of the native Norwalk virus antigen in serologic assays and some epidemiologic observations. *Journal of clinical microbiology*, 31(8), pp.2185–2191.

Guo, L. et al., 2009. A recombinant adenovirus prime-virus-like particle boost regimen elicits effective and specific immunities against norovirus in mice. *Vaccine*, 27(38), pp.5233–5238.

Guo, L. et al., 2008. Intranasal administration of a recombinant adenovirus expressing the norovirus capsid protein stimulates specific humoral, mucosal, and cellular immune responses in mice. *Vaccine*, 26(4), pp.460–468.

Hale, A.D. et al., 1998. Homotypic and heterotypic IgG and IgM antibody responses in adults infected with small round structured viruses. *Journal of medical virology*, 54(4), pp.305–312.

Hall, A.J. et al., 2013. Norovirus disease in the United States. *Emerging infectious diseases*, 19(8), pp.1198–1205.

Hall, A.J. et al., 2014. Vital signs: foodborne norovirus outbreaks - United States, 2009-2012. *MMWR. Morbidity and mortality weekly report*, 63(22), pp.491–495.

Harrington, P.R. et al., 2002. Binding of Norwalk virus-like particles to ABH histo-blood group antigens is blocked by antisera from infected human volunteers or experimentally vaccinated mice. *Journal of virology*, 76(23), pp.12335–12343.

He, W. et al., 2015. Broadly neutralizing anti-influenza virus antibodies: enhancement of neutralizing potency in polyclonal mixtures and IgA backbones. T. S. Dermody, ed. *Journal of virology*, 89(7), pp.3610–3618.

Heijne, J.C.M. et al., 2009. Enhanced hygiene measures and norovirus transmission during an outbreak. *Emerging infectious diseases*, 15(1), pp.24–30.

Herbst-Kralovetz, M.M. et al., 2013. Lack of norovirus replication and histo-blood group antigen expression in 3-dimensional intestinal epithelial cells. *Emerging infectious diseases*, 19(3), pp.431–438.

Huang, W. et al., 2014. Identification of human single-chain antibodies with broad reactivity for noroviruses. *Protein engineering, design & selection : PEDS*, 27(10), pp.339–349.

Iritani, N. et al., 2007. Humoral immune responses against norovirus infections of children. *Journal of medical virology*, 79(8), pp.1187–1193.

Janeway, C.A., Jr, 2001. *Immunobiology*,

Jiang, X. et al., 1992. Expression, self-assembly, and antigenicity of the Norwalk virus capsid protein. *Journal of virology*, 66(11), pp.6527–6532.

Johnson, P.C. et al., 1990. Multiple-challenge study of host susceptibility to Norwalk gastroenteritis in US adults. *The Journal of infectious diseases*, 161(1), pp.18–21.

Jones, M.K. et al., 2014. Enteric bacteria promote human and mouse norovirus infection of B cells. *Science*, 346(6210), pp.755–759.

Kageyama, T. et al., 2003. Broadly reactive and highly sensitive assay for Norwalk-like viruses based on real-time quantitative reverse transcription-PCR. *Journal of clinical microbiology*, 41(4), pp.1548–1557.

Kapikian, A.Z., 2000. The discovery of the 27-nm Norwalk virus: an historic perspective. *The Journal of infectious diseases*, 181 Suppl 2(s2), pp.S295–302.

Kapikian, A.Z. et al., 1972. Visualization by immune electron microscopy of a 27-nm particle associated with acute infectious nonbacterial gastroenteritis. *Journal of virology*, 10(5),

pp.1075–1081.

Karst, S.M. & Baric, R.S., 2015. What is the reservoir of emergent human norovirus strains? S. Schultz-Cherry, ed. *Journal of virology*, 89(11), pp.5756–5759.

Koho, T. et al., 2012. Production and characterization of virus-like particles and the P domain protein of GII.4 norovirus. *Journal of virological methods*, 179(1), pp.1–7.

Koromyslova, A.D. & Hansman, G.S., 2017. Nanobodies targeting norovirus capsid reveal functional epitopes and potential mechanisms of neutralization. B. Sherry, ed. *PLoS pathogens*, 13(11), p.e1006636.

Kou, B. et al., 2015. Characterization of cross-reactive norovirus-specific monoclonal antibodies. R. L. Hodinka, ed. *Clinical and vaccine immunology : CVI*, 22(2), pp.160–167.

Kubota, T. et al., 2012. Structural basis for the recognition of Lewis antigens by genogroup I norovirus. *Journal of virology*, 86(20), pp.11138–11150.

Lay, M.K. et al., 2010. Norwalk virus does not replicate in human macrophages or dendritic cells derived from the peripheral blood of susceptible humans. *Virology*, 406(1), pp.1–11.

Leroux-Roels, G. et al., 2018. Safety and Immunogenicity of Different Formulations of Norovirus Vaccine Candidate in Healthy Adults: A Randomized, Controlled, Double-Blind Clinical Trial. *The Journal of infectious diseases*, 217(4), pp.597–607.

Leshem, E. et al., 2013. Effects and clinical significance of GII.4 Sydney norovirus, United States, 2012-2013. *Emerging infectious diseases*, 19(8), pp.1231–1238.

Lindesmith, L. et al., 2005. Cellular and humoral immunity following Snow Mountain virus challenge. *Journal of virology*, 79(5), pp.2900–2909.

Lindesmith, L. et al., 2003. Human susceptibility and resistance to Norwalk virus infection. *Nature medicine*, 9(5), pp.548–553.

Lindesmith, L.C. et al., 2013. Emergence of a norovirus GII.4 strain correlates with changes in evolving blockade epitopes. *Journal of virology*, 87(5), pp.2803–2813.

Lindesmith, L.C. et al., 2008. Mechanisms of GII.4 norovirus persistence in human populations. B. A. Lopman, ed. *PLoS medicine*, 5(2), p.e31.

Lindesmith, L.C. et al., 2015. Serum Immunoglobulin A Cross-Strain Blockade of Human

Noroviruses. *Open forum infectious diseases*, 2(3), p.ofv084.

Lindesmith, L.C., Beltramello, M., et al., 2012. Immunogenetic mechanisms driving norovirus GII.4 antigenic variation. T. C. Pierson, ed. *PLoS pathogens*, 8(5), p.e1002705.

Lindesmith, L.C., Debbink, K., et al., 2012. Monoclonal antibody-based antigenic mapping of norovirus GII.4-2002. *Journal of virology*, 86(2), pp.873–883.

Lochridge, V.P. et al., 2005. Epitopes in the P2 domain of norovirus VP1 recognized by monoclonal antibodies that block cell interactions. *The Journal of general virology*, 86(Pt 10), pp.2799–2806.

Loisy, F. et al., 2005. Real-time RT-PCR for norovirus screening in shellfish. *Journal of virological methods*, 123(1), pp.1–7.

Lopman, B.A. et al., 2016. The Vast and Varied Global Burden of Norovirus: Prospects for Prevention and Control. *PLoS medicine*, 13(4), p.e1001999.

McCoy, A.J. et al., 2007. Phaser crystallographic software. *Journal of applied crystallography*, 40(Pt 4), pp.658–674.

McLean, G.R. et al., 2000. Human and murine immunoglobulin expression vector cassettes. *Molecular immunology*, 37(14), pp.837–845.

Nordgren, J. et al., 2016. Innate Resistance and Susceptibility to Norovirus Infection. R. E. Dutch, ed. *PLoS pathogens*, 12(4), p.e1005385.

Pang, X. & Lee, B.E., 2015. Laboratory diagnosis of noroviruses: present and future. *Clinics in laboratory medicine*, 35(2), pp.345–362.

Parker, T.D. et al., 2005. Identification of Genogroup I and Genogroup II broadly reactive epitopes on the norovirus capsid. *Journal of virology*, 79(12), pp.7402–7409.

Parra, G.I. et al., 2013. Identification of a Broadly Cross-Reactive Epitope in the Inner Shell of the Norovirus Capsid. R. Jhaveri, ed. *PloS one*, 8(6), p.e67592.

Parra, G.I. et al., 2012. Multiple antigenic sites are involved in blocking the interaction of GII.4 norovirus capsid with ABH histo-blood group antigens. *Journal of virology*, 86(13), pp.7414–7426.

Pires, S.M. et al., 2015. Aetiology-Specific Estimates of the Global and Regional Incidence and

Mortality of Diarrhoeal Diseases Commonly Transmitted through Food. L. A. Selvey, ed. *PloS one*, 10(12), p.e0142927.

Pletneva, M.A., Sosnovtsev, S.V. & Green, K.Y., 2001. The genome of hawaii virus and its relationship with other members of the caliciviridae. *Virus genes*, 23(1), pp.5–16.

Prasad, B.V. et al., 1994. Three-dimensional structure of baculovirus-expressed Norwalk virus capsids. *Journal of virology*, 68(8), pp.5117–5125.

Prasad, B.V. et al., 1999. X-ray crystallographic structure of the Norwalk virus capsid. *Science*, 286(5438), pp.287–290.

Ramani, S. et al., 2015. Mucosal and Cellular Immune Responses to Norwalk Virus. *The Journal of infectious diseases*, p.jiv053.

Ramirez, K. et al., 2012. Intranasal vaccination with an adjuvanted Norwalk virus-like particle vaccine elicits antigen-specific B memory responses in human adult volunteers. *Clinical immunology (Orlando, Fla.)*, 144(2), pp.98–108.

Reeck, A. et al., 2010. Serological correlate of protection against norovirus-induced gastroenteritis. *The Journal of infectious diseases*, 202(8), pp.1212–1218.

Richardson, C. et al., 2013. Norovirus virus-like particle vaccines for the prevention of acute gastroenteritis. *Expert review of vaccines*, 12(2), pp.155–167.

Rocha-Pereira, J. et al., 2016. Post-exposure antiviral treatment of norovirus infections effectively protects against diarrhea and reduces virus shedding in the stool in a mortality mouse model. *Antiviral research*, 132, pp.76–84.

Rockx, B.H.G. et al., 2005. Experimental norovirus infections in non-human primates. *Journal of medical virology*, 75(2), pp.313–320.

Rossignol, J.-F. & El-Gohary, Y.M., 2006. Nitazoxanide in the treatment of viral gastroenteritis: a randomized double-blind placebo-controlled clinical trial. *Alimentary pharmacology & therapeutics*, 24(10), pp.1423–1430.

Schreiber, D.S., Blacklow, N.R. & Trier, J.S., 1973. The mucosal lesion of the proximal small intestine in acute infectious nonbacterial gastroenteritis. *The New England journal of medicine*, 288(25), pp.1318–1323.

Shanker, S. et al., 2014. Structural analysis of determinants of histo-blood group antigen binding

specificity in genogroup I noroviruses. *Journal of virology*, 88(11), pp.6168–6180.

Smith, S.A. & Crowe, J.E., 2015. Use of Human Hybridoma Technology To Isolate Human Monoclonal Antibodies. *Microbiology spectrum*, 3(1), pp.AID–0027–2014.

Smith, S.A. et al., 2013. The potent and broadly neutralizing human dengue virus-specific monoclonal antibody 1C19 reveals a unique cross-reactive epitope on the bc loop of domain II of the envelope protein. *mBio*, 4(6), pp.e00873–13.

Sok, D. et al., 2014. Recombinant HIV envelope trimer selects for quaternary-dependent antibodies targeting the trimer apex. *Proceedings of the National Academy of Sciences of the United States of America*, 111(49), pp.17624–17629.

Souza, M. et al., 2007. Cytokine and antibody responses in gnotobiotic pigs after infection with human norovirus genogroup II.4 (HS66 strain). *Journal of virology*, 81(17), pp.9183–9192.

Souza, M. et al., 2008. Pathogenesis and immune responses in gnotobiotic calves after infection with the genogroup II.4-HS66 strain of human norovirus. *Journal of virology*, 82(4), pp.1777–1786.

Storch, G.A., 2000. Diagnostic virology. L. B. Reller & M. P. Weinstein, eds. *Clinical infectious diseases : an official publication of the Infectious Diseases Society of America*, 31(3), pp.739–751.

Subekti, D.S. et al., 2002. Experimental infection of Macaca nemestrina with a Toronto Norwalk-like virus of epidemic viral gastroenteritis. *Journal of medical virology*, 66(3), pp.400–406.

Tamminen, K. et al., 2016. Mucosal Antibodies Induced by Intranasal but Not Intramuscular Immunization Block Norovirus GII.4 Virus-Like Particle Receptor Binding. *Viral immunology*, 29(5), pp.315–319.

Tan, M. & Jiang, X., 2012. Norovirus P particle: a subviral nanoparticle for vaccine development against norovirus, rotavirus and influenza virus. *Nanomedicine (London, England)*, 7(6), pp.889–897.

Tan, M. et al., 2011. Norovirus P particle, a novel platform for vaccine development and antibody production. *Journal of virology*, 85(2), pp.753–764.

Tegerstedt, K. et al., 2006. [Virus-like particles as cancer vaccine. Great expectations--not only for papillomavirus associated cancer]. *Lakartidningen*, 103(37), pp.2650–2652.

Terwilliger, T.C. et al., 2008. Iterative model building, structure refinement and density modification with the PHENIX AutoBuild wizard. *Acta crystallographica. Section D, Biological crystallography*, 64(Pt 1), pp.61–69.

Teunis, P.F.M. et al., 2008. Norwalk virus: how infectious is it? *Journal of medical virology*, 80(8), pp.1468–1476.

Thornburg, N.J. et al., 2013. Human antibodies that neutralize respiratory droplet transmissible H5N1 influenza viruses. *The Journal of clinical investigation*, 123(10), pp.4405–4409.

Tian, P. et al., 2010. Specificity and kinetics of norovirus binding to magnetic bead-conjugated histo-blood group antigens. *Journal of applied microbiology*, 109(5), pp.1753–1762.

Treanor, J.J. et al., 1993. Subclass-specific serum antibody responses to recombinant Norwalk virus capsid antigen (rNV) in adults infected with Norwalk, Snow Mountain, or Hawaii virus. *Journal of clinical microbiology*, 31(6), pp.1630–1634.

Tudor, D. et al., 2012. Isotype modulates epitope specificity, affinity, and antiviral activities of anti-HIV-1 human broadly neutralizing 2F5 antibody. *Proceedings of the National Academy of Sciences of the United States of America*, 109(31), pp.12680–12685.

Vajdy, M., 2008. *Immunity Against Mucosal Pathogens*, Springer Science & Business Media.

Vega, E. et al., 2014. RNA populations in immunocompromised patients as reservoirs for novel norovirus variants. *Journal of virology*, 88(24), pp.14184–14196.

Vinjé, J., 2015. Advances in laboratory methods for detection and typing of norovirus. G. V. Doern, ed. *Journal of clinical microbiology*, 53(2), pp.373–381.

Wallace, A.C., Laskowski, R.A. & Thornton, J.M., 1995. LIGPLOT: a program to generate schematic diagrams of protein-ligand interactions. *Protein engineering*, 8(2), pp.127–134.

White, P.A., 2014. Evolution of norovirus. *Clinical microbiology and infection : the official publication of the European Society of Clinical Microbiology and Infectious Diseases*, 20(8), pp.741–745.

Williams, J.V. et al., 2007. A recombinant human monoclonal antibody to human metapneumovirus fusion protein that neutralizes virus in vitro and is effective therapeutically in vivo. *Journal of virology*, 81(15), pp.8315–8324.

Wyatt, R.G. et al., 1974. Comparison of three agents of acute infectious nonbacterial

gastroenteritis by cross-challenge in volunteers. *The Journal of infectious diseases*, 129(6), pp.709–714.

Xi, J.N. et al., 1990. Norwalk virus genome cloning and characterization. *Science*, 250(4987), pp.1580–1583.

Zachos, N.C. et al., 2016. Human Enteroids/Colonoids and Intestinal Organoids Functionally Recapitulate Normal Intestinal Physiology and Pathophysiology. *The Journal of biological chemistry*, 291(8), pp.3759–3766.

Zheng, D.-P. et al., 2006. Norovirus classification and proposed strain nomenclature. *Virology*, 346(2), pp.312–323.